



Pontifical Catholic University of Chile  
Faculty of Physics

# On the effects of the modification of the metric in the gravitational context

by

Carlos Rubio

A dissertation presented by Carlos Rubio  
to the Faculty of Physics  
in partial fulfillment of the requirements  
for the degree of Ph.D. in Physics.

Thesis advisor : Dr. Jorge Alfaro (PUC)  
Informant Committee : Dr. Benjamin Koch (PUC)  
Dr. Rolando Düner (PUC)  
Dr. Sergio Hojman (Universidad de Chile,  
Universidad Adolfo Ibañez)  
Dr. Gonzalo Palma (Universidad de Chile)

September 2020, Santiago, Chile

©2020, Carlos Rubio



# Declaration of authorship

I, Carlos Rubio, declare that this thesis titled, ‘On the effects of the modification of the metric in the gravitational context’ and the work presented in it are my own. I confirm that:

- This work was done wholly or mainly while in candidature for a research degree at this University.
- Where any part of this thesis has previously been submitted for a degree or any other qualification at this University or any other institution, this has been clearly stated.
- Where I have consulted the published work of others, this is always clearly attributed.
- Where I have quoted from the work of others, the source is always given. With the exception of such quotations, this thesis is entirely my own work.
- I have acknowledged all main sources of help.
- Where the thesis is based on work done by myself jointly with others, I have made clear exactly what was done by others and what I have contributed myself.

Signed:

---

Date:

---



*“I do not know what I may appear to the world, but to myself, I seem to have been only like a boy playing on the seashore, and diverting myself in now and then finding a smoother pebble or a prettier shell than ordinary, whilst the great ocean of truth lay all undiscovered before me.”*

Isaac Newton



Pontifical Catholic University of Chile

# *Abstract*

Ph.D. in Physics

by Carlos Rubio

This thesis is split into two parts: In the first one we study the minimal geometric deformation approach in order to generate anisotropic solutions from Einstein's equation and its observational effects of such anisotropies when measuring the surface redshift.

On the other hand, we develop the theory of perturbation of Delta Gravity at first order, we discuss the gauge transformations for metric and a perfect fluid in order to present the equations of the evolution of cosmological fluctuations using the hydrodynamic approximation. Then we compute the temperature fluctuations for photons coming from the time of last scattering  $t_L$ . Finally, we present a formula for temperature multipole coefficients for scalar modes, which can be used to compare the theory with astronomical observations.





# *Acknowledgements*

It is a great pleasure to thank my advisor, Dr. Jorge Alfaro, for an excellent supervision and to encourage me to carry out my own ideas. He inspired me to go beyond the standard theories yet never forgetting the observational constraints. In addition, his experience, his ability, and his view of how physics works helped me to improve my own point of view about physics.

Thanks to the members of my thesis committee Dr. Benjamin Koch, Dr. Rolando Dünner, Dr. Segio Hojman and Dr. Gonzalo Palma, for the constructive criticism, useful comments and suggestions.

I would like to thank the Physics Department of the Pontifical Catholic University of Chile for its warmest hospitality all these years. Thanks to the Chilean government who supported me by Conicyt PhD Fellowship No. 21150314.

I would like to thank Raúl, Dr. Matías, Renzo, Cristopher, Ivania, Chirri, Iván, Dr. Francisco, among others, for their support and useful collaboration.

Thanks to my collaborators: Dr. Ángel Rincón, Dr. Luciano Gabbanelli, Dr. Felipe Asenjo and Marco San Martín for their help and support in different projects.

Thanks to our group: Alex Soto, Mauricio Gamonal, Joaquín Sureda, Loreto Osorio and Robinson Mancilla for their help and comments during my stay in the program.

Thanks to my family, to Alexandra and my friends for all their support and love.



# Contents

<b>Declaration of authorship</b>	<b>iii</b>
<b>Abstract</b>	<b>vii</b>
<b>Acknowledgements</b>	<b>ix</b>
<b>1 Preliminar</b>	<b>1</b>
1.1 Motivations . . . . .	1
1.2 Introduction . . . . .	2
<b>2 Gravitational decoupled anisotropies in compact stars</b>	<b>11</b>
2.1 Anisotropic effective field equations . . . . .	11
2.2 Minimal geometric deformation approach . . . . .	14
2.3 Anisotropic Durgapal-Fuloria compact star . . . . .	17
2.3.1 Pressure-like constraint for the anisotropy . . . . .	18
2.3.1.1 Matching conditions . . . . .	19
2.3.2 Density-like constrain for the anisotropy . . . . .	23
2.3.2.1 Matching conditions . . . . .	24
2.3.3 On the detectability and observational differences for anisotropic dis- tributions . . . . .	26
2.4 Anisotropizing an anisotropic Durgapal-Fuloria star . . . . .	27
2.5 Conclusions . . . . .	33
<b>3 Delta Gravity</b>	<b>35</b>
3.1 Definition of Delta Gravity . . . . .	35
3.2 Perfect fluid . . . . .	37
3.3 Test Particle . . . . .	38
3.3.1 Massive Particles . . . . .	38
3.3.2 Massless Particles . . . . .	40
3.4 Cosmology in DG . . . . .	42

3.4.1	Harmonic gauge in an Isotropic and Homogeneous Universe . . . . .	42
3.4.2	Photon Trajectory . . . . .	43
3.4.3	Einstein's Equations . . . . .	45
3.4.4	Delta Sector . . . . .	46
3.4.5	Thermodynamics in DG . . . . .	48
3.4.6	Equality time $t_{EQ}$ . . . . .	50
3.4.7	Conclusions . . . . .	51
<b>4</b>	<b>Cosmological Fluctuations in Delta Gravity</b>	<b>53</b>
4.1	Perturbation Theory . . . . .	53
4.1.1	Choosing a gauge . . . . .	54
4.1.2	$T_{\mu\nu}$ and $\tilde{T}_{\mu\nu}$ . . . . .	56
4.1.3	Gauge Transformations for the Energy-Momentum tensors . . . . .	59
4.1.4	Fields equations and energy momentum conservation in synchronous gauge . . . . .	62
4.2	Evolution of cosmological fluctuations . . . . .	64
4.2.1	Matter era . . . . .	70
4.3	Summary and Conclusions . . . . .	75
<b>5</b>	<b>Temperature Fluctuations</b>	<b>77</b>
5.1	Derivation of temperature fluctuations . . . . .	77
5.1.1	Gauge transformations . . . . .	83
5.1.2	Single modes . . . . .	85
5.2	Coefficients of multipole temperature expansion: Scalar modes . . . . .	86
5.3	Summary and Conclusions . . . . .	94
<b>6</b>	<b>Discussion and conclusions</b>	<b>95</b>
<b>7</b>	<b>Afterword</b>	<b>99</b>
<b>A</b>	<b>WKB approximation</b>	<b>101</b>
A.1	$R$ and $\tilde{R} \neq 0$ . . . . .	101
A.2	Landau Damping . . . . .	104

*Dedicated to my Family: those who have supported me  
throughout this journey.*



# Chapter 1

## Preliminar

### 1.1 Motivations

When we speak about the greatest contribution to the physics of the twentieth century, we can undoubtedly affirm that Quantum Mechanics and General Relativity occupy the podium. Both theories have been tested in different scenarios achieving to explain many phenomena and thanks to them we can understand Nature in a much deeper way.

In particular, General Relativity, proposed by Einstein in 1916 has allowed us to understand the nature of gravity, and with this, we can now figure out how extensive is our Universe and how its constituents take part in it. The evolution of the understanding of the Universe from the first habitants until the modern Cosmology has taught us about the infinite power of the knowledge of mathematics and of the technological development involved.

Richard Feynman said that *to those who do not know mathematics it is difficult to get across a real feeling as to the beauty, the deepest beauty, of nature... if you want to learn about nature, to appreciate nature, it is necessary to understand the language that she speaks in*. I could not agree more with his words, in my young career I have seen how mathematics can not only describe phenomena yet it can predicts how nature behaves or the existence of new particles such the case of neutrinos.

I will never forget one of my first classes of mechanics, where the professor Victor Muñoz said that *the calculator is dumb* when he was referring to approximations in physics and how the intuition will be one of the most powerful skills when solving problems, since that moment I fell in love with physics and I knew that I wanted to be a physicist, and is this

feeling who has driven me to this point where I am concluding the Ph.D. Along this road, I have learned about many fields in physics, both theoretical and experimental. And despite I am aware of Physics is an experimental science, I felt very intrigued when I see an equation that describes an experiment.

With this hungry, I met Einstein's Special Relativity. I am still impressed with how he imagined that space and time behaved the way we understand today. But even more, is how using mathematics he could present his theory and how it was verified with accuracy later. It is not hard to describe my admiration when I went deeper and I studied Einstein's General Relativity. This was the moment when I realized that I wanted to dedicate my life to understand the most possible about this theory. Predictions from the curvature of the space-time which was verified a few years after its publication, the form and the evolution of the Universe which is still in controversy, to gravitational waves which took almost 100 years for its measurement motivated me to do my research in this area.

This thesis tries to give a humble extension of the considerations when solving Einstein's equations, where all the information is encoded as much as in the geometry which is referenced to the metric, as in the content of matter in the Universe. Here are present two main results which have in common a naively simple consideration: the modification of the geometry (or the metric) permits to extend some solutions of GR to explain astronomical observations. I hope these results could go in the right direction to the final answer to the current controversies that the General Relativity is facing through.

## 1.2 Introduction

We know that general relativity (GR) has been tested from scales larger than a millimeter to solar-system scales [1, 2]. Nevertheless, its quantization has proved to be difficult. The theory is non-renormalizable, which prevents its unification with the other forces of nature. There are some theories which have tried to make sense of quantum GR, like string theories, Loop Quantum Gravity among others, but none of them has been accepted as the correct and final answer to the problem of quantum gravity.

The study of analytical solutions of Einstein field equations plays a crucial role in the discovery and understanding of relativistic phenomena. Theoretical grounds provide many exact and non exact isotropic solutions in GR; however most of them have no physical relevance and do not pass elementary test of astrophysical observations[3–6]. There are very few solutions



under static and spherically symmetric assumptions. Worst yet, ever fewer of these solutions have physical relevance passing elementary tests of astrophysical observations. Furthermore, no astronomical object is constituted of perfect fluid only; hence isotropic approximation is likely to fail.

Anisotropic configurations have continuously attracted interest and are still an active field of research. Strong evidence suggests that a variety of very interesting physical phenomena gives rise to a quite large number of local anisotropies, either for low or high density regimes (see [7] and references therein). For instance, among high density regimes, there are highly compact astrophysical objects with core densities ever higher than nuclear density ( $\sim 3 \times 10^{17} \text{ kg/m}^3$ ) that may exhibit an anisotropic behaviour [8]. Certainly, the nuclear interactions of these objects must be treated relativistically. The anisotropic behaviour is produced when the standard pressure is split in two different contributions: i) the radial pressure  $p_r$  and ii) the transverse pressure  $p_t$ , which are not likely to coincide.

Anisotropies in fluid pressure usually arise due to the presence of a mixture of fluids of different types, rotation, viscosity, the existence of a solid core, the presence of a superfluid or a magnetic field [9]. Even anisotropies are produced by some kind of phase transitions or pion condensation among others [10, 11]. The sources of anisotropies have been widely studied in the literature, particularly for different highly compact astrophysical objects such as compact stars or black holes, either in 4 dimensions [12, 13] as well as in the context of braneworld solution in higher dimensions [14–16].

The main purpose of this part of the Thesis is to generalize anisotropic analogous solutions of a particular kind of isotropic compact objects by means of the so-called *minimal geometric deformation* approach (MGD hereinafter) [17, 18]. This method was originally proposed in the context of the Randall–Sundrum braneworld [19, 20] and was designed to deform the standard Schwarzschild solution [21, 22]. It describes the 4D geometry of a brane stellar distribution, hence obtaining braneworld corrections to standard GR solutions. Therefore, it is a suitable method to obtain spherically symmetric and inhomogeneous stellar distributions that are physically admissible in the braneworld. The key point of this approach is that the isotropic and anisotropic sectors can be split. Thus, the decoupling of both gravitational sources can be done in a simple and systematic way establishing a new window to search for new families of anisotropic solutions of Einstein field equations.

We applied a gravitational decoupling through the MGD approach to derive exact and physically acceptable anisotropic interior solutions analogous to the Durgapal and Fuloria superdense star [23]. There have been several proposals of anisotropic models analogous to Durgapal–Fuloria compact stars [24, 25]; the MGD method seems to generalize them. The details of this method will be shown in the next chapter, however the main lines goes as follows: Let us start with a well known spherically symmetric gravitational source  $T_{\mu\nu}^{(0)}$ . This source can be as simple as one would desire; one can start with any known perfect fluid or even with vacuum itself. Any classical solution works as a seed for this method. After this, one switch on a new source of anisotropy

$$\tilde{T}_{\mu\nu} = T_{\mu\nu}^{(0)} + \alpha T_{\mu\nu}^{(1)}. \quad (1.1)$$

When gravitational sources are coupled via gravity only, i.e. they do not exchange energy-momentum among each other, the set of equations can be split into two contributions. On the one hand, a well known sector is identified with the classical field equations of the chosen seed; the Durgapal-Fuloria solution for compact stars in our case. On the other hand, one is left with a simpler set of ‘pseudo-Einstein’ equations for the sources of the anisotropy, to be solved. Combining both sectors a full anisotropic and physically consistent solution of Einstein field equations is obtained. Of course one can switch on as many arbitrary sources of anisotropies  $T_{\mu\nu}^{(i)}$  as desired, as long as a strategy to solve the new sector can be found.

This method for decoupling non-linear differential equations can be applied in a systematic way and has a vast unexplored territory where it could give different novel perspectives. MGD does not only give consistent interior solutions for different isotropic perfect fluid in GR; it could also be conveniently exploited in relevant theories such as  $f(R)$ -gravity [26, 27], intrinsically anisotropic theories as Hořava–aether gravity [28] or to study the stability of novel proposals of Black Holes, described by Bose Einstein gravitational condensate systems of gravitons [29–31]. This is a robust method to extend physical solutions into an anisotropic domain preserving the physical acceptability.

The results of this part are presented in the publication *Gravitational decoupled anisotropies in compact stars*[32] and will be explained detaily in Chapter 2.

On the other hand, recent discoveries in cosmology have revealed that most part of matter is in the form of unknown matter, dark matter, and that the dynamics of the expansion of the Universe is governed by a mysterious component that accelerates its expansion, the so called dark energy. Although GR is able to accommodate both dark matter and dark energy, the

interpretation of the dark sector in terms of fundamental theories of elementary particles is problematic. Even though exist candidates that could play the role of dark matter, none of them have been detected yet.

In GR, dark energy can be explained if a small cosmological constant ( $\Lambda$ ) is present. At early times, this constant is irrelevant, but at the later stages of the evolution of the Universe  $\Lambda$  will dominate the expansion, explaining the observed acceleration. Such small  $\Lambda$  is very difficult to generate in quantum field theory (QFT) models, because  $\Lambda$  is the vacuum energy, which is usually predicted to be very large. Worse yet,  $\Lambda$ CDM which is the actual cosmological model is showing inconsistencies between the early and late Universe description[33]. The problem appears in different cosmological parameters such as the Hubble constant[34, 35], the curvature[36] and  $S_8$  tension[37]. Measuring the cosmic microwave background (CMB) radiation, the Planck team found a local expansion rate of  $H_0 = 67.37 \pm 0.54$  Km/s/Mpc, which is consistent with a flat  $\Lambda$  CDM model[38] (where the Hubble constant must be derived taking into account other observations like BAOs). On the other hand, the SH0ES collaboration found a larger value  $H_0 = 73.52 \pm 1.62$  Km/s/Mpc through model-independent measurements of the local Universe[34], at  $\gtrsim 3.5\sigma$  discrepancy with Planck value. This tension between early and late Universe exists even without Planck CMB data or the SH0ES distance ladder[33]. Another direct measurement of  $H_0 = 72.5^{+2.1}_{-2.3}$  Km/s/Mpc[39] from the H0LiCOW collaboration based on lensing time delays is in moderate tension with Planck, while a constraint from Big Bang nucleosynthesis (BBN) combined with baryon acoustic oscillation (BAO) data of  $H_0 = 66.98 \pm 1.18$  Km/s/Mpc[33] is inconsistent with SH0ES.

Other studies have tried to explain this discrepancy, suggesting that due to cosmic variance, the Hubble constant determined from nearby SNe-Ia may differ from that measured from the CMB by  $\pm 0.8$  percent at  $1\sigma$  statistical significance. Still, this difference does not explain the discrepancy between SNe-Ia and CMB.[40] Nevertheless, in an extreme case, observers located in the centers of the immense voids could measure a Hubble constant from SNe-Ia biased high by 5 percent.

From the first publication of the  $H_0$  tension [41] there have been many questions about the origin of this discrepancy. It has been suggested that could be errors in the calibration of Cepheids that contribute to systematic errors. This possible error has been discarded in an extensive discussion made by Riess et. al. [42].

There are many works which have tried to solve the acceleration evidence, including anisotropies at local scales. Using SNe-Ia data [43] they found evidence of anisotropies associated with

the direction and the amplitude of the bulk flow. Nevertheless, the effect of dipolar distribution dark energy cannot be excluded at high redshift. Also, there is another publication [44] where the anisotropies in cosmic acceleration are related to the Dark Energy, in their words, *the cosmic acceleration deduced from supernovae may be an artifact of our being non-Copernican observers, rather than evidence for a dominant component of "dark energy" in the Universe..* Other studies [45] conclude that even in the case of anisotropy, the Dark Energy could not be completely ruled out. This solution could provide solutions to explain variations on the local scale, for example, different measurements on the local Hubble constant. But this kind of hypothesis could defy all the analyses made by Planck using  $\Lambda$ CDM model because the Dark Energy component is essential for the evolution of photons of the CMB from the last Scattering Surface until now, even more, the sum over  $\Omega$  for every component in the Universe would drastically change. Many other suggestions about discrepancies have appeared, not only related to SNe-Ia measurements, but also within the Planck data itself. The anisotropies in these measurements have been debated and could be ruled out because the uncertainty tends to be very high, and the results can be very inconsistent. Even hypothesis about the possibility of a Universe with less Dark Energy [46] have appeared.

Another source of errors in the local measurement could be an inhomogeneity in the local density. [47] In this scenario the presence of local structure does not appear to impede the possibility of measuring the Hubble constant to 1% precision, and there is no evidence of a change in the Hubble constant corresponding to an inhomogeneity.

Today, there are different methods to obtain the Hubble constant, even with SNe-II, [48]. In this research, they used SN-II as standardizable candles to obtain an independent measurement of the Hubble constant. The value obtained was  $H_0 = 75.8^{+5.2}_{-4.9}$  km /s/Mpc. the local  $H_0$  is higher than the value from the early Universe with a confidence level of 95%. They concluded that there is no evidence that SNe Ia are the source of the  $H_0$  tension. Even, from SNe-Ia, other publication concluded, from analyzing SNe-Ia as standard candles in the near-infrared, that  $H_0 = 72.8 \pm 1.6$  (statistical)  $\pm 2.7$  (systematic) km/s/Mpc. Indeed, they concluded that the tension in the competing  $H_0$  distance ladders is likely not a result of supernova systematic.

Other proposals have tried to reconcile Planck and SNe-Ia data, including modifications in the physics of the DE. In other words, introducing a [49] equation of state of interacting dark energy component, where  $w$  is allowed to vary freely, could solve the  $H_0$  tension. Also, decaying dark matter model has been proposal in order to alleviate the  $H_0$  and  $\sigma_8$  anomalies[50], in

their work they reduce the tension for both measurements when only consider Planck CMB data and the local SH0ES prior on  $H_0$ , however when BAOs and JLA supernova dataset are included their model is weakened.

Other controversies are related to inconsistencies with curvature (and other parameters needed to describe the CMB) [36], or are related to the tension between measurements of the amplitude of the power spectrum of density perturbations (inferred using CMB) and directly measured by large-scale structure (LSS) on smaller scales. [51], Through the time, the tension between Planck and SNe-Ia persist [38, 42], where the  $H_0$  is the most significant tension. Furthermore, the Universe is composed principally by DE, but we still do not know what it is.

Delta Gravity (DG) [52] is an extension of General Relativity (GR), where new fields are added to the Lagrangian by a new symmetry (for more details see [52–54]). This model is very similar to classical GR, but could make sense at the quantum level. In this construction, the authors consider two different points. The first is that GR is finite on shell at one loop in vacuum, so renormalization is no necessary at this level. The second is a type of gauge theories,  $\tilde{\delta}$  gauge theories (DGT), presented in [55, 56], which main properties are: (a) a new kind of field  $\tilde{\phi}_I$  is introduced, different from the original set  $\phi_I$ . (b) The classical equations of motion of  $\phi_I$  are satisfied in the full quantum theory. (c) The model lives at one loop. (d) The action is obtained through the extension of the original gauge symmetry of the model, introducing an extra symmetry that they called  $\tilde{\delta}$  symmetry, since it is formally obtained as the variation of the original symmetry. When we apply this prescription to GR we obtain  $\tilde{\delta}$  Gravity (DG). This theory predicts an accelerating Universe without a cosmological constant  $\Lambda$ , and a Hubble parameter  $H_0 = 74.47 \pm 1.63$  Km/s/Mpc[57] when fitting SN-Ia Data, which is in agreement with SH0ES.

Although DG gives good results for local measurements, we need to study its cosmological predictions. In particular, the information provided by the anisotropies of matter and energy fluctuations in the Cosmic Microwave Background (CMB) could allow us to understand the physical meaning of this new fields which are included.

The temperature correlations give us information about the constituents of the Universe, such as baryonic and dark matter. Therefore we have to study the evolution of the CMB fluctuations from the last scattering (denoted by  $t_{ls}$ ) to the present. Usually, these computations are carried out by codes such as CMBFast[58, 59] or CAMB<sup>1</sup>[60], where Boltzmann

---

<sup>1</sup><http://camb.info/>

equations for the fluids and its interactions provide us well-known results that are in agreement with Planck measurements.[38]

Nevertheless, one can get a good approximation of this complex problem[61, 62]. In this work, we used an analytical method that consists of two steps instead of study the evolution of the scalar perturbations using Boltzmann equations. First, we used a hydrodynamic approximation, which assumes photons and baryonic plasma as a fluid in thermal equilibrium at recombination time, where there is a high rate of collisions between free electrons and photons. Second, we study the propagation of photons [52], by radial geodesics from the moment when the Universe switch from opaque to transparent at time  $t_{ls}$  until now.

In this research, we presented the first steps of this essential procedure, developing the theory of scalar perturbations at first order. We discussed the gauge transformations in an extended Friedmann-Lemaître-Robertson-Walker (FRLW) Universe. Then we showed how to get an expression for temperature fluctuations, and we demonstrated that they are gauge invariant, which is a crucial test from a theoretical point of view. With this result, we derived a formula for the scalar contribution to temperature multipole coefficients. This formula will be useful to test the theory, and could give a sign of the physical consequence of the “delta matter”, introduced in this theory.

The CMB provides cosmological constraints that are crucial to test a model. Many cosmological parameters can be obtained directly from the CMB Power Spectrum, such as  $h^2\Omega_b, h^2\Omega_c, 100\theta, \tau, A_s$  and  $n_s$  [38], but others can be derived from constraining CMB observation with SNe-Ia or BAOs. With the study of the CMB anisotropies, we can study two aspects: the compatibility between CMB Power Spectrum and DG fluctuations and the compatibility between CMB and SNe-Ia in the DG theory.

Throughout the Ph. D. preliminary results were presented in the following conferences:

- **XI SILAFAE: Latin American Symposium of High Energy Physics, CMB Power Spectrum in Delta Gravity**, Nov. 2016, Antigua, Guatemala.
- **La parte y el Todo: Tópicos Avanzados en Física de Altas Energías y Gravitación, CMB Power Spectrum in Delta Gravity**, Jan. 2017, Afunallhue, IX Región de la Araucanía, Chile.
- **XXI Simposio Chileno de Física, Temperature Fluctuations of CMB in Delta Gravity**, Nov. 2018, Antofagasta, Chile.

- **XII SILAFAE: Latin American Symposium of High Energy Physics, *Temperature Fluctuations of CMB in Delta Gravity***, Nov. 2018, Lima, Perú.

This Thesis is divided in four additional chapters, the first one is self-consistent with respect to the other two in the sense that can be read separately without the need of having read the preceding chapter. Finally, we add concluding chapter which sum up the main results of this Thesis.

The second chapter is subdivided as follow: we present the Einstein field equations for an anisotropic fluid. In Section 2.2 we explain how the MGD approach is implemented to generate arbitrary anisotropic solutions. Section 2.3 is dedicated to apply this method to a particular seed, the Durgapal-Fuloria model for compact stars. In Section 2.4 we extend the method to seeds which are already anisotropic. The last two sections are dedicated to discuss the main results and summarize our conclusions.

The third chapter introduce the model of DG and its results that will be useful for the develop of the fourth and fifth chapter. In Section 3.1 we introduce the  $\tilde{\delta}$  symmetry, and how it used to extend an action. Then we applied this symmetry to Einstein-Hilbert action to build the action of Delta Gravity, after that we present the equations of motion of this theory. In Section 3.2 we show the form of the energy-momentum tensors for a perfect fluid and the normalization of the velocity fields. In Section 3.3 we show how massive and massless particles move in a gravitational field induced by DG. After that, in Section 3.4 we present the main results of this theory for an extended FRLW-Universe. In Section 3.4.1 we derive the form of the metric in the harmonic gauge. Then, in Section 3.4.2 we study the trajectory of photons in this background. This define a modified scale factor which will replace the usual scale factor of GR for observable distances. After that, in Sections 3.4.3 and 3.4.4 we solve the complete system of equations of the theory and discuss some implications of these results. Then, in Section 3.4.5 we impose the first lay of Thermodynamics to DG and we can distinguish whether the solutions are physical or not. Also we show that if we require that the black body distribution of photons that travel from the moment of the decoupling until reaching us remain unchanged, the temperature should fall with the modified scale factor. After that, in Section 3.4.6 we show the implication of considering the moment when the density of radiation was equal to the density of Non Relativistic matter was the same for both GR and DG. This gives a physical meaning of a parameter of DG. Finally, in Section



3.4.7 we summarize the previous results of the Chapter and discuss some points of the theory about its foundation.

The fourth chapter presents the cosmological fluctuations in Delta Gravity. In Section 4.1 we perturb the FLRW metric using the scalar-vector-tensor decomposition. Then, in Sections 4.1.1 we study the gauge transformations for those perturbations. In Sections 4.1.2 and 4.1.3 we repeat the procedure for the energy-momentum tensor and present some gauge fixing scenarios. After that, in Section 4.1.4 we present the fields equations and energy-momentum conservation in the synchronous gauge.

In Section 4.2 we analyze the evolution of cosmological perturbation and solve them in the radiation era for adiabatic solutions. Then we do the same for the matter-dominated era in Section 4.2.1. Finally we present a summary of the chapter with some conclusions.

In Chapter 5 we study the fluctuations of temperature in DG. In Section 5.1 we derive how the perturbed FLRW background redshifts the temperature fluctuations. After that, in Section 5.1.1 we study the gauge transformations of these fluctuations, this will be a theoretical test of DG, because those fluctuations have to be gauge invariants. Then in Section 5.1.2 we consider scalar contributions dominated by a unique mode. With this consideration, we derive the coefficients for the multipole temperature expansion in Section 5.2. Here we find a formula for the CMB multipoles that will be useful to fit the data with DG. However, this procedure is not part of this Thesis. Finally, we summarize the results obtained in this Chapter and conclude over them.

To finish this Thesis, in Section 6 we present the main features of this work, and we give some traces for future investigations.



# Chapter 2

## Gravitational decoupled anisotropies in compact stars

This work was done in collaboration with Dr. Luciano Gabbanelli and Dr. Ángel Rincón, with whom I am very grateful to work.

### 2.1 Anisotropic effective field equations

The simplest approach to describe compact distributions modelling stellar structures, is to restrict the metric to be static and spherically symmetric. In the usual Schwarzschild-like coordinates the line element takes the standard form

$$ds^2 = e^\nu dt^2 - e^\lambda dr^2 - r^2 (d^2\theta + \sin^2\theta d^2\phi); \quad (2.1)$$

where the functions  $\nu \equiv \nu(r)$  and  $\lambda \equiv \lambda(r)$  depend on the radial coordinate only. The encoded metric is a generic solution of the Einstein field equations

$$R_{\mu\nu} - \frac{1}{2}R g_{\mu\nu} = \kappa \tilde{T}_{\mu\nu}, \quad (2.2)$$

describing an anisotropic fluid sphere. The coupling constant between matter is given by  $\kappa = 8\pi G/c^4$ . Along these lines we will work in relativistic geometrized units,  $G = c = 1$ . The observable features of the object will be determined by the exterior metric that will

describe the geometry of the outer part. In the present article to maintain the treatment as simpler as possible, we will suppose a Schwarzschild vacuum outside.

The corresponding anisotropic effective stress-energy tensor  $\tilde{T}_{\mu\nu}$  is characterized by its diagonal components  $\tilde{\rho}$ ,  $\tilde{p}_r$  and  $\tilde{p}_t$ , that are related to the geometric functions  $\mu$ ,  $\nu$  through (2.2). Explicitly,

$$\kappa\tilde{\rho} = \frac{1}{r^2} - e^{-\lambda} \left( \frac{1}{r^2} - \frac{\lambda'}{r} \right), \quad (2.3)$$

$$-\kappa\tilde{p}_r = \frac{1}{r^2} - e^{-\lambda} \left( \frac{1}{r^2} + \frac{\nu'}{r} \right), \quad (2.4)$$

$$-\kappa\tilde{p}_t = -\frac{1}{4}e^{-\lambda} \left( 2\nu'' + \nu'^2 - \lambda'\nu' + 2\frac{\nu' - \lambda'}{r} \right). \quad (2.5)$$

The prime stand for derivatives w.r.t.  $r$ . There is another equation consequence of the Bianchi identities: the covariant conservation of the stress-energy tensor

$$\nabla^\nu \tilde{T}_{\mu\nu} = 0. \quad (2.6)$$

Since the discovery of the first interior stellar solution by Schwarzschild [63] and for several years, stars interior were supposed to be constituted by perfect fluids. It was not until 1933 when Lemaître [64] develop that spherical symmetry do not require the isotropic condition  $\tilde{p}_r = \tilde{p}_t$ , but only the equality of the two tangential pressures  $\tilde{p}_\theta = \tilde{p}_\phi = \tilde{p}_t$ . The system of equations (2.3)–(2.6) governs the matter distribution within the star, which is assumed to be locally anisotropic (the radial and tangential pressure do not coincide). It is necessary to solve for five unknowns functions: two geometric functions,  $\nu(r)$  and  $\lambda(r)$ ; and three effective scalar functions,  $\tilde{\rho}(r)$ ,  $\tilde{p}_r(r)$  and  $\tilde{p}_t(r)$ . However there are more unknowns than equations, hence the system is undetermined and constraints must be imposed. Some of them must be chosen by consistency of regularity, stability and (or) energy conditions of relativistic models; see for instance [7, 9, 65].

Throughout this chapter we will make use of the following representation for the effective energy-momentum tensor

$$\tilde{T}_{\mu\nu} = T_{\mu\nu}^{(PF)} + \alpha \theta_{\mu\nu}. \quad (2.7)$$

The first term encodes a perfect fluid with isotropic pressure  $p = p_r = p_t$ ,

$$T_{\mu\nu}^{(PF)} = (\rho + p) u_\mu u_\nu - p g_{\mu\nu}. \quad (2.8)$$

$u_\mu$  is the normalized four-velocity field that accomplish  $u_\mu u_\nu g^{\mu\nu} = 1$ . In our case, the perfect fluid will invariably be given by the Durgapal–Fuloria interior solution. Under this representation, the anisotropic sector is described by the  $\theta$ -term. It describes additional gravitational sources responsible for the anisotropies. These source may contain new fields, whether scalar, vector or (and) tensor fields, coupled to gravity by means of a free dimensionless and constant parameter  $\alpha$ . One of the simplest and most treated examples in the literature are the anisotropies that may arise due to extra interactions resulting from the presence of charge [66]; besides there are plenty of complex treatments of anisotropies generated by other sophisticated physical fields [67].

The effective stress–energy tensor (2.7) contributes at the level of Einstein equations with an effective energy density  $\tilde{\rho}$ , an effective radial pressure  $\tilde{p}_r$  and an effective tangential pressure  $\tilde{p}_t$  defined as

$$\tilde{\rho} = \rho + \alpha \theta_t^t, \quad (2.9)$$

$$\tilde{p}_r = p - \alpha \theta_r^r, \quad (2.10)$$

$$\tilde{p}_t = p - \alpha \theta_\varphi^\varphi. \quad (2.11)$$

Thus, each magnitude is written as a deviation from the GR solution due to the presence of the  $\theta$ -term. The additive structure for the anisotropies allows the theory to have a straightforward limit to GR; setting  $\alpha = 0$  the standard Einstein equations for the perfect fluid are recovered.

Since the Einstein tensor is divergence free, under the representation taken in (2.7) the covariant conservation equation (2.6) yields

$$p' + \frac{\nu'}{2} (\rho + p) - \alpha \left[ (\theta_r^r)' + \frac{\nu'}{2} (\theta_r^r - \theta_t^t) + \frac{2}{r} (\theta_r^r - \theta_\varphi^\varphi) \right] = 0. \quad (2.12)$$

This equation is a linear combination of (2.3) and (2.5), as commonly happens in perfect fluid solutions of Einstein equations.

As this point let us remark the appearance of the anisotropy: there is not an *a priori* restriction for the components of  $\theta_{\mu\nu}$ ; however, if  $\theta_r^r \neq \theta_\varphi^\varphi$  when solving the equation

system (2.3)–(2.5), we will be in the presence of the pressure anisotropy

$$\Pi \equiv \tilde{p}_t - \tilde{p}_r = \alpha (\theta_r^r - \theta_\varphi^\varphi). \quad (2.13)$$

Therefore, an isotropic stellar distribution (perfect fluid) becomes anisotropic when the  $\theta$ -term is turned on. In these lines we will follow a different approach to tackle the equation system (2.3)–(2.5); we will address this system by means of the MGD method. This theory decouples the Einstein field equations when deforming the metric of the corresponding GR solution [17, 18, 68, 69].

## 2.2 Minimal geometric deformation approach

With the aim of approaching the system of equations (2.3)–(2.5) in an alternative manner, a briefly review on the MGD procedure will be presented. This method produces anisotropic corrections to standard GR solutions providing physically admissible non-uniform and spherically symmetric stellar distributions. The input (seed) is a known solution of Einstein equations: for instance the thermodynamic parameters satisfying (2.8), and the corresponding geometric functions  $\lambda(r)$  and  $\nu(r)$ . When a perfect fluid solution is taken as a seed, the isotropic condition  $p_r = p_t = p$  is automatically accomplished. The method will produce a drift in the effective pressures such that  $\tilde{p}_r \neq \tilde{p}_t$ . For doing so, one implements the most generic *minimal geometric deformation* over the metric without breaking the spherical symmetry of the initial solution; this is

$$e^{+\nu(r)} \rightarrow e^{\nu(r)} + \alpha e^*(r), \quad (2.14)$$

$$e^{-\lambda(r)} \rightarrow \mu(r) + \alpha f^*(r), \quad (2.15)$$

with  $e$  and  $f$  generic functions parametrizing the metric deformation. In Figure 2.1 a schematic picture exemplifies how this method extends GR solutions to anisotropic domains when releasing  $\alpha$ . Even though the theory does not impose limits for the coupling strength, the physical acceptability of the new solution does so; if  $\alpha$  is increased, the anisotropies become at some point unstable.

Although nothing prevent us from deforming the temporal component of the metric, it is general enough to start setting  $e^* = 0$ ; hence the effects of the  $\theta_{\mu\nu}$  source undergo in a deformation over the radial coordinate only. The peculiarity of the MGD method is that it

entails in its formulation a decoupling of the equations of motion. As a consequence of taking the  $\theta$ -sector as responsible of the *minimal distortion* of the metric, the system of equations (2.3)–(2.5) results quasi-decoupled: we obtain the Einstein equations for the chosen perfect fluid; and an effective ‘pseudo-Einstein’ system of equations governing the  $\theta$ -sector. The only parameter that connects the two sectors is the temporal geometric function  $\nu(r)$ . At the same order as before, the temporal, radial and angular equations of motion relating the geometry of the spacetime to the thermodynamic characteristic of the perfect fluid sector reduce to

$$\kappa \rho = \frac{1}{r^2} - \frac{\mu}{r^2} - \frac{\mu'}{r}, \quad (2.16)$$

$$-\kappa p = \frac{1}{r^2} - \mu \left( \frac{1}{r^2} + \frac{\nu'}{r} \right), \quad (2.17)$$

$$-\kappa p = -\frac{1}{4} \left[ \mu \left( 2\nu'' + \nu'^2 + 2\frac{\nu'}{r} \right) + \mu' \left( \nu' + \frac{2}{r} \right) \right]. \quad (2.18)$$

The definition of a perfect fluid entails in itself the covariant conservation of the stress-energy tensor, i.e.

$$\nabla^\nu T_{\mu\nu}^{(PF)} = 0. \quad (2.19)$$

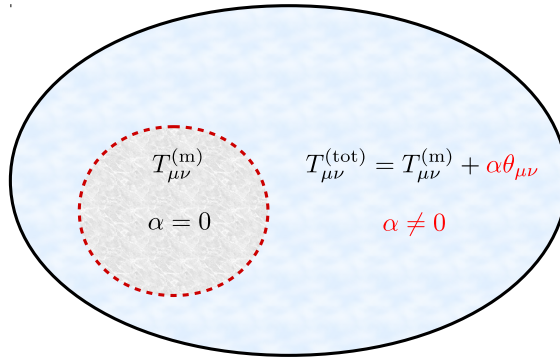


**Figure 2.1:** Any perfect fluid solution can be extended via the MGD approach [18]. When  $\alpha = 0$  we are in the space of isotropic solution of Einstein equations, delimited by the red dashed line.

This solution has a smooth extension to the anisotropic domain releasing the  $\alpha$  to be nonnull.

The resulting equation is again a linear combination of the temporal and angular equations, (2.16) and (2.18), and yields

$$p' + \frac{1}{2}\nu'(\rho + p) = 0. \quad (2.20)$$

It is worth noting that this system of equations is equivalent to Eqs. (2.3)–(2.5) if the coupling between the two sectors is set to zero; that is if the anisotropic sector vanishes.

The temporal component of the metric must satisfy binding conditions in the anisotropic sector: these are the remaining ‘pseudo–Einstein’ field equations for the  $\theta$ –sector

$$\kappa \theta_t^t = -\frac{f^*}{r^2} - \frac{f^{*'}}{r}, \quad (2.21)$$

$$\kappa \theta_r^r = -f^* \left( \frac{1}{r^2} + \frac{\nu'}{r} \right), \quad (2.22)$$

$$\kappa \theta_\varphi^\varphi = -\frac{1}{4} \left[ f^* \left( 2\nu'' + \nu'^2 + \frac{2}{r}\nu' \right) + f^{*'} \left( \nu' + \frac{2}{r} \right) \right]. \quad (2.23)$$

Once again, one has the corresponding conservation equation that is a consequence of (2.6) and (2.19) being satisfied separately. This equation is

$$\nabla^\nu \theta_{\mu\nu} = 0, \quad (2.24)$$

and it is explicitly written as

$$(\theta_t^t)' - \frac{1}{2}\nu'(\theta_t^t - \theta_r^r) + \frac{2}{r}(\theta_r^r - \theta_\varphi^\varphi) = 0. \quad (2.25)$$

This time the latter equation is not necessary linearly dependent of the ‘pseudo–Einstein’ equations, and there is no reason why it should be. At this point it makes explicit that the interaction between the two sectors is purely gravitational; that is, from (2.19) and (2.24) is clear that each sector is separately conserved and there is no exchange of energy-momentum between them.

To conclude this section, let us summarize. First we started with an indeterminate system of equations (2.3)–(2.5). Then, we performed a linear mapping of the radial geometric function of the metric (2.15) that results in a ‘decoupling’ of the Einstein field equations. We ended with two sets of equations: a perfect fluid sector  $\{\rho; p; \nu; \mu\}$ , given by (2.16)–(2.20) where everything is known once a perfect solution of GR is chosen; and a simpler

sector of three linearly independent equations that can be chosen from (2.21) to (2.25), for determining four unknown functions  $\{f^*; \theta_t^t; \theta_r^r; \theta_\varphi^\varphi\}$ . Once the second sector is solved, we can identify directly the effective physical quantities introduced in (2.9), (2.10) and (2.11). At this point, is mandatory to recall that the underlying anisotropic effect which appears as a consequence of breaking the isotropic condition over the effective pressures,  $\tilde{p}_t \neq \tilde{p}_r$ , causes the appearance of the anisotropy  $\Pi(\alpha; r)$  defined in Eq. (2.13).

## 2.3 Anisotropic Durgapal-Fuloria compact star

Let us proceed now to apply the MGD method with the aim of solving the Einstein field equations for the interior of anisotropic superdense stars. In the present work we will take as a seed the well-known Durgapal-Fuloria solution  $\{\nu; \mu; \rho; p\}$  modeling compact stars. As explained before, once the MGD method is applied the system of equations (2.3)–(2.5) is decoupled. Half of the decoupled equations (2.16)–(2.18) are already solved once the relativistic perfect fluid is chosen. For instance, the thermodynamic functions that characterize the Durgapal-Fuloria solution are

$$\rho(r) = \frac{C(9 + 2Cr^2 + C^2r^4)}{7\pi(1 + Cr^2)^3}, \quad (2.26)$$

$$p(r) = \frac{2C(2 - 7Cr^2 - C^2r^4)}{7\pi(1 + Cr^2)^3}, \quad (2.27)$$

with  $C$  an integration constant. The gravitational mass of a sphere of radius  $r$  is obtained integrating the density inside the corresponding volume; in spherical coordinates is

$$m(r) = \int_V \rho dV = \frac{4Cr^3(3 + Cr^2)}{7(1 + Cr^2)^2}. \quad (2.28)$$

This mass function has a well defined behaviour, vanishing at the center of the compact object, i.e.  $m(r=0) = 0$ . It also determines the total mass evaluating the mass function at the surface,  $m(r=R) = M$ .

A massive object deforms the surrounding spacetime; the Durgapal-Fuloria solution is defined by the following metric components

$$e^{\nu(r)} = A (1 + Cr^2)^4, \quad (2.29)$$

$$\mu(r) = 1 - \frac{2m}{r}. \quad (2.30)$$

It is a custom in GR to write the radial component of the metric with the so-called *compactness parameter*, given by  $\xi = 2m/r$ . The spacetime results regular everywhere, even at the center where  $e^{\lambda(r=0)} \equiv \mu(r=0) = 1$ ;  $m$  vanishes faster than  $r$  as one can easily check from (2.28) inside (2.30).  $A$  is the second (and last) integration constant to be determined using boundary conditions over the surface  $r = R$ . In the present article the outer metric will be chosen to satisfy the Schwarzschild form—for simplicity, an uncharged compact star. Both constants  $A$  and  $C$  are positive; however they are expected to change as far as anisotropies begin to be considered.

The remaining equations after the decoupling, (2.21) to (2.23), have to be solved if a generic anisotropic self-gravitating system is desired. The system of equation is as explain before underdetermined. A reasonable constrain is needed to close the system, but it is mandatory not to lose the physical acceptability of the solution. These issues will be discussed in what follows when three different anisotropic solutions (of many) are presented.

### 2.3.1 Pressure-like constraint for the anisotropy

In order to close the system of equations (2.21)–(2.23), additional information is needed. For instance, an equation of state for the source  $\theta_{\mu\nu}$  or some physically motivated constrain on  $f^*(r)$ . A first acceptable interior solution is deduced when forcing the associated radial pressure  $\theta_r{}^r$  to mimic a physically acceptable pressure

$$\theta_r{}^r(r) = p(r). \quad (2.31)$$

This means that one simple choice is to require that the stress-energy tensor for the perfect fluid coincides with the anisotropy in that direction. As a consequence of (2.31), the radial Einstein equations for the GR solution (2.17) and the radial ‘pseudo-Einstein’ equation (2.22)



are equal. This gives immediately an expression for the radial component metric deformation

$$f^*(r) = -\mu + \frac{1}{1 + r\nu'} . \quad (2.32)$$

The temporal component of the metric (2.29) remains non-deformed, so  $\nu'$  is computed directly. The resulting deformed component, the radial one in (2.15), then becomes

$$e^{-\lambda(r)} \rightarrow (1 - \alpha)\mu + \alpha \frac{1 + Cr^2}{1 + 9Cr^2} . \quad (2.33)$$

It is explicit that when the  $\alpha \rightarrow 0$  limit is taken, one gets the non-perturbed Durgapal-Fuloria solution; particularly for the radial component of the metric,  $e^{-\lambda(r)} = \mu(r)$ .

With the above considerations, the metric can be written in terms of an effective mass function of the anisotropic sphere given by

$$\tilde{m}(r) = m - \alpha \frac{r f^*}{2} . \quad (2.34)$$

Expressed in this form, it is obtained one branch of MGD metrics that govern anisotropic interiors of GR solutions, whatever the GR solution is chosen. This branch corresponds to the pressure constrain imposed over the radial anisotropy. Therefore, the metric (2.1) is deformed to

$$ds^2 = e^\nu dt^2 - \left(1 - \frac{2\tilde{m}}{r}\right)^{-1} dr^2 - r^2 d\Omega^2 . \quad (2.35)$$

As we have closed the system of equations with the constrain (2.31), we can compute all the effective magnitudes that characterized the fluid; but first, the values of the integration constants  $A$  and  $C$  are needed to be fixed. This will be done by means of consistent matching conditions.

### 2.3.1.1 Matching conditions

A crucial aspect in the study of stellar distributions is the matching conditions at the star surface between the interior and the exterior spacetime geometries [70, 71]. In our case, the interior stellar geometry is given by the MGD metric (2.35); while the outer part is assumed to be empty. Hence for  $r \geq R$  the solution is given by the Schwarzschild vacuum solution.

The continuity of the first fundamental form at the star surface  $\Sigma$  (defined by  $r = R$ ) is given by  $[ds^2]_\Sigma = 0$ . This equation implies the continuity of the metric when crossing the surface and reads for the relevant components ( $tt$  and  $rr$ -components) as

$$g_{tt} \Big|_{r=R^-} = g_{rr}^{-1} \Big|_{r=R^-} = 1 - \frac{2 M_{Schw}}{R^+} . \quad (2.36)$$

The superindices stand for the region from where we approach the surface, either from inside with a minus sign, or from outside using the plus sign.

We must also take into account the Israel-Darmois matching condition at the stellar surface  $\Sigma$  that gives the continuity of the second fundamental form  $[G_{\mu\nu} x^\nu]_\Sigma = 0$ ;  $x^\nu$  is a unit vector. If we make use of the field equations (2.2), the continuity reads as  $[\tilde{T}_{\mu\nu} x^\nu]_\Sigma = 0$ . Using the full stress-energy tensor (2.7) and projecting in the radial direction  $x^r = r$ , is written as  $[(T_{rr}^{(PF)} + \alpha \theta_{rr}) r]_\Sigma = 0$ . This leads to

$$\tilde{p}_r \Big|_{r=R^-} = (p - \alpha \theta_r^r) \Big|_{r=R^-} = 0 ; \quad (2.37)$$

where the effective pressure comes from Eq. (2.10). On the r.h.s. we are in vacuum, hence the pressure must nullify. The equation system has been closed with the constrain (2.31), therefore  $\tilde{p}(R) = 0$  is equivalent to request  $p(R) = 0$  in (2.27). This equivalence makes the constant  $C$  not to vary from the perfect fluid solution once the anisotropies are considered. The value is

$$CR^2 = \frac{-7 + \sqrt{57}}{2} . \quad (2.38)$$

With the constant fixed, we have fully determined the effective radial pressure of the anisotropic Durgapal-Fuloria solution

$$\tilde{p}_r(r; \alpha) = (1 - \alpha) p . \quad (2.39)$$

A natural bound is obtained,  $\alpha < 1$ . In Figure 2.2, it is shown the dependence of the pressure with a dimensionless radial coordinate  $r/R$  for different values of  $\alpha$ . At first sight one can observe that the higher  $\alpha$  is, the smaller the radial pressure becomes. The decreasing of the radial pressure is needed to produce the pressure anisotropy that is reflected in a change over

the tangential pressure along the surface. The expression for the later pressure is written as

$$\tilde{p}_t(r; \alpha) = \tilde{p}_r + \alpha \frac{6 C^2 r^2 (1 + 3 C r^2)}{\pi (1 + C r^2) (1 + 9 C r^2)^2}. \quad (2.40)$$

The pressure (in both directions) must be a decreasing function along the radial coordinate. This condition restricts even more the values of  $\alpha$ ; higher values immediately triggers instabilities. In light of what was written in (2.37), the tangential pressure (2.40) determines another physical constrain for  $\alpha$ : this pressure is meaningful as long as it remains positive everywhere  $\tilde{p}_t(r) > 0$ ; hence, so must be  $\alpha > 0$  to not contradict this statement in the surface where  $\tilde{p}_r(R) = 0$ . From the latter equation, the anisotropy is directly computed; comparing

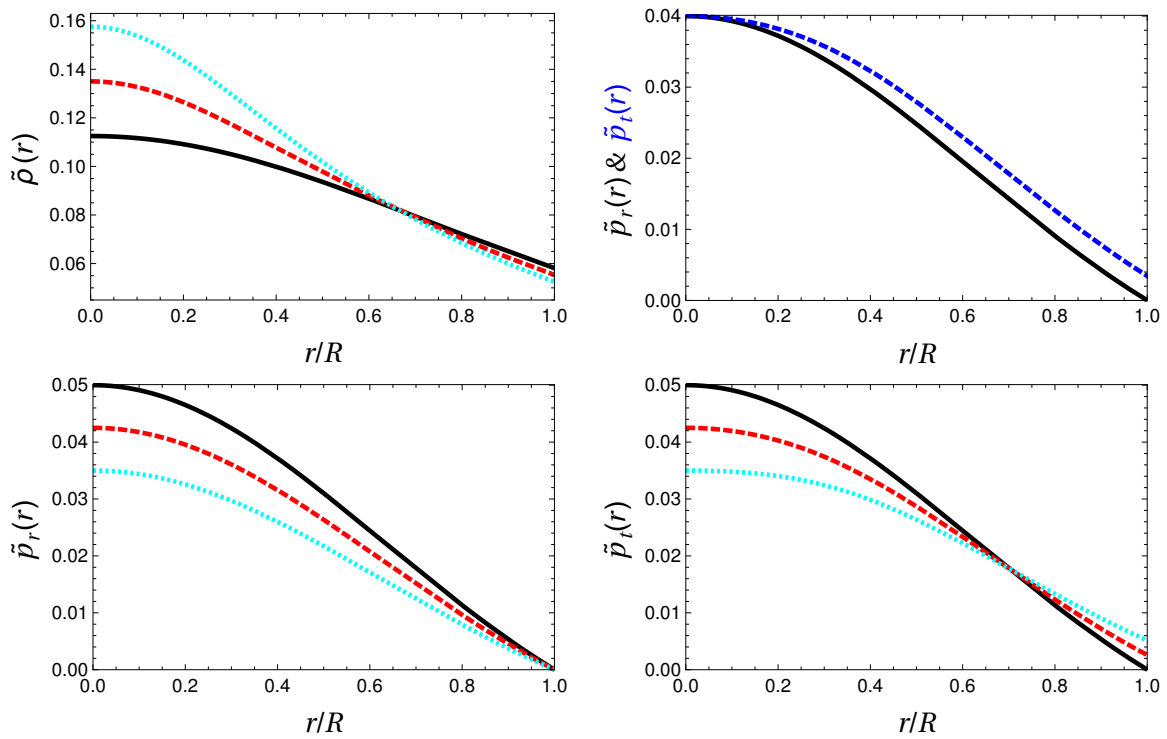


**Figure 2.2:** Effective thermodynamic quantities for different values of  $\alpha$  when the constrain mimics the standard pressure in the radial direction  $\theta_r{}^r = p$ . All curves share the same color code:  $\alpha = 0$  (solid black line) represents the standard Durgapal–Fuloria solution;  $\alpha = 0.15$  (dashed red line) and  $\alpha = 0.3$  (dotted cyan line) represent two anisotropic solutions. The second curve shows a comparison between the radial and transverse pressure ( $\alpha = 0.2$ ). The anisotropy becomes larger when approaching the surface, hence the pressures values drift apart.

with Eq. (2.13), we obtain

$$\Pi(r; \alpha) \equiv \alpha \frac{6 C^2 r^2 (1 + 3 C r^2)}{\pi (1 + C r^2) (1 + 9 C r^2)^2}. \quad (2.41)$$

One can go on computing the remaining thermodynamic parameters. For instance the density can be expressed following (2.9) with the temporal component of the anisotropy given by (2.21)

$$\tilde{\rho}(r; \alpha) = \rho + \alpha \frac{2 C (6 - 18 C r^2 - 257 C^2 r^4 + 15 C^3 r^6 - 9 C^4 r^8)}{7 \pi (1 + C r^2)^3 (1 + 9 C r^2)^2}. \quad (2.42)$$

Some comments are pertinent. The Durgapal-Fuloria solution is a fluid sphere with a solid crust. In Figure 2.2 the density shows a discontinuity in the surface. The anisotropy smoothes this jump; the bigger the parameter  $\alpha$  is, the lower the value of the density on the surface of the star. This behaviour immediately triggers the question on the profile of the effective mass function. This parameter has been defined in (2.34) and together with (2.32), is written as

$$\tilde{m}(r; \alpha) = \left[ 1 + \alpha \frac{2 (2 - 7 C r^2 + C^2 r^4)}{(3 + C r^2)(1 + 9 C r^2)} \right] m(r). \quad (2.43)$$

An observer outside the star, would see a resulting mass  $M_{Schw}$  surrounded by vacuum as it has been requested in (2.36). The continuity of the radial component of the metric (when crossing the star surface  $\Sigma$ ) is direct: (2.35) identifies the Schwarzschild mass seen from outside with the effective mass of our solution ; i.e.  $M_{Schw} \equiv \tilde{m}(R)$ . Even more, a closer look at the mass function shows that the correction  $(\alpha r f^*)/2$  in (2.34) vanishes at the surface  $r = R$ . This means that the effective total mass of the star is the same as the isotropic total standard mass;  $\tilde{m}(R) \equiv m(R)$  from (2.28). This issue is not surprising at all. The anisotropy mimics the radial pressure, hence the radial and tangential pressure start to drift apart in the region close to the solid surface. For this anisotropic behaviour to happen, both pressures must decrease in magnitude at the inner region. Of course this pressure discrepancy with respect to the isotropic solution makes the density to be disturbed. The equilibrium between gravitational collapse and pressure repulsion is modified; hence the mass function is redistributed to the center of the star. Despite this, the total mass of the anisotropic object remains unmodified.

To conclude this section, let us determine the value of the remaining constant  $A$  from (2.36).

The temporal component of the MGD metric (2.29) should match smoothly with the outer Schwarzschild region

$$g_{tt} \Big|_{r=R^-} = A(1 - C r^2) \Big|_{r=R^-} = 1 - \frac{2 M_{Schw}}{R^+}. \quad (2.44)$$

The constant  $A$  remains unchanged. This constant close one branch ( $\alpha$ -dependent) of anisotropic solutions analogous to Durgapal-Fuloria; namely  $\{\nu; \lambda; \tilde{\rho}; \tilde{p}_r; \tilde{p}_t\}$ . Of course, this solution is not unique. Different anisotropic solutions can be obtained starting from the Durgapal-Fuloria solution by means of requiring different constrains when closing the indeterminate system of equations. In next section we will consider a different constrain and we will see that a different anisotropic solution is obtained.

### 2.3.2 Density-like constrain for the anisotropy

Another useful constrain that gives an acceptable physical solution, is to impose that the anisotropy ‘mimics’ a density. This requirement is written as

$$\theta_t^t(r) \equiv \rho(r) \quad (2.45)$$

and closes the system of equations (2.21)–(2.23). The consequence of this ansatz is direct, the temporal Einstein equation for the perfect fluid (2.16) is identical to the temporal equation of motion for the  $\theta_{\mu\nu}$ -tensor (2.21). Equaling both equations, one notes immediately that the resulting equation has a total derivative structure. The integration is straightforward

$$r(1 - \mu + f^*) = K \quad \implies \quad f^*(r) = \mu - 1 \quad (2.46)$$

where  $K = 0$  must be imposed for the invariants  $R$ ,  $R_{\mu\nu}R^{\mu\nu}$  and  $R_{\mu\nu\gamma\sigma}R^{\mu\nu\gamma\sigma}$  to remain smooth and finite all over the inner region. Note that with this constraint the radial deformation is again totally determined by the solution of the perfect fluid. Eventually, one computes the relevant component of the metric; the minimally deformed component is written as in (2.15) (naming  $\beta$  to the coupling between sectors) as

$$e^{-\lambda(r)} \rightarrow (1 + \beta)\mu - \beta \equiv \mu - \beta \frac{8Cr^2(3 + Cr^2)}{7(1 + Cr^2)^2}. \quad (2.47)$$

We can write the metric with the structure used in (2.35). The effective mass is written as a minimal deviation from the GR mass  $m(r)$  presented in (2.28)

$$\tilde{m}(r) = m + \beta \frac{\kappa}{2} \int \rho r^2 dr = (1 + \beta) m. \quad (2.48)$$

In the latter equality, if we make use of spherical coordinates and the corresponding relations, we have  $\int \rho r^2 dr = m/\Omega_4$ ; where the 4-dimensional solid angle is  $\Omega_4 = \iint d\Omega$  and  $2\Omega_4/\kappa = 1$ . Of course, this is not surprising at all, the constrain for the anisotropy is to mimic the density, therefore the effective mass mimics the mass being proportional one to the other (unlike the previous case where the mass is exactly the same with respect to the standard GR solution).

Once the system is closed and the minimal deformation obtained, the remaining magnitudes are easily derived. As before this will be done by means of the smooth matching between the inner and outer region of the star.

### 2.3.2.1 Matching conditions

Here we will reproduce the same steps that we have done before in order to find the constants  $A$  and  $C$ ; this time for the density ansatz (2.45). It is already known that the constant  $C$  is determined by the second fundamental form (2.37). Its value is

$$CR^2 = \frac{-7(1 + 2\beta) + \sqrt{(57 + 169\beta)(1 + \beta)}}{2 + 9\beta}. \quad (2.49)$$

In this case, the anisotropic sector has an influence on the integration constant. It is explicitly seen that in the limit of no coupling  $\beta \rightarrow 0$  the constant from Durgapal-Fuloria is recovered.

Because of the ansatz where it has been required for the anisotropy to mimic the density, the effective value of the density is modified

$$\tilde{\rho}(r; \beta) = (1 + \beta) \rho. \quad (2.50)$$

This is in complete accordance with the changes experienced by the mass. In what follows we will show that this solution only admits a *minimal geometric deformation* over the metric in only one ‘direction’; the ‘direction’ to where the density and the mass is increase. The anisotropies restricted to the present constrain change the integration constants; for instance

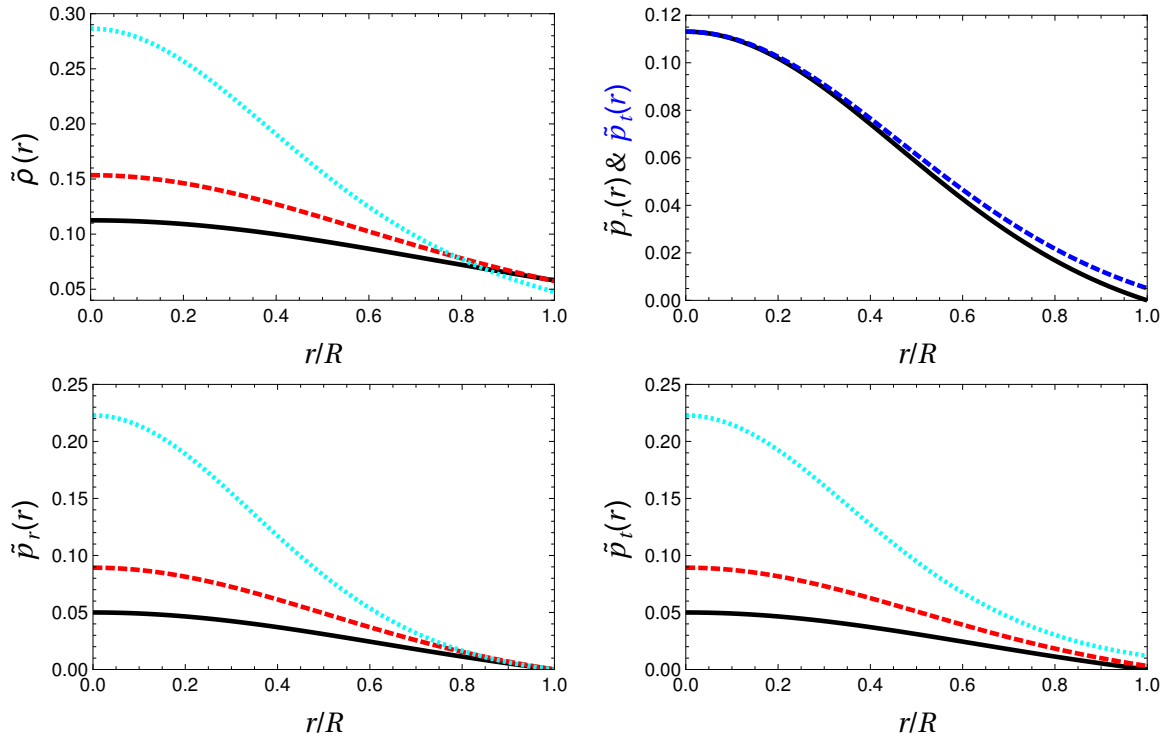


**Figure 2.3:** Effective thermodynamic quantities for different values of  $\beta$  when the anisotropy is forced to act as a density,  $\theta_t^t = \rho$ . The standard Durgapal-Fuloria solution has  $\beta = 0$  (solid black line);  $\beta = -0.16$  (dashed red line) and  $\beta = -0.32$  (dotted cyan line) represent two anisotropic solutions. The second set of curves shows the anisotropy over the pressure,  $\tilde{p}_r \neq \tilde{p}_t$  for  $\beta = -0.2$ .

$C$  is  $\beta$  dependent. An analysis over Eq. (2.49) shows that  $C$  increases when  $\beta$  becomes more negative. This behaviour makes Eqs. (2.48) and (2.50) to increase when  $\beta$  increases in modulus. Of course, both parameters can not increase without a limit; as in the previous case, anisotropies develop instabilities. In the first curve of Figure 2.3 it is seen how the density function increases in the inner region, while it slightly decreases its value over the surface's surroundings softening the crust. The mass function rises throughout the interior and the total effective mass is also increased.

The remaining thermodynamic parameters are the effective radial pressure

$$\tilde{p}_r(r; \beta) = p - \beta \frac{C(3 + Cr^2)(1 + 9Cr^2)}{7\pi(1 + Cr^2)^3} \quad (2.51)$$

and the effective tangential pressure

$$\tilde{p}_t(r; \beta) = \tilde{p}_r - \beta \frac{C^2 r^2}{\pi(1 + Cr^2)^2}. \quad (2.52)$$

As can be seen in the second graph of Figure 2.3, being the latter pressure different from the former, the anisotropy is developed. In the third and fourth set of curves, it is seen that both pressures are enhanced for the anisotropy to take place. When the mass increases, the enhancement of the density requires higher pressures for stability reasons.

In order to get some insight in the underlying sign for  $\beta$  in the new solution, we will focus ourselves in the anisotropy, given by

$$\Pi(r; \beta) = -\beta \frac{C^2 r^2}{\pi(1 + Cr^2)^2}. \quad (2.53)$$

It is worth to note that this magnitude can not be negative (let us remind that  $C > 0$ ) because if this were so, over the surface of the star where  $\tilde{p}_r(R) = 0$ , we would have a negative tangential pressure  $\tilde{p}_t(R) < 0$  which is not physically acceptable. Therefore, positive pressures implies negative values for  $\beta$ . Now we have a physical domain for  $\beta$ . The constant  $A$  is found in an analogous manner than in the previous section, i.e. by means of Eq. (2.44). The value of this constant changes with  $\beta$ . The usual constant of Durgapal-Fuloria is recovered in the limit of  $\beta \rightarrow 0$  as it should be.

### 2.3.3 On the detectability and observational differences for anisotropic distributions

One of the many remarkable predictions of the theory of general relativity is the time dilation within a gravitational well. This results in footprints in the lines of the spectrum shifting towards the red. Although it is a useful quantity, particularly for astronomers, which allows to get some insight into compact stars physics, this effect is extremely difficult to deal with because of its complexity to be disentangle from the displacements and alterations due to various causes such as the Doppler, Zeeman and pressure effects among others. Theoretical derivations states that the redshift factor associated to a star comes when relating the proper time  $\tau$  of the object with the observer clock  $t$ . This relation is given by the standard formula  $d\tau^2 = g_{tt} dt^2$  that yields the following for the surface redshift

$$1 + z = \frac{\nu_e}{\nu_o} = \frac{1}{\sqrt{g_{tt}(R)}}. \quad (2.54)$$

Therefore the relation between the emitted and observed frequency makes the redshift manifest [72].



Over the years, the study of anisotropies in compact objects has received considerable attention and this parameter is a simple way to contrast theory with observations. Formula (2.54) relates the measured redshift with the *compactness parameter*  $\xi = 2m/r$  of the star (that depends on the anisotropic coupling in this case  $\alpha/\beta$ ) introduced after Eq. (2.29). An observer outside would see the Schwarzschild metric, hence the redshift, that depends on  $\xi$ , is directly related with the total mass of the star (we are generating anisotropic contributions over fixed radius stars). Now, we want to investigate how this parameter evolve in our particular solutions.

Let us start with the first solution derived in Section 2.3.1. The interest should focus in the mass function (2.43) evaluated over the surface. As we have explained after this equation the Schwarzschild mass remains unmodified with respect to the Durgapal-Fuloria mass,  $M_{Schw} \equiv \tilde{m}(R) = m^{(DF)}(R)$ . Hence, there is no observational evidence to differentiate an isotropic star from these anisotropic counterpart.

On the contrary, things change in the second case. The solution obtained in Section 2.3.1 is based on an increment of the total mass. Then a shift occurs when observing this anisotropic configuration

$$z(\beta) = \left[ 1 - \frac{2M_{Schw}(\beta)}{R} \right]^{-1/2} - 1. \quad (2.55)$$

The Schwarzschild mass coincides with the mass function over the surface; i.e.  $M_{Schw} = \tilde{m}(R)$  in Eq. (2.48). As it has been explained, the mass increases when  $\beta$  increases in modulus. Therefore, the compactness parameter is also increased; the star becomes more and more denser with  $\beta$ . Then, the parenthesis in (2.55) decrease and  $z(\beta)$  grows when  $|\beta|$  grows. This means that these anisotropic contributions increases the gravitational redshift as it is expected when the stars are more dense.

## 2.4 Anisotropizing an anisotropic Durgapal-Fuloria star

In section 2.2, we present a method to generate different anisotropic solutions of Einstein field equations using any well known perfect fluid as a seed. After this, we apply this prescription to the Durgapal-Fuloria perfect sphere. In section 2.3, with some reasonable constrains we found two novel physical anisotropic solutions analogous to the Durgapal-Fuloria compact star.

The decomposition of Einstein equations (2.3)–(2.5) stem on the minimal geometric deformation (2.15); the anisotropic sector (2.21)–(2.23) is decoupled with respect to any perfect fluid sector (2.16)–(2.18). However, there is no need for the known sector to be a perfect fluid solution exclusively. Whatever solution of Einstein field equations, either a perfect or an anisotropic fluid, work as a seed for implementing the MGD decomposition. For instance, we can take any of the two previous found solutions; e.g. the one obtained in section 2.3.1 given by  $\{\nu; \tilde{\mu}; \tilde{p}_r; \tilde{p}_t\}$ . So as not to obscure how the method works, we will *minimally deform* the anisotropic solution along the radial component of the metric. While the temporal geometric function in Eq. (2.29) remains unchanged, the minimal distortion takes place only over the radial component

$$e^{-\tilde{\lambda}(r)} \rightarrow e^{-\bar{\lambda}(r)} = \tilde{\mu}(r) + \beta g^*(r). \quad (2.56)$$

of an anisotropic metric solution of Einstein equation; in this case (2.35). This deformation is caused by new generic sources of anisotropies (called  $\psi_{\mu\nu}$  in order to avoid confusion with the deformed seed by  $\theta_{\mu\nu}$ ) that acts over the anisotropic energy momentum tensor (2.7)

$$\bar{T}_{\mu\nu} = \tilde{T}_{\mu\nu} + \beta \psi_{\mu\nu}. \quad (2.57)$$

The Einstein field equations connecting the latter effective stress-energy tensor to the space-time curvature are

$$\kappa \bar{\rho} = \frac{1}{r^2} - e^{-\bar{\lambda}} \left( \frac{1}{r^2} - \frac{\bar{\lambda}'}{r} \right), \quad (2.58)$$

$$-\kappa \bar{p}_r = \frac{1}{r^2} - e^{-\bar{\lambda}} \left( \frac{1}{r^2} + \frac{\nu'}{r} \right), \quad (2.59)$$

$$-\kappa \bar{p}_t = -\frac{1}{4} e^{-\bar{\lambda}} \left( 2\nu'' + \nu'^2 - \bar{\lambda}'\nu' + 2\frac{\nu' - \bar{\lambda}'}{r} \right). \quad (2.60)$$

The *minimal geometric deformation* (2.56) decouples the two anisotropic sectors. On the one hand, the seed sector characterized by the density given by (2.42), the radial pressure  $\tilde{p}_r$  (2.39) and the tangential anisotropic pressure  $\tilde{p}_t$  obtained in (2.40). This parameters solve

the already known equation system

$$\kappa \tilde{\rho} = \frac{1}{r^2} - \frac{\tilde{\mu}}{r^2} - \frac{\tilde{\mu}'}{r}, \quad (2.61)$$

$$-\kappa \tilde{p}_r = \frac{1}{r^2} - \tilde{\mu} \left( \frac{1}{r^2} + \frac{\nu'}{r} \right), \quad (2.62)$$

$$-\kappa \tilde{p}_t = -\frac{1}{4} \left[ \tilde{\mu} \left( 2\nu'' + \nu'^2 + 2\frac{\nu'}{r} \right) + \tilde{\mu}' \left( \nu' + \frac{2}{r} \right) \right]; \quad (2.63)$$

and on the other hand, we are left with the new anisotropic sector for  $\psi_{\mu\nu}$  completely decoupled. In this sector we have the following ‘pseudo-Einstein’ equations

$$\kappa \psi_t^t = -\frac{g^*(r)}{r^2} - \frac{g^{*'}(r)}{r}, \quad (2.64)$$

$$\kappa \psi_r^r = -g^* \left( \frac{1}{r^2} + \frac{\nu'}{r} \right), \quad (2.65)$$

$$\kappa \psi_\varphi^\varphi = -\frac{1}{4} \left[ g^* \left( 2\nu'' + \nu'^2 + \frac{2}{r} \nu' \right) + g^{*'} \left( \nu' + \frac{2}{r} \right) \right]. \quad (2.66)$$

Subsequently, a constrain over the solution must be imposed; the system is indeterminate. Until now we used a constrain that mimics the pressure to obtain the seed solution; a density constrain will be applied now to combine both previously found solutions. The ansatz then is to require

$$\psi_t^t \equiv \tilde{\rho}(r). \quad (2.67)$$

Now the steps that follow are known. Eqs. (2.61) and (2.64) equals and give a total derivative equivalent to (2.46). The solution for the second minimal deformation function is straightforward because the constant of integration is again null

$$g^* = \tilde{\mu} - 1. \quad (2.68)$$

The radial metric component from (2.56) then promotes to

$$e^{-\bar{\lambda}(r)} = (1 - \alpha)(1 + \beta)\mu + \frac{\alpha(1 + \beta)}{1 + r\nu'} - \beta; \quad (2.69)$$

where the anisotropic radial component of the metric (2.33) has been used.

The effective radial pressure  $\bar{p}_r = \tilde{p}_r - \beta\psi_r{}^r$  is computed from (2.59)

$$\bar{p}_r(r; \alpha, \beta) = [1 - \alpha(1 + \beta)]p - \beta \frac{C(3 + Cr^2)(1 + 9Cr^2)}{7\pi(1 + Cr^2)^3}. \quad (2.70)$$

The first integration constant  $C$  is obtain by means of the continuity of the second fundamental form, analogous condition to (2.37). Imposing the annulment of the latter effective radial pressure at the surface  $\Sigma$ , we get

$$CR^2 = \frac{-7[1 - \alpha + \beta(2 - \alpha)] + \sqrt{[57(1 - \alpha) + \beta(169 - 57\alpha)](1 - \alpha)(1 + \beta)}}{2(1 - \alpha) + \beta(9 - 2\alpha)}. \quad (2.71)$$

Both the integration constant  $C$  as well as the effective pressure  $\bar{p}_r$  recover the corresponding values: (2.38) and (2.39) in the limit of  $\beta \rightarrow 0$  or (2.49) and (2.51) when  $\alpha \rightarrow 0$ . Besides, this constant is required to plot the thermodynamic parameters.

In Figure 2.4 we present the corresponding evolution of the parameters of the theory: for a comparison, we include also the Durgapal–Fuloria isotropic solution ( $\alpha = \beta = 0$  in solid line). If for instance, one of the couplings move away from zero but the other remains null, the thermodynamic quantities behave as in Figures 2.2 (if  $\alpha \neq 0$ ) or 2.3 (if  $\beta \neq 0$ ), as it is expected. After this, we plot the anisotropic seed to be *minimally deformed* by fixing the coupling  $\alpha$  (red dashed-line). Finally,  $\beta$  drifts away the parameters again. We choose one smaller order of magnitude for the second deformation to make notorious the effect over the seed solution. An important statement is that as the seed is anisotropic and the corresponding tangential pressure is nonnull over the surface, then there is no restriction for

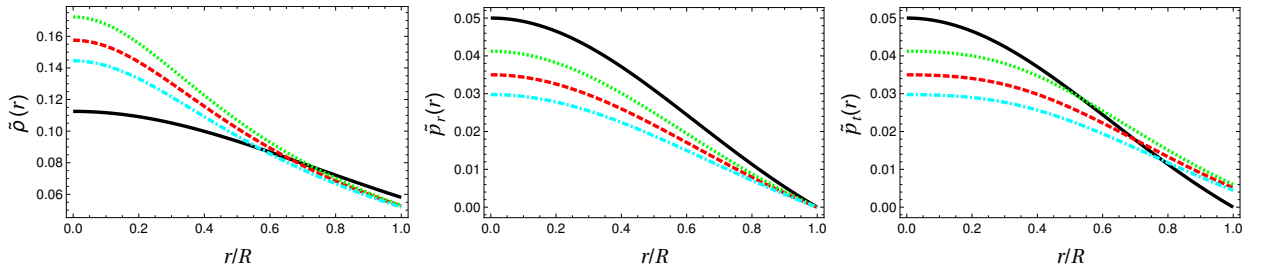


**Figure 2.4:** Effective thermodynamic quantities for different values of the parameters  $\{\alpha, \beta\}$ . The solid black line represents the standard Durgapal–Fuloria solution ( $\alpha = \beta = 0$ ). The dashed red line is the anisotropic solution used as a seed  $\{\alpha = 0.3, \beta = 0\}$ . This configuration is *minimally deformed* by a  $\psi$ -sector. Two different solutions are presented: dotted green line for  $\{\alpha = 0.3, \beta = 0.03\}$  and the dotted-dashed cyan line for  $\{\alpha = 0.3, \beta = -0.03\}$ .

$\beta$  to be negative.  $\beta$  is allowed to be positive until either it decrease the tangential pressure until it becomes null, or the anisotropy becomes unstable.

Lest we forget, we include the expression of the two remaining parameters: first the effective density  $\bar{\rho} = \tilde{\rho} + \beta\psi_t^t$ , whose structure is analogous to (2.50),

$$\bar{\rho}(r; \alpha, \beta) = (1 + \beta)\tilde{\rho} \quad (2.72)$$

with  $\tilde{\rho}$  the seed density (2.42). And secondly, the anisotropic tangential pressure  $\bar{p}_t = \tilde{p}_t - \beta\psi_\varphi^\varphi$  that can be written as

$$\bar{p}_t(r; \alpha, \beta) = \bar{p}_r(r; \alpha, \beta) + \Pi(r; \alpha, \beta). \quad (2.73)$$

The anisotropy is now written as

$$\Pi(r; \alpha, \beta) = -\beta \frac{C^2 r^2}{\pi(1 + Cr^2)^2} + (1 + \beta)\alpha \frac{6C^2 r^2(1 + 3Cr^2)}{\pi(1 + Cr^2)(1 + 9Cr^2)^2}. \quad (2.74)$$

It is important to remark that in all expressions we recover both previous limits when either  $\alpha$  or  $\beta$  are set to zero, and the standard Durgapal-Fuloria solution for  $\alpha = \beta = 0$ . Let us conclude presenting the profile of the anisotropy over the surface  $\Sigma$  of the sphere. In Figure 2.5, we plot the function  $\Pi$  from Eq. (2.74) versus the couplings  $\alpha$  and  $\beta$ . Nearby  $\alpha$  closer to zero and  $\beta$  positive, the anisotropy becomes unphysical ( $\Pi < 0$ ); thus deformations with this parameters are prohibited and excluded from the physical surface. In particular this procedure extends the range of physical values for  $\beta$ . Each time  $\alpha$  grows, new possible values of  $\beta > 0$  are released.

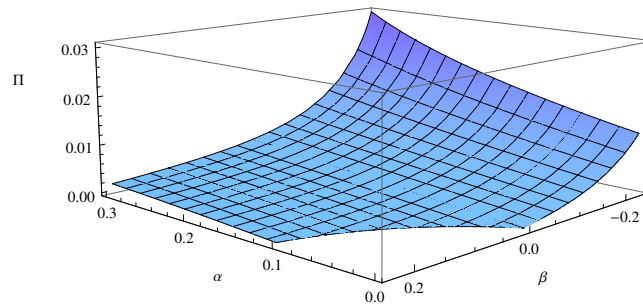


**Figure 2.5:** The figure illustrate the anisotropy  $\Pi$  as a function of the couplings  $\{\alpha, \beta\}$  evaluated at the star's surface  $\Sigma$ . The region where  $\alpha < 0.1$  and  $\beta > 0$ , the anisotropy is unphysical.

Besides should be noted that the anisotropy can be interpreted as a lineal combination of the first two cases studied

$$\Pi(r; \alpha, \beta) = \Pi(r; \beta) + (1 + \beta)\Pi(r; \alpha); \quad (2.75)$$

Each single parameter anisotropy have been computed in (2.41) and (2.53). In this case, the resulting  $\Pi(\alpha, \beta)$  no longer coincides with  $\beta(\psi_r^r - \psi_t^t)$  as mentioned in (2.13), because the seed is no more an isotropic fluid. Immediately, the linearity is translated to the stress-energy tensor; the components of the new  $\psi$ -sector can be written as a combination of the single *minimal geometric deformations* computed in Section 2.3

$$\psi_{\mu\nu} = \theta_{\mu\nu}^{(density)} + \alpha \theta_{\mu\nu}^{(pressure)}. \quad (2.76)$$

making the ‘additive’ character of the method manifest. If one starts with any perfect solution of GR,  $T_{\mu\nu}^{(PF)}$ , a *minimal deformation* induced by an anisotropy subjected to a pressure structure, makes the stress energy tensor to become  $\tilde{T}_{\mu\nu} = T_{\mu\nu}^{(PF)} + \alpha \theta_{\mu\nu}^{(pressure)}$ . After this, a second *minimal deformation* acts over the already anisotropic solution, but now subjected to a density constrain. The new contribution is given by (2.76), therefore the effective energy-momentum tensor (2.57) is decomposed as

$$\bar{T}_{\mu\nu} = T_{\mu\nu}^{(PF)} + \alpha \theta_{\mu\nu}^{(pressure)} + \beta [\theta_{\mu\nu}^{(density)} + \alpha \theta_{\mu\nu}^{(pressure)}]. \quad (2.77)$$

This expression states the noncommutative structure of the MGD-decoupling method; the order in which the deformations take place matters. For instance, if we take as a seed the solution found in Section 2.3.2 where the deformation obeys a density-like constrain, and then we deform the anisotropic solution with a different constrain analogous to (2.31), the noncommutative character of the theory becomes manifest. The equations (2.75) and (2.76) change their form and become

$$\begin{aligned} \Pi(r; \beta, \alpha) &= \Pi(r; \alpha) + (1 - \alpha)\Pi(r; \beta), \\ \psi_{\mu\nu} &= \theta_{\mu\nu}^{(pressure)} - \beta \theta_{\mu\nu}^{(density)}; \end{aligned} \quad (2.78)$$

respectively. Likewise, the effective energy-momentum tensor (2.77) becomes

$$\bar{T}_{\mu\nu} = T_{\mu\nu}^{(PF)} + \beta \theta_{\mu\nu}^{(density)} + \alpha [\theta_{\mu\nu}^{(pressure)} - \beta \theta_{\mu\nu}^{(density)}] \quad (2.79)$$

when the order of the two anisotropizations is reversed. The reason of the noncommutativity is that the coefficients involved in the linear combinations of the components of the anisotropic tensor  $\theta_{\mu\nu}$  depends explicitly on the coupling constants. This is not surprising at all; we are dealing with nonlinear differential equations. The commutativity is likely to be lost in this kind of systems.

From a perturbation theory point of view, one can think that the deformations over the metric (*zero* order) is due to the existence of the anisotropic term which acts at  $\mathcal{O}(\alpha)$ ; being  $\alpha$  the coupling strength to the anisotropies. We must emphasize that, although the MGD approach seems like a perturbation technique, the method, in fact, is not, and this is easily visualized by noticing that the couplings do not necessarily have to be small, which is a crucial ingredient in perturbation theories. The deformation being a perturbation is just a well behaved limit of the theory, and means that we can softly deform the seed configuration. Being the theory noncommutative, successive and mixed perturbative deformations give different configurations depending on the order in which each of them are implemented. This provides infinite manners of deforming realistic configurations controlling rigorously the physical acceptability of the resulting anisotropic distribution.

## 2.5 Conclusions

In this work we have presented different branches of solutions that determines non-rotating and uncharged anisotropic superdense stars. Each branch opens a possibility for new physically acceptable anisotropic configuration for these objects. They were obtained by guided deformations using as a starting point the isotropic Durgapal-Fuloria model for compact stars, and exemplify some possible anisotropic distributions among the many that the MGD-method generates. This prescription has been design to decouple the field equations of static and spherically symmetric self-gravitating systems. It associates the anisotropic sector with a deformation over the geometric potentials. Hence, after the decoupling, one obtains a sector which solution is already known (seed sector) and the anisotropic sector which obeys a set of simpler ‘pseudo-Einstein’ equations associated to the metric deformation. It is worth to note that the *minimal geometric deformations* stems in an exclusively gravitational interaction between sectors; i.e. there is no exchange of energy-momentum among sectors.

We have then proceed to solve the decoupled anisotropic sector. When the equations are forced to be decoupled, no new information is introduced. Then we have an underdetermined

system of equations; consistent constraints are needed. We have shown how intuitive constraint leads to new physical anisotropic solutions. Variations in the couplings between the seed and the anisotropic sector reveals consistent evolution of the thermodynamical parameter giving to the MGD-method a new proof of validity. We also have discussed the observational features of the anisotropic sectors. When the anisotropy changes the compactness of the star, the observed redshift increases as it is expected. Not all anisotropic contributions have observational effects, because some anisotropies only redistribute the thermodynamical parameters in the interior. However, when the anisotropy tweaks the compactness parameter, the star suffers a redshift. Therefore, observational data would bound the parameters of the model.

After presenting two branches of solutions that provides an infinite number of physical configurations, we have proceeded to deform anisotropic solutions. Any solution of Einstein equation admits a minimal deformation. Different anisotropic sources have additive effect, however these effects are noncommutative. The path to the final configuration matters, and same deformations in reversed order produces different resulting configurations. Hence, the method provides a 'fine-tuning structure' that generates an enormous amount of different physically acceptable anisotropic stars.



# Chapter 3

## Delta Gravity

### 3.1 Definition of Delta Gravity

In this section, we present the action as well all the symmetries of the model and derive the equations of motion.

These approaches are based on the application of a variation called  $\tilde{\delta}$ . And it has the usual properties of a variation such as:

$$\begin{aligned}\tilde{\delta}(AB) &= (\tilde{\delta}A)B + A(\tilde{\delta}B), \\ \tilde{\delta}\delta A &= \delta\tilde{\delta}A, \\ \tilde{\delta}(\Phi_\mu) &= (\tilde{\delta}\Phi)_\mu,\end{aligned}\tag{3.1}$$

where  $\delta$  is another variation. The main point of this variation is that, when it is applied on a field (function, tensor, etc), it produces new elements that we define as  $\tilde{\delta}$  fields, which we treat them as an entirely new independent object from the original,  $\tilde{\Phi} = \tilde{\delta}(\Phi)$ . We use the convention that a tilde tensor is equal to the  $\tilde{\delta}$  transformation of the original tensor when all its indexes are covariant.

Now we will present the  $\tilde{\delta}$  prescription to a general action. The extension of the new symmetry is given by:

$$S_0 = \int d^n x \mathcal{L}_0(\phi, \partial_i \phi) \rightarrow S = \int d^n x (\mathcal{L}_0(\phi, \partial_i \phi) + \tilde{\delta}\mathcal{L}_0(\phi, \partial_i \phi)),\tag{3.2}$$

where  $S_0$  is the original action and  $S$  is the extended action in Delta Gauge Theories. When we apply this formalism to the Einstein-Hilbert action of GR, we get [52]

$$S = \int d^4x \sqrt{-g} \left( \frac{R}{2\kappa} + L_M - \frac{1}{2\kappa} (G^{\alpha\beta} - \kappa T^{\alpha\beta}) \tilde{g}_{\alpha\beta} + \tilde{L}_M \right), \quad (3.3)$$

where  $\kappa = \frac{8\pi G}{c^2}$ ,  $\tilde{g}_{\mu\nu} = \delta g_{\mu\nu}$ ,  $L_M$  is the matter Lagrangian and:

$$T^{\mu\nu} = \frac{2}{\sqrt{-g}} \frac{\delta}{\delta g_{\mu\nu}} [\sqrt{-g} L_M], \quad (3.4)$$

$$\tilde{L}_M = \tilde{\phi}_I \frac{\delta L_M}{\delta \phi_I} + (\partial_\mu \tilde{\phi}_I) \frac{\delta L_M}{\delta (\partial_\mu \phi_I)}, \quad (3.5)$$

with  $\tilde{\phi} = \delta\phi$  are the  $\delta$  matter fields or “delta matter” fields. The equations of motion are given by the variation of  $g_{\mu\nu}$  and  $\tilde{g}_{\mu\nu}$ , it is easy to see that we get the usual Einstein’s equations varying the action (3.3) with respect to  $\tilde{g}_{\mu\nu}$ . By the other hand, variations with respect to  $g_{\mu\nu}$  give the equations for  $\tilde{g}_{\mu\nu}$ :

$$\begin{aligned} F^{(\mu\nu)(\alpha\beta)\rho\lambda} D_\rho D_\lambda \tilde{g}_{\alpha\beta} &+ \frac{1}{2} R^{\alpha\beta} \tilde{g}_{\alpha\beta} g^{\mu\nu} + \frac{1}{2} R \tilde{g}^{\mu\nu} - R^{\mu\alpha} \tilde{g}_\alpha^\nu - R^{\nu\alpha} \tilde{g}_\alpha^\mu + \frac{1}{2} \tilde{g}_\alpha^\alpha G^{\mu\nu} \\ &= \frac{\kappa}{\sqrt{-g}} \frac{\delta}{\delta g_{\mu\nu}} \left[ \sqrt{-g} \left( T^{\alpha\beta} \tilde{g}_{\alpha\beta} + 2\tilde{L}_M \right) \right], \end{aligned} \quad (3.6)$$

with:

$$\begin{aligned} F^{(\mu\nu)(\alpha\beta)\rho\lambda} &= P^{((\rho\mu)(\alpha\beta))} g^{\nu\lambda} + P^{((\rho\nu)(\alpha\beta))} g^{\mu\lambda} - P^{((\mu\nu)(\alpha\beta))} g^{\rho\lambda} - P^{((\rho\lambda)(\alpha\beta))} g^{\mu\nu} \\ P^{((\alpha\beta)(\mu\nu))} &= \frac{1}{4} (g^{\alpha\mu} g^{\beta\nu} + g^{\alpha\nu} g^{\beta\mu} - g^{\alpha\beta} g^{\mu\nu}), \end{aligned} \quad (3.7)$$

where  $(\mu\nu)$  denotes the totally symmetric combination of  $\mu$  and  $\nu$ . It is possible to simplify (3.6) (see [52]) to get the following system of equations:

$$G^{\mu\nu} = \kappa T^{\mu\nu}, \quad (3.8)$$

$$F^{(\mu\nu)(\alpha\beta)\rho\lambda} D_\rho D_\lambda \tilde{g}_{\alpha\beta} + \frac{1}{2} g^{\mu\nu} R^{\alpha\beta} \tilde{g}_{\alpha\beta} - \frac{1}{2} \tilde{g}^{\mu\nu} R = \kappa \tilde{T}^{\mu\nu}, \quad (3.9)$$

where  $\tilde{T}^{\mu\nu} = \tilde{\delta} T^{\mu\nu}$ . Besides, the energy momentum conservation now is given by

$$D_\nu T^{\mu\nu} = 0, \quad (3.10)$$

$$D_\nu \tilde{T}^{\mu\nu} = \frac{1}{2} T^{\alpha\beta} D^\mu \tilde{g}_{\alpha\beta} - \frac{1}{2} T^{\mu\beta} D_\beta \tilde{g}_\alpha^\alpha + D_\beta (\tilde{g}_\alpha^\beta T^{\alpha\mu}). \quad (3.11)$$

Then, we are going to work with equations (3.8), (3.9), (3.10) and (3.11). It is very important to notice that as Einstein's equations (3.8) and (3.10) do not change in this theory, the standard results of GR holds in DG, and they will be important to solve the delta sector (3.9) and (3.11).

## 3.2 Perfect fluid

The derivation of the  $T_{\mu\nu}$  and  $\tilde{T}_{\mu\nu}$  is explained in detail in [53], here we present the final results which will be useful henceforth. In particular,  $u^T$  is related to the new velocity field coming from the new symmetry, however, we have to emphasize that  $\tilde{\delta} u_\alpha \neq u_\alpha^T$ . Also, we have set the speed of light  $c = 1$  and we will explicitly put it back when it needed.

The energy-momentum tensors  $T_{\mu\nu}$  and  $\tilde{T}_{\mu\nu}$  now read

$$T_{\mu\nu} = p(\rho) g_{\mu\nu} + (\rho + p(\rho)) u_\mu u_\nu \quad (3.12)$$

$$\begin{aligned} \tilde{T}_{\mu\nu} = & p(\rho) \tilde{g}_{\mu\nu} + \frac{\partial p}{\partial \rho}(\rho) \tilde{\rho} g_{\mu\nu} + \left( \tilde{\rho} + \frac{\partial p}{\partial \rho}(\rho) \tilde{\rho} \right) u_\mu u_\nu \\ & + (\rho + p(\rho)) \left( \frac{1}{2} (u_\nu u^\alpha \tilde{g}_{\mu\alpha} + u_\mu u^\alpha \tilde{g}_{\nu\alpha}) + u_\mu^T u_\nu + u_\mu u_\nu^T \right). \end{aligned} \quad (3.13)$$

With extended normalization conditions

$$u^\alpha u_\alpha = -1 \quad (3.14)$$

$$u^\alpha u_\alpha^T = 0. \quad (3.15)$$

The condition (3.15) is interesting because will give similar results on the background of DG as when we set a particular gauge condition in the perturbation theory of GR. Nevertheless, we point out that delta sector is not a perturbation of GR sector, it could be understood better as a modification of GR. We will deepen to this point later.

### 3.3 Test Particle

As DG include a new gravitational field, it is necessary to describe the particles trajectories in this new approach, here we will review the trajectory for both massive and massless particles.

#### 3.3.1 Massive Particles

The action for a test particle is given by:

$$S_0[\dot{x}, g] = -m \int dt \sqrt{-g_{\mu\nu} \dot{x}^\mu \dot{x}^\nu}, \quad (3.16)$$

with  $\dot{x}^\mu = \frac{dx^\mu}{dt}$ . This action is invariant under reparametrizations,  $t' = t - \epsilon(t)$ . This means, in the infinitesimal form, that:

$$\delta_R x^\mu = \dot{x}^\mu \epsilon. \quad (3.17)$$

In DG, we have a new test particle action. To obtain this action, we need to evaluate (3.16) in (3.2):

$$S[\dot{x}, y, g, \tilde{g}] = m \int dt \left( \frac{\bar{g}_{\mu\nu} \dot{x}^\mu \dot{x}^\nu + \frac{1}{2}(2g_{\mu\nu} \dot{y}^\mu \dot{x}^\nu + g_{\mu\nu,\rho} y^\rho \dot{x}^\mu \dot{x}^\nu)}{\sqrt{-g_{\alpha\beta} \dot{x}^\alpha \dot{x}^\beta}} \right), \quad (3.18)$$

where  $\bar{g}_{\mu\nu} = g_{\mu\nu} + \frac{1}{2}\tilde{g}_{\mu\nu}$  and  $y^\mu = \tilde{\delta}x^\mu$ . This action is invariant under reparametrization transformations, given by (3.17), plus  $\tilde{\delta}$  reparametrization transformations:

$$\delta_R y^\mu = \dot{y}^\mu \epsilon + \dot{x}^\mu \tilde{\epsilon}. \quad (3.19)$$

The presence of  $y^\mu$  introduce a new system of coordinates. Because we do not want new coordinates, we impose that  $2g_{\mu\nu} \dot{y}^\mu \dot{x}^\nu + g_{\mu\nu,\rho} y^\rho \dot{x}^\mu \dot{x}^\nu = 0$  like a gauge condition on  $\tilde{\delta}$  reparametrization, fixing  $\tilde{\epsilon}$ . With this we eliminate this new symmetry, however the general coordinate transformations as well as time reparametrizations continue to be preserved. Finally, (3.18) is reduced to:

$$S[\dot{x}, g, \tilde{g}] = m \int dt \left( \frac{\bar{g}_{\mu\nu} \dot{x}^\mu \dot{x}^\nu}{\sqrt{-g_{\alpha\beta} \dot{x}^\alpha \dot{x}^\beta}} \right). \quad (3.20)$$

Now, if we vary (3.20) with respect to  $x^\mu$ , we obtain the equation of motion for a massive test particle. That is:

$$\hat{g}_{\mu\nu} \ddot{x}^\nu + \hat{\Gamma}_{\mu\alpha\beta} \dot{x}^\alpha \dot{x}^\beta = \frac{1}{4} \tilde{K}_{,\mu}, \quad (3.21)$$

with:

$$\begin{aligned}
\hat{\Gamma}_{\mu\alpha\beta} &= \frac{1}{2}(\hat{g}_{\mu\alpha,\beta} + \hat{g}_{\beta\mu,\alpha} - \hat{g}_{\alpha\beta,\mu}) \\
\hat{g}_{\alpha\beta} &= \left(1 + \frac{1}{2}\tilde{K}\right) g_{\alpha\beta} + \tilde{g}_{\alpha\beta} \\
\tilde{K} &= \tilde{g}_{\alpha\beta}\dot{x}^\alpha\dot{x}^\beta
\end{aligned}$$

and, if we choose  $t$  equal to the proper time, then  $g_{\mu\nu}\dot{x}^\mu\dot{x}^\nu = -1$ . The equation of motion of a free massive particle is a second-order equation, but there is no longer a geodesic in an effective metric.

### 3.3.2 Massless Particles

When considering massless particles, action (3.16) is useless, because it is null when  $m = 0$ . To solve this problem, it is common to start from the action:

$$S_0[\dot{x}, g, v] = \frac{1}{2} \int dt \left( vm^2 - v^{-1} g_{\mu\nu} \dot{x}^\mu \dot{x}^\nu \right), \quad (3.22)$$

where  $v$  is a Lagrange multiplier. From (3.22), we can obtain the equation of motion for  $v$ :

$$v = -\frac{\sqrt{-g_{\mu\nu}\dot{x}^\mu\dot{x}^\nu}}{m}. \quad (3.23)$$

If we substitute (3.23) in (3.22), we recover (3.16). In other words, (3.22) is a good action that includes the massless case. So, we must substitute (3.22) in (3.2) to obtain the modified test particle action. That is:

$$S[\dot{x}, g, \tilde{g}, v, \tilde{v}] = \frac{1}{2} \int dt \left[ vm^2 - v^{-1} (g_{\mu\nu} + \tilde{g}_{\mu\nu}) \dot{x}^\mu \dot{x}^\nu + \tilde{v} (m^2 + v^{-2} g_{\mu\nu} \dot{x}^\mu \dot{x}^\nu) \right], \quad (3.24)$$

where we must discard  $y^\mu$  for the same reason used in Section 3.3.1. Besides, two Lagrange multiplier are unnecessary, so we will eliminate one of them. The equation of motion for  $\tilde{v}$  is:

$$\tilde{v} = \frac{m^2 + v^{-2} (g_{\mu\nu} + \tilde{g}_{\mu\nu}) \dot{x}^\mu \dot{x}^\nu}{2v^{-3} g_{\alpha\beta} \dot{x}^\alpha \dot{x}^\beta}. \quad (3.25)$$

If we now replace (3.25) in (3.24), we obtain our  $\tilde{\delta}$  Test Particle Action:

$$S[\dot{x}, g, \tilde{g}, v] = \int dt \left( m^2 v - \frac{(g_{\mu\nu} + \tilde{g}_{\mu\nu}) \dot{x}^\mu \dot{x}^\nu}{4v} + \frac{m^2 v^3}{4g_{\alpha\beta} \dot{x}^\alpha \dot{x}^\beta} (m^2 + v^{-2} \tilde{g}_{\mu\nu} \dot{x}^\mu \dot{x}^\nu) \right). \quad (3.26)$$

Therefore, we can use (3.26) to represent the trajectory of a particle in the presence of a gravitational field, given by  $g$  and  $\tilde{g}$ , for the massless and massive case. In the previous section, we have developed the massive case, so we need to study the massless case now. Evaluating  $m = 0$  in (3.22) and (3.26), they are respectively:

$$S_0^{(m=0)}[\dot{x}, g, v] = -\frac{1}{2} \int dt v^{-1} g_{\mu\nu} \dot{x}^\mu \dot{x}^\nu \quad (3.27)$$

$$S^{(m=0)}[\dot{x}, g, \tilde{g}, v] = -\frac{1}{4} \int dt v^{-1} \mathbf{g}_{\mu\nu} \dot{x}^\mu \dot{x}^\nu, \quad (3.28)$$

with  $\mathbf{g}_{\mu\nu} = g_{\mu\nu} + \tilde{g}_{\mu\nu}$ . In the usual and modified case, the equation of motion for  $v$  implies that a massless particle will move in a null-geodesic. In the usual case we have  $g_{\mu\nu} \dot{x}^\mu \dot{x}^\nu = 0$ , but in this model the null-geodesic is  $\mathbf{g}_{\mu\nu} \dot{x}^\mu \dot{x}^\nu = 0$ .

All this means that, in DG, the equation of motion of a free massless particle is given by:

$$\begin{aligned} \mathbf{g}_{\mu\nu} \ddot{x}^\nu + \Gamma_{\mu\alpha\beta} \dot{x}^\alpha \dot{x}^\beta &= 0 \\ \mathbf{g}_{\mu\nu} \dot{x}^\mu \dot{x}^\nu &= 0, \end{aligned} \quad (3.29)$$

with:

$$\Gamma_{\mu\alpha\beta} = \frac{1}{2}(\mathbf{g}_{\mu\alpha,\beta} + \mathbf{g}_{\beta\mu,\alpha} - \mathbf{g}_{\alpha\beta,\mu}).$$

To summarize, we obtained how a test particle moves when it is coupled to  $g_{\mu\nu}$  and  $\tilde{g}_{\mu\nu}$ , given by (3.21) or (3.29) if we have a massive or massless particle respectively. It is important to emphasize that the proper time is given by  $g_{\mu\nu}$ . This will be important when we study the cosmology of DG. Also, we notice the importance of a gauge condition in order to remove new coordinates. This will be the characteristic of this model, because as we will see, in the cosmological case we will need to fix another gauge to reduce the system, this fix will break explicitly the delta symmetry and therefore both sector will evolved independently.

## 3.4 Cosmology in DG

Now we are able to present the solutions and its implications on the Cosmology in DG.

### 3.4.1 Harmonic gauge in an Isotropic and Homogeneous Universe

When we consider an isotropic and homogeneous Universe, the most generic solution in GR is

$$g_{\mu\nu}dx^\mu dx^\nu = -A(t)c^2dt^2 + a^2(t)(dx^2 + dy^2 + dz^2), \quad (3.30)$$

where  $a(t)$  is the scale factor. Usually the function  $A(t)$  is setted to 1, however the reason for this election is just a gauge condition known as the harmonic gauge<sup>1</sup>. That is

$$\Gamma^\mu \equiv g^{\alpha\beta}\Gamma_{\alpha\beta}^\mu = 0. \quad (3.31)$$

---

<sup>1</sup>for more details, see Section 7.4, Chapter 8 and Chapter 9. Gravitation and Cosmology: Principles and Applications of the General Theory of Relativity. Weinberg



Under general coordinate transformation  $x \rightarrow x'$ ,  $\Gamma^\mu$  transform:

$$\Gamma'^\mu = \frac{\partial x'^\mu}{\partial x^\alpha} \Gamma^\alpha - g^{\alpha\beta} \frac{\partial^2 x'^\mu}{\partial x^\alpha \partial x^\beta}.$$

Therefore, if  $\Gamma^\alpha$  does not vanish, we can define a new coordinate system  $x'^\mu$  where  $\Gamma'^\mu = 0$ . So, it is always possible to choose an harmonic coordinate system. When we use (3.31) with the metric (3.30) we obtain  $A(t) = 1$ .

The extension of the harmonic gauge to  $\tilde{g}_{\mu\nu}$  is natural if we consider

$$\tilde{\delta}(\Gamma^\mu) \equiv g^{\alpha\beta} \tilde{\delta}(\Gamma_{\alpha\beta}^\mu) - \tilde{g}^{\alpha\beta} \Gamma_{\alpha\beta}^\mu = 0, \quad (3.32)$$

where  $\tilde{\delta}(\Gamma_{\alpha\beta}^\mu) = \frac{1}{2} g^{\mu\lambda} (D_\beta \tilde{g}_{\lambda\alpha} + D_\alpha \tilde{g}_{\beta\lambda} - D_\lambda \tilde{g}_{\alpha\beta})$ . Then, a generic solution for  $\tilde{g}_{\mu\nu}$  is

$$\tilde{g}_{\mu\nu} dx^\mu dx^\nu = -F_a(t) c^2 dt^2 + F_b(t) R^2(t) (dx^2 + dy^2 + dz^2) \quad (3.33)$$

After the condition (3.32), the solution for those functions are  $F_a(t) = 3F_b(t) \equiv F(t)$ . With the harmonic gauge fixed, we can solve the system of equation in the cosmological case.

### 3.4.2 Photon Trajectory

While a photon emitted from a source travels to the Earth, the Universe is expanding. Then the photon is affected by the cosmological Doppler effect. If we consider a radial trajectory from  $r_1$  to  $r = 0$  in a null geodesic we have

$$-(1 + 3F(t))c^2 dt^2 + a^2(t)(1 + F(t))dr^2 = 0.$$

In GR, we have that  $cdt = -R(t)dr$ . So, in the DG we can define the effective scale factor:

$$a_{DG}(t) = a(t) \sqrt{\frac{1 + F(t)}{1 + 3F(t)}} \quad (3.34)$$

such that  $cdt = -a_{DG}(t)dr$  now. If we integrate this expression from  $r_1$  to 0, we obtain:

$$r_1 = c \int_{t_1}^{t_0} \frac{dt}{a_{DG}(t)}, \quad (3.35)$$

where  $t_1$  and  $t_0$  are the emission and reception times. If a second wave crest is emitted at  $t = t_1 + \Delta t_1$  from  $r = r_1$ , it will reach  $r = 0$  at  $t = t_0 + \Delta t_0$ , so:

$$r_1 = c \int_{t_1 + \Delta t_1}^{t_0 + \Delta t_0} \frac{dt}{a_{DG}(t)}. \quad (3.36)$$

Therefore, for  $\Delta t_1, \Delta t_0$  small, which is appropriate for light waves, we get:

$$\frac{\Delta t_0}{\Delta t_1} = \frac{a_{DG}(t_0)}{a_{DG}(t_1)} \quad (3.37)$$

or:

$$\frac{\Delta \nu_1}{\Delta \nu_0} = \frac{a_{DG}(t_0)}{a_{DG}(t_1)}, \quad (3.38)$$

where  $\nu_0$  is the light frequency detected at  $r = 0$ , corresponding to a source emission at frequency  $\nu_1$ . So, the redshift is now:

$$1 + z(t_1) = \frac{a_{DG}(t_0)}{a_{DG}(t_1)} \equiv \frac{1}{Y_{DG}}. \quad (3.39)$$

We see that  $Y_{DG}(t)$  replaces the usual scale factor  $a(t)$  to compute  $z$ . This means that distances such the luminosity distance changes and need to be redefine. This was done in [57], where they used this result to fit SNe-Ia without a Dark Energy component. In Chapter 4 we will present the redefinition of the important distances involved in the CMB.

### 3.4.3 Einstein's Equations

Now lets review the main results of Einstein's equation in the cosmological case. It is usual to use  $u_\alpha = (c, 0, 0, 0)$ , then the equations for  $g_{\mu\nu}$  are just the Friedmann's equations

$$\left(\frac{\dot{a}(t)}{a(t)}\right)^2 = \frac{\kappa c^2}{3} \sum_i \rho_i(t) \quad (3.40)$$

$$\dot{\rho}_i(t) = -\frac{3\dot{a}(t)}{a(t)}(\rho_i(t) + p_i(t)), \quad (3.41)$$

with  $\dot{f} = df/dt(t)$ . In order to solve (3.40)–(3.41) it is necessary equations of state  $p_\alpha = \omega_\alpha \rho_\alpha$ . Where  $\alpha$  could be non-relativistic matter (cold dark matter, baryonic matter) where  $\omega_{NR} = 0$  and radiation (photons, massless particles) where  $\omega_R = 1/3$ . Replacing in (3.40)–(3.41) we get

$$\begin{aligned} \rho(Y) &= \rho_M(Y) + \rho_R(Y) \\ &= \frac{3H_0^2 \Omega_R}{\kappa c^2 C} \frac{Y + C}{Y^4}, \end{aligned} \quad (3.42)$$

$$\begin{aligned} p(Y) &= \frac{1}{3} \rho_R(t) \\ &= \frac{H_0^2 \Omega_R}{\kappa c^2} \frac{1}{Y^4}, \end{aligned} \quad (3.43)$$

$$t(Y) = \frac{2\sqrt{C}}{3H_0\sqrt{\Omega_R}} \left( \sqrt{Y+C}(Y-2C) + 2C^{\frac{3}{2}} \right), \quad (3.44)$$

with  $Y = a(t)/a(t=0) = a(t)$  because we set  $a(t=0) = 1$  the value of the scale factor in the present.  $H_0 = \dot{a}/a$  evaluated at the present, however this is not longer the physical Hubble constant.  $C = \Omega_{R0}/\Omega_{M0}$ , where  $\Omega_{R0}$  and  $\Omega_{M0}$  are the values at the present for those

density parameters, and they are defined as.

$$\Omega_R = \frac{\rho_{R0}}{\rho_c} \quad (3.45)$$

$$\Omega_M = \frac{\rho_{M0}}{\rho_c} \quad (3.46)$$

$$\rho_c = \frac{3H_0^2}{8\pi G}. \quad (3.47)$$

This definition is useful because as we only have radiation and non-relativistic matter the first Friedmann equation at the present reads

$$1 = \Omega_R + \Omega_M \rightarrow \Omega_R = \frac{C}{1+C} \quad (3.48)$$

Then the value  $C$  defines the values of  $\Omega_R$  and  $\Omega_M$ .

### 3.4.4 Delta Sector

After fixing the harmonic gauge the delta symmetry was broken explicitly, then the delta sector evolved independently. So, using (3.42)-(3.44), then (3.9) and (3.11) equations are reduced to:

$$u_\mu^T = 0 \quad (3.49)$$

$$F(Y) = \frac{3}{2}(2C_2 - C_1) \frac{Y}{C} \left( \sqrt{\frac{Y}{C} + 1} \ln \left( \frac{\sqrt{\frac{Y}{C} + 1} + 1}{\sqrt{\frac{Y}{C} + 1} - 1} \right) - 2 \right) - 2C_2 + C_3 \frac{Y}{C} \sqrt{\frac{Y}{C} + 1} \quad (3.50)$$

$$\tilde{\rho}_M(Y) = \frac{9H_0^2\Omega_R}{2\kappa c^2 C} \frac{(C_1 - F(Y))}{Y^3} \quad (3.51)$$

$$\tilde{\rho}_R(Y) = \frac{6H_0^2\Omega_R}{\kappa c^2} \frac{(C_2 - F(Y))}{Y^4}, \quad (3.52)$$

where  $C_1$ ,  $C_2$  and  $C_3$  are integration constants. In [53] and [57], they set  $C_1 = C_2 = 0$  because those terms in (3.51) and (3.52) produce a contribution of matter of the same nature that was obtained in the GR sector. And we are not interested in that contribution. Besides, DG

was expected to explain Dark Energy, so if we use (3.50) in (3.34) we can see that

$$a_{DG} \simeq \sqrt{\frac{1 - 2k_2 C_2}{1 - 6k_2 C_2}} Y + O(Y^2)$$

when  $Y \ll C$ . As Dark Energy is irrelevant in the early Universe, we impose that  $a_{DG} = Y + O(Y^2)$ . For this, we must use  $C_2 = 0$ . Under this analysis, we can not say anything about  $C_1$ , but as we explained before, we are not interested in delta matter which has the same nature that the standard matter of GR.

For completeness, we point out that DG has a Big-Rip, when  $a_{DG} = \infty$ . We need a Big-Rip to explain the accelerated expansion of the universe because we want that  $a_{DG}$  to grow quickly when  $Y$  is bigger.

The effective scale factor is:

$$a_{DG}(Y, L, C) = Y \sqrt{\frac{1 - L \frac{Y}{3} \sqrt{Y + C}}{1 - LY \sqrt{Y + C}}}, \quad (3.53)$$

where we used  $C_3 = -\frac{C^{\frac{3}{2}} L}{3}$  and  $L \sim 1$ . That is because we need that  $C_3 \sim C^{\frac{3}{2}} \ll 1$ . If we use  $C_3 = 0$  ie  $L = 0$ , the Big-Rip is not produced and we cannot explain the expansion of the universe. Therefore, we need to consider that  $1 \gg C \neq 0$ . To see the Big-Rip we must analyze (3.53) for  $Y \gg C$ :

$$a_{DG}(Y, L, C) \simeq Y \sqrt{\frac{3 - LY^{\frac{3}{2}}}{3(1 - LY^{\frac{3}{2}})}} + O(C^{\frac{1}{2}}). \quad (3.54)$$

It is clear that the Big-Rip is produced when:

$$Y_{Rip} = \left(\frac{1}{L}\right)^{\frac{2}{3}}. \quad (3.55)$$

In summary, we have that  $a_{DG} \sim Y$  when  $Y \ll C$ , so the Universe evolves normally at its beginning, without differences with GR. But, when  $Y \gg C$ , an accelerated expansion is produced, ending in a Big-Rip when the denominator is null.

### 3.4.5 Thermodynamics in DG

Now we will study some implications of thermodynamics in DG. This results are crucial in the understanding of the theory and the interpretation of physical quantities.

In Section 3.4.4 we show that the geometry which photons follow is given by a modified scale factor

$$a_{DG}(t) = a(t) \sqrt{\frac{1 + F(t)}{1 + 3F(t)}}$$

Then the volume of a cosmological sphere is now

$$V = \frac{4}{3} \pi r^3 a_{DG}^3$$

where  $r$  is the radial coordinate. Thus, any physical fluid has a density given by

$$\rho = \frac{U}{c^2 V} \quad (3.56)$$

where  $U$  is the internal energy and  $V$  is the volume. From the first law of Thermodynamics we have

$$\frac{dU}{dt} = T \frac{dS}{dt} - P \frac{dV}{dt} \quad (3.57)$$

We will assume that the Universe evolved adiabatically as in GR (see for instance [73]). This means  $\dot{S} = 0$ . Then we get the well known relation for the energy conservation

$$\dot{\rho} = -3H_{DG} \left( \rho + \frac{P}{c^2} \right) \quad (3.58)$$

with  $H_{DG} = \dot{a}_{DG}/a_{DG}$ . In order to know the evolution of  $\rho$  we need an equation of state  $P(\rho)$ . In [57] they showed that  $H_{DG}(t)$  replaces the first Friedmann equation, now we know that the second Friedmann equation is the thermodynamics statement that the Universe evolves adiabatically, so the physical densities must satisfy eq. (3.58). If we

assume  $P = c^2 \omega \rho$  we found

$$\rho a_{DG}^{3(1+\omega)} = \rho_0 a_{DG0}^{3(1+\omega)} \quad (3.59)$$

where  $\rho_0$  is the density at the present. A crucial point in this theory is that GR equations (3.8) and (3.10) are valid, then we also have a similar relation for the densities of GR, but with the standard scale factor  $a(t)$ , explicitly

$$\rho_{GR} a^{3(1+\omega)} = \rho_{GR0} a_0^{3(1+\omega)} \quad (3.60)$$

These solution for  $\rho_{GR}$  are the same as (3.42). Then we can relate both densities by the ratio between them

$$\frac{\rho}{\rho_{GR}} \left( \sqrt{\frac{1+F(t)}{1+3F(t)}} \right)^{3(1+\omega)} = \text{constant}(\omega) \quad (3.61)$$

This ratio will be vitally important when we study the perturbations of the system. Because we will study the evolution of fractional perturbations at the last-scattering time defined as

$$\delta_{GR\alpha} = \frac{\delta \rho_{GR\alpha}}{\bar{\rho}_{GR\alpha} + \bar{p}_{GR\alpha}} \quad (3.62)$$

where  $\alpha$  runs between  $\gamma$ ,  $\nu$ ,  $B$  and  $D$  (photons, neutrinos, baryons and dark matter, respectively). If we consider the results from [57] ( $C \sim 10^{-4}$  and  $L \sim 0.45$ ), at the moment of last-scattering ( $T \sim 3000$  K) we get

$$\sqrt{\frac{1+F(t_{ls})}{1+3F(t_{ls})}} \sim 1 \quad (3.63)$$

This mean that at that moment the physical density was proportional to the densities of GR, and without lost of generality we can take

$$\delta_{phys\alpha}(t_{ls}) = \delta_{GR\alpha}(t_{ls}) = \delta_{\alpha}(t_{ls}) \quad (3.64)$$

as it will be introduce in Section 4.2. In facts, (3.63) is valid for a wide range of times, from the beginning of the Universe ( $z \rightarrow \infty$ ) until  $z \sim 10$ , so this approximation is valid in the study of primordial perturbations in DG when using the equations of GR.

On the other hand, the number density (number of photons over the volume) at equilibrium

with matter at temperature  $T$  is

$$n_T(\nu)d\nu = \frac{8\pi\nu^2 d\nu}{e^{\frac{h\nu}{k_B T}} - 1}; \quad (3.65)$$

After decoupling photons travel freely from the surface of last scattering to us. So the number of photons is conserved

$$dN = n_{T_{ls}}(\nu_{ls})d\nu_{ls}dV_{ls} = n_T(\nu)d\nu dV \quad (3.66)$$

as frequencies are redshifted by  $\nu = \nu_{ls}a_{DG}(t_{ls})/a_{DG}$ , and the volume  $V = V_{ls}a_{DG}^3/a_{DG}^3(t_{ls})$  we find that in order to keep the form of a black body distribution, the temperature in the number density should evolves as

$$Ta_{DG} = constant \rightarrow T = \frac{T_0}{Y_{DG}}, \quad (3.67)$$

where  $T_0 = 2.73 \text{ K}$  is the temperature of the Universe at the present based on the black body radiation of the CMB.

To summarize this Section, thermodynamics establish that the physical densities diluted with  $Y_{DG}$  and not with  $Y$ , this means that  $\Omega_R$  and  $\Omega_M$  defined before are not the physical density parameter which Planck measures. However, as we know exactly the evolution of  $\rho_{GR}$  because Friedmann's equation's are valid in DG, we can use (3.61) to know the evolution of the physical densities. By the other side, in DG temperature must fall with the modified scale factor  $Y_{DG}$  (or  $a_{DG}$ ). This is important because we will study how the temperature of the photons coming from the CMB decreased until the actual temperature.

### 3.4.6 Equality time $t_{EQ}$

After concluding this chapter, there is an ansatz that we need to propose in order to be completely consistent when solving the cosmological perturbation theory in the next chapter. This is about when the radiation was equal to the non-relativistic matter. The relevance of this moment is due we will solve the perturbed equation when the Universe was dominated by radiation and when it was dominated by matter. We state that the moment when radiation and matter were equal at some  $t_{EQ}$  is the same as in GR as in DG. The implication of this statement is the following: Let us consider the ratio of the matter and radiation densities of



GR (3.60)

$$\frac{\rho_{GR\,M}}{\rho_{GR\,R}} = \frac{Y}{C}, \quad (3.68)$$

we remind that  $C = \Omega_R/\Omega_M$ . Then the moment of equality in GR correspond to  $Y_{EQ} = C$ . On the other side, if we consider the same ratio but now between the physical densities using (3.59), we get

$$\frac{\rho_{phys;M}}{\rho_{phys\,R}} = \frac{Y_{DG}}{C_{DG}}, \quad (3.69)$$

where  $C_{DG} = \Omega_{DG\,R}/\Omega_{DG\,M}$ . Then in the equality we need to impose  $Y_{DG}(Y_{EQ}) = C_{DG}$ , explicitly

$$C_{DG} = C \frac{\sqrt{\frac{1+F(C)}{1+3F(C)}}}{\sqrt{\frac{1+F(1)}{1+3F(1)}}}, \quad (3.70)$$

if we take the value from [57],  $C \sim 10^{-4}$  and  $L \sim 0.45$  implies  $F(C) \sim 10^{-3} \ll 1$  and  $F(1) \sim -L/3$ , then

$$C_{DG} = C \sqrt{\frac{1-L}{1-L/3}} \quad (3.71)$$

This means that total density of matter and radiation today depends explicitly on the geometry measured with  $L$ .

### 3.4.7 Conclusions

We have presented the definition of Delta Gravity, showing how this delta symmetry acts on an general action, in particular in the Einstein-Hilbert action. We presented the system of equations of the model, and we emphasize that General Relativity equations are valid in this theory. Then we just present the form of the energy-momentum tensors  $T_{\mu\nu}$  and  $\tilde{T}_{\mu\nu}$  and the normalization of the velocity fields. After that, we described how particles move in this theory, concluding that massive particles do not move in geodesics, while massless particles do in an effective metric  $\mathbf{g}_{\mu\nu} = g_{\mu\nu} + \tilde{g}_{\mu\nu}$ .

Then we presented cosmological solutions for an isotropic and homogeneous Universe, showing that in order to reduce the free functions of the theory it is necessary to impose the extended harmonic gauge. It is important to notice that after fixing this gauge the delta

symmetry is broken and both sectors evolves independently. Then we described the trajectory of photons coming from a source in a radial trajectory until reaching us, this introduce a new scale factor which defines the geometry and the redshift. After that we presented the solutions of Einstein's equation and the delta sector, with only radiation and non-relativistic matter and its delta versions, where we consider the same equation of state for each species in both GR and delta sector. Here we consider that in order to explain the CMB and Nucleosynthesis, DG must be equal to GR for early times, while it predicts a Big-Rip in the future.

Then, we discussed the implications of the first law of thermodynamics in the modified geometry of this model. We distinguish the physical densities from the GR densities in terms of which scale factor they dilute. However knowing the solutions of the GR sector is enough for us to know about the behavior of the physical densities. Also, if we consider that the number of photons is conserved after the moment of decoupling, the black body distribution should keep the form, and that means that temperature is redshifted with the modified scale factor  $Y_{DG}$ . Finally, we stated the ansatz that the moment of equality between radiation and matter was the same in GR and in DG and we showed it implications in some parameters of the theory.

We will use all this results as the background of the theory, and in the next Chapter we will study the scalar perturbations of CMB.

Before finishing this Chapter, let's discuss the foundations of DG. We have solved completely the system in the harmonic gauge, this gave us solutions that we will use as background in the following chapters. However, when solving GR linear perturbation theory in the comoving gauge [74] where one uses  $\delta u = 0$ , one gets exactly the same equations for DG but now as a perturbed equations from GR, because we imposed  $u^T = 0$ . Nevertheless, we emphasize that DG is not a perturbation theory of GR, so solutions of the delta sector could have the same or even more weight that GR solutions because in DG the delta fields are unbounded whereas perturbations are valid in a certain range.

# Chapter 4

## Cosmological Fluctuations in Delta Gravity

In this Chapter we present the perturbation theory of DG in the cosmological FRLW background described in Chapter 3. As the physics of DG should be the same as in GR, we will use of the equation of GR in order to describe the evolution of the physical perturbations. We follow the prescription given by Weinberg[62] step by step, translating their results to this theory.

### 4.1 Perturbation Theory

Let's start with a perturbation as follows:

$$g_{\mu\nu} = \bar{g}_{\mu\nu} + h_{\mu\nu}, \quad (4.1)$$

$$\tilde{g}_{\mu\nu} = \tilde{\bar{g}}_{\mu\nu} + \tilde{h}_{\mu\nu} \quad (4.2)$$

where  $h, \tilde{h} \ll 1$ . The bar means the background solutions which was obtained before. However we remind that in the harmonic gauge we have

$$\bar{g}_{\mu\nu} dx^\mu dx^\nu = -c^2 dt^2 + a^2(t)(dx^2 + dy^2 + dz^2) \quad (4.3)$$

$$\tilde{\bar{g}}_{\mu\nu} dx^\mu dx^\nu = -3F(t)c^2 dt^2 + F(t)a^2(t)(dx^2 + dy^2 + dz^2). \quad (4.4)$$

Then, we follow the standard method, known as Scalar-Vector-Tensor decomposition [75]. This process allows us to study those sectors independently. Therefore, the perturbations are

$$h_{00} = -E \quad h_{i0} = a \left[ \frac{\partial H}{\partial x^i} + G_i \right] \quad h_{ij} = a^2 \left[ A\delta_{ij} + \frac{\partial^2 B}{\partial x^i \partial x^j} + \frac{\partial C_i}{\partial x^j} + \frac{\partial C_j}{\partial x^i} + D_{ij} \right], \quad (4.5)$$

where

$$\frac{\partial C_i}{\partial x^i} = \frac{\partial G_i}{\partial x^i} = 0 \quad \frac{\partial D_{ij}}{\partial x^j} = 0 \quad D_{ii} = 0. \quad (4.6)$$

This decomposition must be equivalent for  $\tilde{h}_{\mu\nu}$  (by group theory):

$$\tilde{h}_{00} = -\tilde{E} \quad \tilde{h}_{i0} = a \left[ \frac{\partial \tilde{H}}{\partial x^i} + \tilde{G}_i \right] \quad \tilde{h}_{ij} = a^2 \left[ \tilde{A}\delta_{ij} + \frac{\partial^2 \tilde{B}}{\partial x^i \partial x^j} + \frac{\partial \tilde{C}_i}{\partial x^j} + \frac{\partial \tilde{C}_j}{\partial x^i} + \tilde{D}_{ij} \right], \quad (4.7)$$

with

$$\frac{\partial \tilde{C}_i}{\partial x^i} = \frac{\partial \tilde{G}_i}{\partial x^i} = 0 \quad \frac{\partial \tilde{D}_{ij}}{\partial x^j} = 0 \quad \tilde{D}_{ii} = 0. \quad (4.8)$$

If we replace perturbations in (3.8), (3.9), (3.10), and (3.11), we get the equations for the perturbations. However, there are degrees of freedom that we have to take into account to have physical solutions. In the next subsection, we show how to choose a gauge to delete those nonphysical solutions.

### 4.1.1 Choosing a gauge

Under a space-time coordinate transformation, the metric perturbations transform as

$$\Delta h_{\mu\nu}(x) = -\bar{g}_{\lambda\nu}(x) \frac{\partial \epsilon^\lambda}{\partial x^\mu} - \bar{g}_{\mu\lambda}(x) \frac{\partial \epsilon^\lambda}{\partial x^\nu} - \frac{\partial \bar{g}_{\mu\nu}}{\partial x^\lambda} \epsilon^\lambda. \quad (4.9)$$

In more detail,

$$\Delta h_{ij} = -\frac{\partial \epsilon_i}{\partial x^j} - \frac{\partial \epsilon_j}{\partial x^i} + 2a\dot{a}\delta_{ij}\epsilon_0, \quad (4.10)$$

$$\Delta h_{i0} = -\frac{\partial \epsilon_i}{\partial t} - \frac{\partial \epsilon_0}{\partial x^i} + 2\frac{\dot{a}}{a}\epsilon_i, \quad (4.11)$$

$$\Delta h_{00} = -2\frac{\partial \epsilon_0}{\partial t}. \quad (4.12)$$

For delta perturbations we get<sup>1</sup>

$$\Delta \tilde{h}_{\mu\nu} = -\tilde{g}_{\mu\lambda}\frac{\partial \epsilon^\lambda}{\partial x^\nu} - \tilde{g}_{\lambda\nu}\frac{\partial \epsilon^\lambda}{\partial x^\mu} - \frac{\partial \tilde{g}_{\mu\nu}}{\partial x^\lambda}\epsilon^\lambda - \tilde{g}_{\mu\lambda}\frac{\partial \tilde{\epsilon}^\lambda}{\partial x^\nu} - \tilde{g}_{\lambda\nu}\frac{\partial \tilde{\epsilon}^\lambda}{\partial x^\mu} - \frac{\partial \tilde{g}_{\mu\nu}}{\partial x^\lambda}\tilde{\epsilon}^\lambda. \quad (4.13)$$

In more detail,

$$\Delta \tilde{h}_{ij} = -F\frac{\partial \epsilon_i}{\partial x^j} - F\frac{\partial \epsilon_j}{\partial x^i} - \frac{\partial \tilde{\epsilon}_j}{\partial x^i} - \frac{\partial \tilde{\epsilon}_i}{\partial x^j} + \left[ \epsilon_0 \left( 2Fa\dot{a} + \dot{F}a^2 \right) + 2\tilde{\epsilon}_0 a\dot{a} \right] \delta_{ij}, \quad (4.14)$$

$$\Delta \tilde{h}_{i0} = -F\frac{\partial \epsilon_i}{\partial t} - 3F\frac{\partial \epsilon_0}{\partial x^i} - \frac{\partial \tilde{\epsilon}_i}{\partial t} - \frac{\partial \tilde{\epsilon}_0}{\partial x^i} + 2F\frac{\dot{a}}{a}\epsilon_i + 2\frac{\dot{a}}{a}\tilde{\epsilon}_i, \quad (4.15)$$

$$\Delta \tilde{h}_{00} = -3\epsilon_0\dot{F} - 6F\frac{\partial \epsilon_0}{\partial t} - 2\frac{\partial \tilde{\epsilon}_0}{\partial t}, \quad (4.16)$$

where  $\epsilon$  and  $\tilde{\epsilon} = \tilde{\delta}\epsilon$  defines the coordinates transformation. Also we raised and lowered index using  $\tilde{g}_{\mu\nu}$ , so  $\epsilon^0 = -\epsilon_0$ ,  $\tilde{\epsilon}^0 = -\tilde{\epsilon}_0$ ,  $\epsilon^i = a^{-2}\epsilon_i$  and  $\tilde{\epsilon}^j = a^{-2}\tilde{\epsilon}_j$ .

Following the standard procedure, we decompose the spatial part of  $\epsilon^\mu$  and  $\tilde{\epsilon}^\mu$  into the gradient of a spatial scalar plus a divergenceless vector:

$$\epsilon_i = \partial_i \epsilon^S + \epsilon_i^V, \quad \partial_i \epsilon^V = 0, \quad (4.17)$$

$$\tilde{\epsilon}_i = \partial_i \tilde{\epsilon}^S + \tilde{\epsilon}_i^V, \quad \partial_i \tilde{\epsilon}^V = 0 \quad (4.18)$$

Thus, we can compare equations (4.5) and (4.7) with (4.10)-(4.12) and (4.14)-(4.16) to obtain the gauge transformations of the metric components:

---

<sup>1</sup>This form is obtained taking the delta symmetry to (4.9), for more details see [52]

$$\begin{aligned}
\Delta A &= \frac{2\dot{a}}{a}\epsilon_0, \quad \Delta B = -\frac{2}{a^2}\epsilon^S, \\
\Delta C_i &= -\frac{1}{a^2}\epsilon_i^V, \quad \Delta D_{ij} = 0, \quad \Delta E = 2\dot{\epsilon}_0, \\
\Delta H &= \frac{1}{a}\left(-\epsilon_0 - \dot{\epsilon}^S + \frac{2\dot{a}}{a}\epsilon^S\right), \quad \Delta G_i = \frac{1}{a}\left(-\dot{\epsilon}_i^V + \frac{2\dot{a}}{a}\epsilon_i^V\right),
\end{aligned} \tag{4.19}$$

and

$$\begin{aligned}
\Delta \tilde{A} &= \left(\frac{2\dot{a}F}{a} + \dot{F}\right)\epsilon_0 + 2\frac{\dot{a}}{a}\tilde{\epsilon}_0, \quad \Delta \tilde{B} = -\frac{2}{a^2}(F\epsilon^S + \tilde{\epsilon}^S), \\
\Delta \tilde{C}_i &= -\frac{1}{a^2}(F\epsilon_i^V + \tilde{\epsilon}_i^V), \quad \Delta \tilde{D}_{ij} = 0, \quad \Delta \tilde{E} = 6F\dot{\epsilon}_0 + 3\dot{F}\epsilon_0 + 2\dot{\tilde{\epsilon}}_0, \\
\Delta \tilde{H} &= \frac{1}{a}\left(-3F\epsilon_0 - \tilde{\epsilon}_0 - F\dot{\epsilon}^S - \dot{\tilde{\epsilon}}^S + \frac{2F\dot{a}}{a}\epsilon^S + \frac{2\dot{a}}{a}\tilde{\epsilon}^S\right), \\
\Delta \tilde{G}_i &= \frac{1}{a}\left(-F\dot{\epsilon}_i^V - \dot{\tilde{\epsilon}}_i^V + \frac{2F\dot{a}}{a}\epsilon_i^V + \frac{2\dot{a}}{a}\tilde{\epsilon}_i^V\right).
\end{aligned} \tag{4.20}$$

There are different scenarios in which we can continue with the calculations when we impose conditions on the parameters  $\epsilon_\mu$  and  $\tilde{\epsilon}_\mu$ . However, before discussing it, we will study the gauge transformations of energy-momentum tensors  $T_{\mu\nu}$  and  $\tilde{T}_{\mu\nu}$ .

#### 4.1.2 $T_{\mu\nu}$ and $\tilde{T}_{\mu\nu}$

Now we will decompose the energy-momentum tensors  $T_{\mu\nu}$  and  $\tilde{T}_{\mu\nu}$  in the same way. For a perfect fluid, we showed

$$T_{\mu\nu} = pg_{\mu\nu} + (\rho + p)u_\mu u_\nu, \tag{4.21}$$

while for  $\tilde{T}_{\mu\nu}$

$$\tilde{T}_{\mu\nu} = \tilde{p}g_{\mu\nu} + \tilde{p}\tilde{g}_{\mu\nu} + (\tilde{\rho} + \tilde{p})u_\mu u_\nu + (\rho + p)\left(\frac{1}{2}(\tilde{g}_{\mu\alpha}u_\nu u^\alpha + \tilde{g}_{\nu\alpha}u_\mu u^\alpha) + u_\mu^T u_\nu + u_\mu u_\nu^T\right), \tag{4.22}$$

where

$$g^{\mu\nu}u_\mu u_\nu = -1, \quad (4.23)$$

$$g^{\mu\nu}u_\mu u_\nu^T = 0. \quad (4.24)$$

Now let us consider

$$\begin{aligned} p &= \bar{p} + \delta p, \\ \rho &= \bar{\rho} + \delta \rho, \\ u_\mu &= \bar{u}_\mu + \delta u_\mu, \\ \tilde{p} &= \tilde{\bar{p}} + \delta \tilde{p}, \\ \tilde{\rho} &= \tilde{\bar{\rho}} + \delta \tilde{\rho}, \\ u_\mu^T &= \bar{u}_\mu^T + \delta u_\mu^T. \end{aligned} \quad (4.25)$$

Usually, the equation of state is given by  $p(\rho)$ , so we could reduce this system. For now, we will work in the generic case. When we work in the frame  $\bar{u}_\mu = (-1, 0, 0, 0)$  we have  $\bar{u}_\mu^T = 0$ , and the normalization conditions (4.23) and (4.24) give

$$\begin{aligned} \delta u^0 &= \delta u_0 = \frac{h_{00}}{2} \\ \delta u_0^T &= \delta u_T^0 = 0 \end{aligned} \quad (4.26)$$

while  $\delta u_i$  and  $\delta u_i^T$  are independent dynamical variables (note that  $\delta u^\mu \equiv \delta(g^{\mu\nu}u_\nu)$  is not given by  $\bar{g}^{\mu\nu}\delta u_\nu$ , the same for  $\delta u_T^\mu$ ). Then, the first-order perturbation for both energy-momentum tensors are

$$\delta T_{\mu\nu} = \bar{p}h_{\mu\nu} + \delta p\bar{g}_{\mu\nu} + (\bar{p} + \bar{\rho})(\bar{u}_\mu\delta u_\nu + \delta u_\mu\bar{u}_\nu) + (\delta p + \delta\rho)\bar{u}_\mu\bar{u}_\nu, \quad (4.27)$$

Therefore,

$$\delta T_{ij} = \bar{p}h_{ij} + a^2\delta_{ij}\delta p, \quad \delta T_{i0} = \bar{p}h_{i0} - (\bar{p} + \bar{\rho})\delta u_i, \quad \delta T_{00} = -\bar{\rho}h_{00} + \delta\rho. \quad (4.28)$$

While

$$\begin{aligned} \delta\tilde{T}_{\mu\nu} &= \tilde{p}h_{\mu\nu} + \delta\tilde{p}\tilde{g}_{\mu\nu} + \tilde{p}\tilde{h}_{\mu\nu} + \delta p\tilde{g}_{\mu\nu} + (\tilde{\rho} + \tilde{p})(\bar{u}_\mu\delta u_\nu + \delta u_\mu\bar{u}_\nu) \\ &+ (\delta\tilde{\rho} + \delta\tilde{p})\bar{u}_\mu\bar{u}_\nu + (\bar{\rho} + \bar{p})\left\{\frac{1}{2}\left[\tilde{g}_{\mu\alpha}(\bar{u}_\nu\delta u^\alpha + \delta u_\nu\bar{u}^\alpha) + \tilde{h}_{\mu\alpha}\bar{u}_\nu\bar{u}^\alpha\right.\right. \\ &+ \left.\tilde{g}_{\nu\alpha}(\bar{u}_\mu\delta u^\alpha + \delta u_\mu\bar{u}^\alpha) + \tilde{h}_{\nu\alpha}\bar{u}_\mu\bar{u}^\alpha\right] + \bar{u}_\mu^T\delta u_\nu + \delta u_\mu^T\bar{u}_\nu + \bar{u}_\mu\delta u_\nu^T + \delta u_\mu\bar{u}_\nu^T\Big\} \\ &+ (\delta\rho + \delta p)\left\{\frac{1}{2}\left[\tilde{g}_{\mu\alpha}\bar{u}_\nu\bar{u}^\alpha + \tilde{g}_{\nu\alpha}\bar{u}_\mu\bar{u}^\alpha\right] + \bar{u}_\mu^T\bar{u}_\nu + \bar{u}_\mu\bar{u}_\nu^T\right\}, \end{aligned} \quad (4.29)$$

and

$$\begin{aligned} \delta\tilde{T}_{00} &= -\tilde{\rho}h_{00} - \tilde{\rho}\tilde{h}_{00} + 3F\delta\rho + \delta\tilde{\rho}, \\ \delta\tilde{T}_{i0} &= \tilde{p}h_{i0} + \tilde{p}\tilde{h}_{i0} - (\tilde{\rho} + \tilde{p})\delta u_i + (\bar{\rho} + \bar{p})\left\{\frac{1}{2}[Fh_{i0} - \tilde{h}_{i0} - 4F\delta u_i] - \delta u_i^T\right\}, \\ \delta\tilde{T}_{ij} &= \tilde{p}h_{ij} + \delta\tilde{p}a^2\delta_{ij} + \tilde{p}\tilde{h}_{ij} + \delta pFa^2\delta_{ij}, \end{aligned} \quad (4.30)$$

where we used  $\delta u^\alpha = \delta(g^{\alpha\beta}u_\beta) = \bar{g}^{\alpha\beta}\delta u_\beta + h^{\mu\nu}\bar{u}_\beta$ . Generally, we decompose  $\delta u_i$  ( $\delta u_i^T$ ) into the gradient of a scalar velocity potential  $\delta u$  ( $\delta\tilde{u}$ ) and a divergenceless vector  $\delta u_i^V$  ( $\delta\tilde{u}_i^V$ ), and the dissipative corrections to the inertia tensor are added as follows

$$\delta T_{ij} = \bar{p}h_{ij} + a^2\left[\delta_{ij}\delta p + \partial_i\partial_j\pi^S + \partial_i\pi_j^V + \partial_j\pi_i^V + \pi_{ij}^T\right], \quad (4.31)$$

$$\delta T_{i0} = \bar{p}h_{i0} - (\bar{p} + \bar{\rho})\left(\partial_i\delta u + \delta u_i^V\right), \quad (4.32)$$

$$\delta T_{00} = -\bar{\rho}h_{00} + \delta\rho, \quad (4.33)$$

and



$$\begin{aligned}\delta\tilde{T}_{ij} &= \tilde{p}h_{ij} + a^2 [\delta_{ij}\delta\tilde{p} + \partial_i\partial_j\tilde{\pi}^S + \partial_i\tilde{\pi}_j^V + \partial_j\tilde{\pi}_i^V + \tilde{\pi}_{ij}^T] + \tilde{p}h_{ij} \\ &+ Fa^2 [\delta_{ij}\delta p + \partial_i\partial_j\pi^S + \partial_i\pi_j^V + \partial_j\pi_i^V + \pi_{ij}^T],\end{aligned}\quad (4.34)$$

$$\begin{aligned}\delta\tilde{T}_{i0} &= \tilde{p}h_{i0} + \tilde{p}\tilde{h}_{i0} - (\tilde{\rho} + \tilde{p})(\partial_i\partial u + \partial u_i^V) \\ &+ (\bar{\rho} + \bar{p}) \left\{ \frac{1}{2}[Fh_{i0} - \tilde{h}_{i0} - 4F(\partial_i\delta u + \delta u_i^V)] - \partial_i\delta\tilde{u} + \delta\tilde{u}_i^V \right\},\end{aligned}\quad (4.35)$$

$$\delta\tilde{T}_{00} = -\tilde{\rho}h_{00} - \tilde{\rho}\tilde{h}_{00} + 3F\delta\rho + \delta\tilde{\rho},\quad (4.36)$$

where  $\pi_i^V$  ( $\tilde{\pi}_i^V$ ),  $\pi_{ij}^T$  ( $\tilde{\pi}_{ij}^T$ ) and  $\delta u_i^V$  ( $\delta\tilde{u}_i^V$ ) satisfy similar conditions to (4.6) and (4.8). These conditions are (expressed before as  $C_i$  ( $\tilde{C}_i$ ),  $D_{ij}$  ( $\tilde{D}_{ij}$ )  $G_i$  ( $\tilde{G}_i$ )):

$$\partial_i\pi_i^V = \partial_i\tilde{\pi}_i^V = \partial_i\delta u_i^V = \partial_i\delta\tilde{u}_i^V = 0 \quad \partial_i\pi_{ij}^T = \partial_i\tilde{\pi}_{ij}^T = 0, \quad \pi_{ii}^T = \tilde{\pi}_{ii}^T = 0. \quad (4.37)$$

The dissipative corrections take into account physical configurations when radial pressure is not longer equal to the tangential pressure; we added it here just for completeness of the development of the theory, however when we solve the system of equations of DG we will set them equal to zero because we consider perfect fluids as sources.

### 4.1.3 Gauge Transformations for the Energy-Momentum tensors

The gauge transformation for  $T_{\mu\nu}$  is given by

$$\Delta\delta T_{\mu\nu}(x) = -\bar{T}_{\lambda\nu}(x)\frac{\partial\epsilon^\lambda}{\partial x^\mu} - \bar{T}_{\mu\lambda}(x)\frac{\partial\epsilon^\lambda}{\partial x^\nu} - \frac{\partial\bar{T}_{\mu\nu}}{\partial x^\lambda}\epsilon^\lambda, \quad (4.38)$$

where the components are

$$\Delta\delta T_{ij} = -\bar{p}\left(\frac{\partial\epsilon_i}{\partial x^j} + \frac{\partial\epsilon_j}{\partial x^i}\right) + \frac{\partial}{\partial t}(a^2\bar{p})\delta_{ij}\epsilon_0, \quad (4.39)$$

$$\Delta\delta T_{i0} = -\bar{p}\frac{\partial\epsilon_i}{\partial t} + \bar{\rho}\frac{\partial\epsilon_0}{\partial x^i} + 2\bar{p}\frac{\dot{a}}{a}\epsilon_i, \quad (4.40)$$

$$\Delta\delta T_{00} = 2\bar{\rho}\frac{\partial\epsilon_0}{\partial t} + \dot{\bar{\rho}}\epsilon_0. \quad (4.41)$$

While the gauge transformation of  $\delta\tilde{T}_{\mu\nu}$  is given by

$$\Delta\delta\tilde{T}_{\mu\nu} = -\tilde{T}_{\mu\lambda}\frac{\partial\epsilon^\lambda}{\partial x^\nu} - \tilde{T}_{\lambda\nu}\frac{\partial\epsilon^\lambda}{\partial x^\mu} - \frac{\partial\tilde{T}_{\mu\nu}}{\partial x^\lambda}\epsilon^\lambda - \bar{T}_{\mu\lambda}\frac{\partial\tilde{\epsilon}^\lambda}{\partial x^\nu} - \bar{T}_{\lambda\nu}\frac{\partial\tilde{\epsilon}^\lambda}{\partial x^\mu} - \frac{\partial\bar{T}_{\mu\nu}}{\partial x^\lambda}\tilde{\epsilon}^\lambda, \quad (4.42)$$

where the components are

$$\begin{aligned} \Delta\delta\tilde{T}_{ij} &= -(\tilde{p} + \bar{p}F)\frac{\partial\epsilon_i}{\partial x^j} - (\tilde{p} + \bar{p}F)\frac{\partial\epsilon_j}{\partial x^i} - \bar{p}\frac{\partial\tilde{\epsilon}_j}{\partial x^i} - \bar{p}\frac{\partial\tilde{\epsilon}_i}{\partial x^j} \\ &+ \left[ \epsilon_0\frac{\partial}{\partial t}[a^2(\tilde{p} + \bar{p}F)] + \frac{\partial}{\partial t}(a^2\bar{p})\tilde{\epsilon}_0 \right] \delta_{ij} \end{aligned} \quad (4.43)$$

$$\begin{aligned} \Delta\delta\tilde{T}_{i0} &= -(\tilde{p} + \bar{p}F)\frac{\partial\epsilon_i}{\partial t} + (\tilde{\rho} + 3F\bar{\rho})\frac{\partial\epsilon_0}{\partial x^i} - \bar{p}\frac{\partial\tilde{\epsilon}_i}{\partial t} + \bar{\rho}\frac{\partial\tilde{\epsilon}_0}{\partial x^i} \\ &+ 2(\tilde{p} + \bar{p}F)\frac{\dot{a}}{a}\epsilon_i + 2\bar{p}\frac{\dot{a}}{a}\tilde{\epsilon}_i \end{aligned} \quad (4.44)$$

$$\Delta\delta\tilde{T}_{00} = \epsilon_0\frac{\partial}{\partial t}(\tilde{\rho} + 3F\bar{\rho}) + 2(\tilde{\rho} + 3F\bar{\rho})\frac{\partial\epsilon_0}{\partial t} + \dot{\rho}\tilde{\epsilon}_0 + 2\bar{\rho}\frac{\partial\tilde{\epsilon}_0}{\partial t}. \quad (4.45)$$

$\epsilon_i$  and  $\tilde{\epsilon}_i$  were decomposed in (4.17) to write these gauge transformations in terms of the scalar, vector and tensor components. The transformations (4.10)-(4.12) and (4.14)-(4.16) with (4.39)-(4.40) and (4.43)-(4.45) give the gauge transformation for the pressure, energy density and velocity potential:

$$\Delta\delta p = \dot{\bar{p}}\epsilon_0, \quad \Delta\delta\rho = \dot{\bar{\rho}}\epsilon_0, \quad \Delta\delta u = -\epsilon_0. \quad (4.46)$$

The other ingredients of the energy-momentum tensor are gauge invariants:

$$\Delta\pi^S = \Delta\pi_i^V = \Delta\pi_{ij}^T = \Delta\delta u_i^V = 0. \quad (4.47)$$

Nevertheless, the other transformations are

$$\begin{aligned}\Delta\delta\tilde{\rho} &= \frac{\partial}{\partial t}(\tilde{\rho} + 3F\bar{\rho})\epsilon_0 + 2(\tilde{\rho} + 3F\bar{\rho})\dot{\epsilon}_0 + \dot{\rho}\tilde{\epsilon}_0 + 2\bar{\rho}\dot{\tilde{\epsilon}}_0 - \tilde{\rho}\Delta E \\ &\quad - 3F\bar{\rho}\Delta\tilde{E} - 3F\Delta\delta\rho, \end{aligned} \quad (4.48)$$

$$\Delta\delta\tilde{p} = \frac{1}{a^2}\frac{\partial}{\partial t}[a^2(\tilde{p} + \bar{p}F)]\epsilon_0 + \frac{1}{a^2}\frac{\partial}{\partial t}(a^2\bar{\rho})\tilde{\epsilon}_0 - \tilde{p}\Delta A - \bar{p}F\Delta\tilde{A} - F\Delta\delta p, \quad (4.49)$$

$$\begin{aligned}\Delta\delta\tilde{u} &= \frac{1}{(\bar{\rho} + \bar{p})} \left\{ (\tilde{p} + \bar{p}F)\dot{\epsilon}^S - (\tilde{\rho} + 3F\bar{\rho})\epsilon_0 + \bar{p}\dot{\tilde{\epsilon}}^S - \bar{\rho}\tilde{\epsilon}_0 - 2(\tilde{p} + \bar{p}F)\frac{\dot{a}}{a}\epsilon^S \right. \\ &\quad \left. - 2\bar{p}\frac{\dot{a}}{a}\tilde{\epsilon}^S + \tilde{p}a\Delta H + \bar{p}a\Delta\tilde{H} - (\bar{\rho} + \bar{p}) \left[ \frac{1}{2}(1-F)a\Delta\tilde{H} + 2F\Delta\delta u \right] \right\}, \end{aligned} \quad (4.50)$$

$$\begin{aligned}\Delta\delta\tilde{u}_i^V &= \frac{1}{(\bar{\rho} + \bar{p})} \left\{ (\tilde{p} + \bar{p}F)\dot{\epsilon}_i^V + \bar{p}\dot{\tilde{\epsilon}}_i^V - 2(\tilde{p} + \bar{p}F)\frac{\dot{a}}{a}\epsilon_i^V - 2\bar{p}\frac{\dot{a}}{a}\tilde{\epsilon}_i^V + \tilde{p}a\Delta G_i \right. \\ &\quad \left. + \bar{p}a\Delta\tilde{G}_i - \frac{1}{2}(\bar{\rho} + \bar{p})(1-F)a\Delta\tilde{G}_i \right\}, \end{aligned} \quad (4.51)$$

$$\Delta\delta\tilde{\pi}^S = -\frac{2}{a^2}(\tilde{p} + \bar{p}F)\epsilon^S - 2\frac{\bar{p}}{a^2}\tilde{\epsilon}^S - \tilde{p}\Delta B - \bar{p}F\Delta\tilde{B}, \quad (4.52)$$

$$\Delta\delta\tilde{\pi}_i^V = -\frac{1}{a^2}(\tilde{p} + \bar{p}F)\epsilon_i^V - \frac{\bar{p}}{a^2}\tilde{\epsilon}_i^V - \tilde{p}\Delta C_i - \bar{p}F\Delta\tilde{C}_i, \quad (4.53)$$

$$\Delta\delta\tilde{\pi}_{ij} = 0. \quad (4.54)$$

The results given in (4.19), (4.20) and (4.46) are used to obtain

$$\Delta\delta\tilde{\rho} = \dot{\tilde{\rho}}\epsilon_0 + (\dot{\rho} - 3F\bar{\rho})\tilde{\epsilon}_0, \quad (4.55)$$

$$\Delta\delta\tilde{p} = \dot{\tilde{p}}\epsilon_0 + \dot{\bar{p}}\tilde{\epsilon}_0, \quad (4.56)$$

$$\begin{aligned}\Delta\delta\tilde{u} &= \left[ (1-3F)\frac{F}{2} - \frac{(\tilde{p} + \tilde{\rho})}{(\bar{p} + \bar{\rho})} \right] \epsilon_0 - \frac{1}{2}(1+F)\tilde{\epsilon}_0 - (1-F)\frac{\dot{a}}{a}(F\epsilon^S + \tilde{\epsilon}^S) \\ &\quad + \frac{1}{2}(1-F)(F\dot{\epsilon}^S + \dot{\tilde{\epsilon}}^S), \end{aligned} \quad (4.57)$$

$$\Delta\delta\tilde{u}_i^V = \frac{1}{2}(1-F)[F\dot{\epsilon}_i^V + \dot{\tilde{\epsilon}}_i^V - 2\frac{\dot{a}}{a}F\epsilon_i^V - 2\frac{\dot{a}}{a}\tilde{\epsilon}_i^V], \quad (4.58)$$

$$\Delta\delta\tilde{\pi}_i^S = 0, \quad (4.59)$$

$$\Delta\delta\tilde{\pi}_i^V = 0, \quad (4.60)$$

$$\Delta\delta\tilde{\pi}_{ij} = 0. \quad (4.61)$$

As we said before, there are different choices for  $\epsilon$  and  $\tilde{\epsilon}$  parameter to fix all the gauge freedoms. The most common and well-known gauges are the Newtonian gauge and Synchronous

gauge[62, 74]. The former fix  $\epsilon^S$  such that  $B = 0$ , and choose  $\epsilon_0$  such that  $H = 0$  ( in equation (4.19) ). In DG, this choice is extended imposing similar conditions in (4.20) for  $\tilde{\epsilon}^S$  and  $\tilde{\epsilon}_0$ , such that  $\tilde{B} = \tilde{H} = 0$ . There is no remaining freedom to make a gauge transformation in this scenario. Nevertheless, in this work, we will use the Synchronous gauge, where we will choose  $\epsilon_0$  such that  $E = 0$ , and  $\epsilon^S$  such that  $H = 0$ , (similar conditions for  $\tilde{\epsilon}_0$  and  $\tilde{\epsilon}^S$ ). In the next section, we present the perturbed equations of motion in this frame and we discuss the suitability of this choice for our purposes.

#### 4.1.4 Fields equations and energy momentum conservation in synchronous gauge

Under this gauge fixing, perturbed Einstein equations Eq. (3.8) reads (at first order):

$$-4\pi G(\delta\rho + 3\delta p + \nabla^2\pi^S) = \frac{1}{2}\left(3\ddot{A} + \nabla^2\ddot{B}\right) + \frac{\dot{a}}{2a}\left(3\dot{A} + \nabla^2\dot{B}\right). \quad (4.62)$$

While the energy-momentum conservation gives

$$\delta p + \nabla^2\pi^S + \partial_0[(\bar{\rho} + \bar{p})\delta u] + \frac{3\dot{a}}{a}(\bar{\rho} + \bar{p})\delta u = 0, \quad (4.63)$$

$$\delta\dot{\rho} + \frac{3\dot{a}}{a}(\delta\rho + \delta p) + \nabla^2\left[a^{-2}(\bar{\rho} + \bar{p})\delta u + \frac{\dot{a}}{a}\pi^S\right] + \frac{1}{2}(\bar{\rho} + \bar{p})\partial_0[3A + \nabla^2B] = 0. \quad (4.64)$$

We define

$$\Psi \equiv \frac{1}{2}[3A + \nabla^2B], \quad (4.65)$$

then,

$$-4\pi G a^2(\delta\rho + 3\delta p + \nabla^2\pi^S) = \frac{\partial}{\partial t}\left(a^2\dot{\Psi}\right), \quad (4.66)$$

$$\delta\dot{\rho} + \frac{3\dot{a}}{a}(\delta\rho + \delta p) + \nabla^2\left[a^{-2}(\bar{\rho} + \bar{p})\delta u + \frac{\dot{a}}{a}\pi^S\right] + \frac{1}{2}(\bar{\rho} + \bar{p})\dot{\Psi} = 0. \quad (4.67)$$

The unperturbed Einstein equations correspond to the Friedmann equations. In the delta sector, computations give the non-perturbed equations:

$$3\dot{F}\frac{\dot{a}}{a} = \kappa(3F\bar{\rho} + \tilde{\rho}) \quad (4.68)$$

, and

$$12F\frac{\ddot{a}}{a} + 6F\left(\frac{\dot{a}}{a}\right)^2 + 3\dot{F}\frac{\dot{a}}{a} - 3\ddot{F} = \kappa(\tilde{\rho} + 3\tilde{p} + 3F\bar{\rho} + 3F\bar{p}). \quad (4.69)$$

The perturbed contribution (at first order) is

$$\begin{aligned} & \left[2\dot{F}\frac{\dot{a}}{a} + \ddot{F}\right] [3A + \nabla^2 B] + \left[6F\frac{\dot{a}}{a} + \frac{5}{2}\dot{F}\right] [3\dot{A} + \nabla^2 \dot{B}] - \left[2\frac{\dot{a}}{a}\right] [3\dot{\tilde{A}} + \nabla^2 \dot{\tilde{B}}] \\ & + 3F [3\ddot{A} + \nabla^2 \ddot{B}] - [3\ddot{\tilde{A}} + \nabla^2 \ddot{\tilde{B}}] = \kappa (3\delta\tilde{p} + \delta\tilde{\rho} + F\delta\rho + 3F\delta p + \nabla^2 \tilde{\pi} + F\nabla^2 \pi) \end{aligned} \quad (4.70)$$

Besides, 00 component of delta Energy-momentum conservation in (3.11) give

$$\begin{aligned} & \delta\dot{\tilde{\rho}} + \frac{3\dot{a}}{a}(\delta\tilde{\rho} + \delta\tilde{p}) + \frac{3\dot{F}}{2}(\delta\rho + \delta p) + \nabla^2 \left[ \frac{(\tilde{\rho} + \tilde{p})}{a^2}\delta u + \frac{(\bar{\rho} + \bar{p})F}{a^2}\delta u + \frac{(\bar{\rho} + \bar{p})}{a^2}\delta\tilde{u} \right] \\ & + \frac{(\tilde{\rho} + \tilde{p})}{2}\partial_0[3A + \nabla^2 B] + \frac{(\bar{\rho} + \bar{p})}{2}\partial_0[3\tilde{A} + \nabla^2 \tilde{B}] - \frac{(\bar{\rho} + \bar{p})}{2}\partial_0(F[3A + \nabla^2 B]) = 0, \end{aligned} \quad (4.71)$$

while the  $i0$  component gives

$$\begin{aligned} & \delta\tilde{p} + \partial_0[(\tilde{\rho} + \tilde{p})\delta u] + \partial_0[(\bar{\rho} + \bar{p})\delta\tilde{u}] - \partial_0[(\bar{\rho} + \bar{p})F\delta u] + 3(\bar{\rho} + \bar{p})\dot{F}\delta u \\ & + \frac{3\dot{a}}{a}(\bar{\rho} + \bar{p})\delta\tilde{u} + \frac{3\dot{a}}{a}(\tilde{\rho} + \tilde{p})\delta u - \frac{3\dot{a}}{a}F(\bar{\rho} + \bar{p})\delta u = 0. \end{aligned} \quad (4.72)$$

Analogous to the standard sector, we define

$$\tilde{\Psi} \equiv \frac{1}{2} [3\tilde{A} + \nabla^2 \tilde{B}] , \quad (4.73)$$

then the gravitational equation becomes

$$\begin{aligned} \left[ 2\dot{F}\frac{\dot{a}}{a} + \ddot{F} \right] a^2\Psi + \left[ 6F\frac{\dot{a}}{a} + \frac{5}{2}\dot{F} \right] a^2\dot{\Psi} + 3Fa^2\ddot{\Psi} - \frac{d}{dt} \left( a^2\dot{\Psi} \right) \\ = \frac{\kappa}{2} (3\delta\tilde{p} + \delta\tilde{\rho} + F\delta\rho + 3F\delta p + \nabla^2\tilde{\pi} + F\nabla^2\pi). \end{aligned} \quad (4.74)$$

Now, the delta energy conservation is given by

$$\begin{aligned} \delta\dot{\rho} + \frac{3\dot{a}}{a}(\delta\tilde{\rho} + \delta\tilde{p}) + \frac{3\dot{F}}{2}(\delta\rho + \delta p) + \nabla^2 \left[ \frac{(\tilde{\rho} + \tilde{p})}{a^2}\delta u + \frac{(\bar{\rho} + \bar{p})F}{a^2}\delta u + \frac{(\bar{\rho} + \bar{p})}{a^2}\delta\tilde{u} \right] \\ + (\tilde{\rho} + \tilde{p})\dot{\Psi} + (\bar{\rho} + \bar{p})\dot{\Psi} - (\bar{\rho} + \bar{p})\partial_0(F\Psi) = 0. \end{aligned} \quad (4.75)$$

The study of the non-perturbed sector was already treated in Alfaro et al.[52–54] and applied to the supernovae observations[57]. In Chapter 3 we presented the results that will be useful for our treatment.

We have to remark that our definition of  $\Psi$  is not the usual since the standard definition[62] is with the time derivative of fields  $A$  and  $B$ , respectively. In the delta sector appears explicitly the combinations of these fields without a time derivative, so if the reader wants to compare results with other works, he or she should take into consideration this definition to analyze the solutions. In the next Section, we will discuss the evolution of the cosmological fluctuations, and why of choosing this particular gauge frame which will help us to calculate the scalar contribution to the CMB.

## 4.2 Evolution of cosmological fluctuations

Until now, we have developed the perturbation theory in DG; now, we are interested in studying the evolution of the cosmological fluctuations to have a physical interpretation of the delta matter fields, which this theory naturally introduces. Even in the standard cosmology, the system of equations that describes these perturbations are complicated to allow analytic solutions, and there are comprehensive computer programs to this task, such as CMBfast[58, 59], and CAMB[60]. However, such computer programs can not give a clear

understanding of the physical phenomena involved. Nevertheless, some good approximations allow the compute of the spectrum of the CMB fluctuations with a rather good agreement with these computer programs[61, 62]. In particular, we are going to extend Weinberg approach for this task. This method consists of two main aspects: first, the hydrodynamic limit, which assumes that near recombination time photons were in local thermal equilibrium with the baryonic plasma, then photons could be treated hydro-dynamically, like plasma and cold dark matter. Second, a sharp transition from thermal equilibrium to complete transparency at the moment  $t_{ls}$  of the last scattering.

Since we will reproduce this approach, we consider the Universe's standard components, which means photons, neutrinos, baryons, and cold dark matter. Then the task is to understand the role of their own delta-counterpart. We will also neglect both anisotropic inertia tensors and took the usual state equation for pressures and energy densities and perturbations. Besides, as we will treat photons and delta photons hydro-dynamically, we will use  $\delta u_\gamma = \delta u_B$  and  $\delta \tilde{u}_\gamma = \delta \tilde{u}_B$ . Finally, as the synchronous scheme does not completely fix the gauge freedom, one can use the remaining freedom to put  $\delta u_D = 0$ , which means that cold dark matter evolves at rest with respect to the Universe expansion. In our theory, the extended synchronous scheme also has extra freedom, which we will use to choose  $\delta \tilde{u}_D = 0$  as its standard part. Now we will present the equations for both sectors. However, we will provide more detail in the delta sector because Weinberg[62] already calculates the solution of Einstein's equations.

Einstein's equations and its energy-momentum conservation in Fourier space are

$$\frac{d}{dt} \left( a^2 \dot{\Psi}_q \right) = -4\pi G a^2 (\delta \rho_{Dq} + \delta \rho_{Bq} + 2\delta \rho_{\gamma q} + 2\delta \rho_{\nu q}) , \quad (4.76)$$

$$\delta \dot{\rho}_{\gamma q} + 4H\delta \rho_{\gamma q} - (4q/3a)\bar{\rho}_\gamma \delta u_{\gamma q} = -(4/3)\bar{\rho}_\gamma \dot{\Psi}_q , \quad (4.77)$$

$$\delta \dot{\rho}_{Dq} + 3H\delta \rho_{Dq} = -\bar{\rho}_D \dot{\Psi}_q , \quad (4.78)$$

$$\delta \dot{\rho}_{Bq} + 3H\delta \rho_{Bq} - (q/a)\bar{\rho}_B \delta u_{\gamma q} = -\bar{\rho}_B \dot{\Psi}_q , \quad (4.79)$$

$$\delta \dot{\rho}_{\nu q} + 4H\delta \rho_{\nu q} - (4q/3a)\bar{\rho}_\nu \delta u_{\nu q} = -(4/3)\bar{\rho}_\nu \dot{\Psi}_q , \quad (4.80)$$

where  $H \equiv \dot{a}/a$ . It is useful to rewrite these equations in term of the dimensionless fractional perturbation

$$\delta_{\alpha q} = \frac{\delta\rho_{\alpha q}}{\bar{\rho}_\alpha + \bar{p}_\alpha}, \quad (4.81)$$

where  $\alpha$  can be  $\gamma$ ,  $\nu$ ,  $B$  and  $D$  (photons, neutrinos, baryons and dark matter, respectively).  $a^4\bar{\rho}_\gamma$ ,  $a^4\bar{\rho}_\nu$ ,  $a^3\bar{\rho}_D$ ,  $a^3\bar{\rho}_B$  are time independent quantities, then (4.76)-(4.80) are

$$\frac{d}{dt} \left( a^2 \dot{\Psi}_q \right) = -4\pi G a^2 \left( \bar{\rho}_D \delta_{Dq} + \bar{\rho}_B \delta_{Bq} + \frac{8}{3} \bar{\rho}_\gamma \delta_{\gamma q} + \frac{8}{3} \bar{\rho}_\nu \delta_{\nu q} \right), \quad (4.82)$$

$$\dot{\delta}_{\gamma q} - (q^2/a^2) \delta u_{\gamma q} = -\dot{\Psi}_q \quad (4.83)$$

$$\dot{\delta}_{Dq} = -\dot{\Psi}_q, \quad (4.84)$$

$$\dot{\delta}_{Bq} - (q^2/a^2) \delta u_{Bq} = -\dot{\Psi}_q \quad (4.85)$$

$$\dot{\delta}_{\nu q} - (q^2/a^2) \delta u_{\nu q} = -\dot{\Psi}_q \quad (4.86)$$

$$\frac{d}{dt} \left( \frac{(1+R) \delta u_{\gamma q}}{a} \right) = -\frac{1}{3a} \delta_{\gamma q} \quad (4.87)$$

$$\frac{d}{dt} \left( \frac{\delta u_{\nu q}}{a} \right) = -\frac{1}{3a} \delta_{\nu q}, \quad (4.88)$$

where  $R = 3\bar{\rho}_B/4\bar{\rho}_\gamma$ . By the other side, in delta sector we will also use a dimensionless fractional perturbation. However, this perturbation is defined as the delta transformation of (4.81)<sup>2</sup>,

$$\tilde{\delta}_{\alpha q} \equiv \tilde{\delta} \delta_{\alpha q} = \frac{\delta \tilde{\rho}_{\alpha q}}{\bar{\rho}_\alpha + \bar{p}_\alpha} - \frac{\tilde{\rho}_\alpha + \tilde{p}_\alpha}{\bar{\rho}_\alpha + \bar{p}_\alpha} \delta_{\alpha q}. \quad (4.89)$$

In Section 3.4.3 and 3.4.4, we presented the solutions for the densities (eqs. (3.42), (3.51) and (3.52), with  $C_1 = C_2 = 0$ ), finding

---

<sup>2</sup>We choose this definition because the system of equations now seems as an homogeneous system exactly equal to the GR sector (where now the variables are the tilde-fields) with external forces mediated by the GR solutions. Maybe the most intuitive solution should be

$$\tilde{\delta}_{\alpha q}^{int} = \frac{\delta \tilde{\rho}_{\alpha q}}{\tilde{\rho}_\alpha + \tilde{p}_\alpha},$$

however these definitions are related by

$$\tilde{\delta}_{\alpha q} = \frac{\tilde{\rho}_\alpha + \tilde{p}_\alpha}{\bar{\rho}_\alpha + \bar{p}_\alpha} \left( \tilde{\delta}_{\alpha q}^{int} - \delta_{\alpha q} \right).$$



$$\frac{\tilde{\rho}_R}{\bar{\rho}_R} = -2F(a) \quad \text{and} \quad \frac{\tilde{\rho}_M}{\bar{\rho}_M} = -\frac{3}{2}F(a) \quad (4.90)$$

We will assume that this quotient holds for every component. Also using the result that  $a^4\tilde{\rho}_\gamma/F$ ,  $a^4\tilde{\rho}_\nu/F$ ,  $a^3\tilde{\rho}_D/F$ ,  $a^3\tilde{\rho}_B/F$  are time independent, the equations for the delta sector are

$$\begin{aligned} & \left[ 2\dot{F}\frac{\dot{a}}{a} + \ddot{F} \right] a^2\Psi_q + \left[ 6F\frac{\dot{a}}{a} + \frac{5}{2}\dot{F} \right] a^2\dot{\Psi}_q + 3Fa^2\ddot{\Psi}_q - \frac{d}{dt} \left( a^2\dot{\Psi}_q \right) = \frac{\kappa}{2}a^2 \left[ \bar{\rho}_D\tilde{\delta}_{Dq} \right. \\ & \left. + \bar{\rho}_B\tilde{\delta}_{Bq} + \frac{8}{3}\bar{\rho}_\gamma\tilde{\delta}_{\gamma q} + \frac{8}{3}\bar{\rho}_\nu\tilde{\delta}_{\nu q} - \frac{F}{2}(\bar{\rho}_D\delta_{Dq} + \bar{\rho}_B\delta_{Bq}) - \frac{8}{3}F(\bar{\rho}_\gamma\delta_{\gamma q} + \bar{\rho}_\nu\delta_{\nu q}) \right] \end{aligned} \quad (4.91)$$

$$\dot{\delta}_{\gamma q} - \frac{q^2}{a^2}(\delta\tilde{u}_{\gamma q} + F\delta u_{\gamma q}) + \dot{\Psi}_q - \partial_0(F\Psi_q) = 0 \quad (4.92)$$

$$\dot{\delta}_{Dq} + \dot{\Psi}_q - \partial_0(F\Psi_q) = 0 \quad (4.93)$$

$$\dot{\delta}_{Bq} - \frac{q^2}{a^2}(\delta\tilde{u}_{\gamma q} + F\delta u_{\gamma q}) + \dot{\Psi}_q - \partial_0(F\Psi_q) = 0 \quad (4.94)$$

$$\dot{\delta}_{\nu q} - \frac{q^2}{a^2}(\delta\tilde{u}_{\nu q} + F\delta u_{\nu q}) + \dot{\Psi}_q - \partial_0(F\Psi_q) = 0 \quad (4.95)$$

$$\begin{aligned} & \frac{\tilde{\delta}_{\gamma q}}{3a} + \frac{d}{dt} \left( \frac{(1+R)\delta\tilde{u}_{\gamma q}}{a} \right) + 2F\frac{d}{dt} \left( \frac{(R-\tilde{R})\delta u_{\gamma q}}{a} \right) - F\frac{d}{dt} \left( \frac{(1+R)\delta u_{\gamma q}}{a} \right) \\ & - 2\dot{F}(\tilde{R}-R)\frac{\delta u_{\gamma q}}{a} = 0 \end{aligned} \quad (4.96)$$

$$\frac{\tilde{\delta}_{\nu q}}{3a} + \frac{d}{dt} \left( \frac{\delta\tilde{u}_{\nu q}}{a} \right) - F\frac{d}{dt} \left( \frac{\delta u_{\nu q}}{a} \right) = 0 \quad (4.97)$$

with  $\tilde{R} = 3\tilde{\rho}_D/4\tilde{\rho}_\gamma$ . Due to the definition of tilde fractional perturbation (4.89), solutions for (4.91)-(4.97) can be obtained easily, putting all solutions of GR equal to zero, then the system is exactly equal to the system of equations (4.82)-(4.88) and the solution of tilde perturbations in the homogeneous system are exactly equal to the GR solutions, and then we only need to "turn on" the GR source and find the complete solutions just like a forced-system.

We will impose initial conditions to find solutions valid up to recombination time. At sufficiently early times the Universe was dominated by radiation, and as Friedmann equations

are valid in our theory (in particular the first equation), we can use as a good approximation that  $a \propto \sqrt{t}$  and  $8\pi G\bar{\rho}_R/3 = 1/4t^2$ , while  $R$  and  $\tilde{R} \ll 1$ . Here

$$\bar{\rho}_M \equiv \bar{\rho}_D + \bar{\rho}_B, \quad \bar{\rho}_R \equiv \bar{\rho}_\gamma + \bar{\rho}_\nu. \quad (4.98)$$

Besides, we are interested in adiabatic solutions, in the sense that all the  $\delta_{\alpha q}$  and  $\tilde{\delta}_{\alpha q}$  become equal at very early times. So, we make the ansatz:

$$\delta_{\gamma q} = \delta_{\nu q} = \delta_{Bq} = \delta_{Dq} = \delta_q \quad \delta u_{\gamma q} = \delta u_{\nu q} = \delta u_q, \quad (4.99)$$

$$\tilde{\delta}_{\gamma q} = \tilde{\delta}_{\nu q} = \tilde{\delta}_{Bq} = \tilde{\delta}_{Dq} = \tilde{\delta}_q \quad \delta \tilde{u}_{\gamma q} = \delta \tilde{u}_{\nu q} = \delta \tilde{u}_q. \quad (4.100)$$

Finally, we drop the term  $q^2/a^2$  because we are considering very early times. Then Equations (4.82)-(4.88) becomes

$$\frac{d}{dt}(t\Psi_q) = -\frac{1}{t}\delta_q, \quad (4.101)$$

$$\dot{\delta}_q = -\Psi_q, \quad (4.102)$$

$$\frac{d}{dt}\left(\frac{\delta u_q}{\sqrt{t}}\right) = -\frac{1}{t}\delta_q. \quad (4.103)$$

While equations (4.91)-(4.97) becomes

$$\left[2\dot{F}\frac{\dot{a}}{a} + \ddot{F}\right]a^2\Psi_q + \left[6F\frac{\dot{a}}{a} + \frac{5}{2}\dot{F}\right]a^2\dot{\Psi}_q + 3Fa^2\ddot{\Psi}_q - \frac{d}{dt}\left(a^2\dot{\Psi}_q\right) = \frac{a^2}{t^2}(\tilde{\delta}_q - F\delta_q), \quad (4.104)$$

$$\dot{\delta}_q + \dot{\tilde{\Psi}}_q - \partial_0(F\Psi_q) = 0, \quad (4.105)$$

$$\frac{\tilde{\delta}_q}{3a} + \frac{d}{dt}\left(\frac{\delta \tilde{u}_q}{a}\right) - F\frac{d}{dt}\left(\frac{\delta u_q}{a}\right) = 0. \quad (4.106)$$

Inspection of Eq. (3.50) show that at this era that for  $Y \ll C = Y_{EQ}$  we have  $F \propto -L_2 a \sqrt{C}/3$  (as we are using  $a_0 = 1$  we have  $Y = a$ ). Also, the time is obtained by (3.44)

$$t(Y) = \frac{2\sqrt{1+C}}{3H_0} \left( \sqrt{Y+C}(Y-2C) + 2C^{\frac{3}{2}} \right), \quad (4.107)$$

we recall that  $H_0 = \dot{a}_0/a_0$  is the usual Hubble parameter which is not longer the physical Hubble parameter observed by Planck[38] and Riess[34]. Thus, in radiation era time and  $a(t)$  was related by  $a(t) = (3H_0\sqrt{C}/\sqrt{1+C})^{1/2}t^{1/2}$ . The complete system Eqs. (4.101)-(4.103) and Eqs. (4.104)-(4.106) has analytical solution:

$$\delta_{\gamma q} = \delta_{Bq} = \delta_{Dq} = \delta_{\nu q} = \frac{q^2 t^2 \mathcal{R}_q}{a^2}, \quad (4.108)$$

$$\dot{\Psi}_q = -\frac{t q^2 \mathcal{R}_q}{a^2}, \quad (4.109)$$

$$\delta u_{\gamma q} = \delta u_{\nu q} = -\frac{2t^3 q^2 \mathcal{R}_q}{9a^2}, \quad (4.110)$$

where<sup>3</sup>

$$q^2 \mathcal{R}_q \equiv -a^2 H \Psi_q + 4\pi G a^2 \delta \rho_q + q^2 H \delta u_q, \quad (4.111)$$

is a gauge invariant quantity, which take a time independent value for  $q/a \ll H$ . Here  $H = \dot{a}/a$  is the GR definition of the Hubble parameter, which we recall is not longer the physical one. On the other hand, we get

$$\tilde{\delta}_q = -\frac{L_2 \sqrt{C} q^2 \mathcal{R}_q t^2}{3a}, \quad (4.112)$$

$$\dot{\tilde{\Psi}}_q = \frac{L_2 \sqrt{C} q^2 \mathcal{R}_q t}{a}, \quad (4.113)$$

$$\delta \tilde{u}_q = \frac{L_2 \sqrt{C} q^2 \mathcal{R}_q t^3}{a} \quad (4.114)$$

We will talk about this initial conditions later. Note that Eq. (4.83) and (4.85) give

---

<sup>3</sup>the definition of  $\mathcal{R}_q$  is given in section 5.4: Conservation outside the horizon, Cosmology, Weinberg.

$$\frac{d}{dt}(\delta_\gamma - \delta_B) = 0. \quad (4.115)$$

This implies that if we start from adiabatic solutions,  $\delta_\gamma = \delta_B$  is true for all the Universe evolution (the same happens for its delta version, from Eq. (4.92) and Eq (4.94)).

### 4.2.1 Matter era

In this era ( $a \gg C$ ) we have  $a \propto t^{2/3}$ , then (still using  $R = \tilde{R} = 0$ ) we have

$$\frac{d}{dt}(a^2 \Psi_q) = -4\pi G \bar{\rho}_D a^2 \delta_{Dq}, \quad (4.116)$$

$$\dot{\delta}_{Dq} = -\Psi_q, \quad (4.117)$$

$$\frac{d}{dt}\left(\frac{\delta u_{\gamma q}}{a}\right) = -\frac{1}{3a}\delta_{\gamma q}, \quad (4.118)$$

$$\frac{d}{dt}\left(\frac{\delta u_{\nu q}}{a}\right) = -\frac{1}{3a}\delta_{\nu q}. \quad (4.119)$$

For the delta sector,

$$\begin{aligned} \left[2\dot{F}\frac{\dot{a}}{a} + \ddot{F}\right] a^2 \Psi_q + \left[6F\frac{\dot{a}}{a} + \frac{5}{2}\dot{F}\right] a^2 \dot{\Psi}_q + 3Fa^2 \ddot{\Psi}_q, \\ -\frac{d}{dt}\left(a^2 \dot{\tilde{\Psi}}_q\right) = \frac{2a^2}{3t^2}\left(\tilde{\delta}_{Dq} - F\frac{\delta_{Dq}}{2}\right), \end{aligned} \quad (4.120)$$

$$\dot{\tilde{\delta}}_{\gamma q} - \frac{q^2}{a^2}(\delta \tilde{u}_{\gamma q} + F\delta u_{\gamma q}) + \dot{\tilde{\Psi}}_q - \partial_0(F\Psi_q) = 0, \quad (4.121)$$

$$\dot{\tilde{\delta}}_{Dq} + \dot{\tilde{\Psi}}_q - \partial_0(F\Psi_q) = 0, \quad (4.122)$$

$$\frac{\tilde{\delta}_{\gamma q}}{3a} + \frac{d}{dt}\left(\frac{\delta \tilde{u}_{\gamma q}}{a}\right) - F\frac{d}{dt}\left(\frac{\delta u_{\gamma q}}{a}\right) = 0 \quad (4.123)$$

Where,

$$a(t) = \left( \frac{3H_0}{2\sqrt{1+C}} \right)^{2/3} t^{2/3}, \quad (4.124)$$

$$F(t) = -\frac{L}{3}a(t)^{3/2}. \quad (4.125)$$

It is remarkable that in GR sector there are exact solutions, given by

$$\delta_{Dq} = \frac{9q^2t^2\mathcal{R}_q\mathcal{T}(\kappa)}{10a^2} \quad (4.126)$$

$$\dot{\Psi}_q = -\frac{3q^2t\mathcal{R}_q\mathcal{T}(\kappa)}{5a^2} \quad (4.127)$$

$$\delta_{\gamma q} = \delta_{\nu q} = \frac{3\mathcal{R}_q}{5} \left[ \mathcal{T}(\kappa) - \mathcal{S}(\kappa) \cos \left( q \int_0^t \frac{dt}{\sqrt{3}a} + \Delta(\kappa) \right) \right], \quad (4.128)$$

$$\delta u_{\gamma q} = \delta u_{\nu q} = \frac{3t\mathcal{R}_q}{5} \left[ -\mathcal{T}(\kappa) + \mathcal{S}(\kappa) \frac{a}{\sqrt{3}qt} \sin \left( q \int_0^t \frac{dt}{\sqrt{3}a} + \Delta(\kappa) \right) \right] \quad (4.129)$$

Where  $\mathcal{T}(\kappa)$ ,  $\mathcal{S}(\kappa)$  and  $\Delta(\kappa)$  are time-independent dimensionless functions of the dimensionless re-scaled wave number

$$\kappa \equiv \frac{q\sqrt{2}}{a_{EQ}H_{EQ}} \quad (4.130)$$

$a_{EQ}$  and  $H_{EQ}$  are, respectively, the Robertson-Walker scale factor and the expansion rate at matter-radiation equality. These are known as transfer functions. (These functions can only depend on  $\kappa$  because they must be independent of the spatial coordinates normalization and are dimensionless. A complete discussion of the behavior of these functions can be found in [62]). On the other side, delta perturbations have not an exact solution, and numerical calculation is needed to find them, however we will not present numerical solutions because there are not part of this Thesis, and we only will estimate the initial conditions of the perturbations at the end of this section.

In order to get all transfer functions we have to compare solutions with the full equation system (with  $\rho_B = \tilde{\rho}_B = 0$ ). To do this task lets make the change of variable  $y \equiv a/a_{EQ} = a/C$ , this means

$$\frac{d}{dt} = \frac{H_{EQ}}{\sqrt{2}} \frac{\sqrt{1+y}}{y} \frac{d}{dy} \quad (4.131)$$

Also, we will use the following parametrization for all perturbations

$$\begin{aligned} \delta_{Dq} &= \kappa^2 \mathcal{R}_q^0 d(y)/4, & \delta_{\gamma q} &= \delta_{\nu q} = \kappa^2 \mathcal{R}_q^0 r(y)/4, \\ \dot{\Psi}_q &= (\kappa^2 H_{EQ}/4\sqrt{2}) \mathcal{R}_q^0 f(y), & \delta u_{\gamma q} &= \delta u_{\nu q} = (\kappa^2 \sqrt{2}/4H_{EQ}) \mathcal{R}_q^0 g(y), \end{aligned}$$

and

$$\begin{aligned} \tilde{\delta}_{Dq} &= \kappa^2 \mathcal{R}_q^0 \tilde{d}(y)/4, & \tilde{\delta}_{\gamma q} &= \tilde{\delta}_{\nu q} = \kappa^2 \mathcal{R}_q^0 \tilde{r}(y)/4 \\ \dot{\tilde{\Psi}}_q &= (\kappa^2 H_{EQ}/4\sqrt{2}) \mathcal{R}_q^0 \tilde{f}(y), & \delta \tilde{u}_{\gamma q} &= \delta \tilde{u}_{\nu q} = (\kappa^2 \sqrt{2}/4H_{EQ}) \mathcal{R}_q^0 \tilde{g}(y). \end{aligned}$$

Then Eqs. (4.116)-(4.119) and Eqs. (4.120)-(4.123) become

$$\sqrt{1+y} \frac{d}{dy} (y^2 f(y)) = -\frac{3}{2} d(y) - \frac{4r(y)}{y}, \quad (4.132)$$

$$\sqrt{1+y} \frac{d}{dy} r(y) - \frac{\kappa^2 g(y)}{y} = -yf(y), \quad (4.133)$$

$$\sqrt{1+y} \frac{d}{dy} d(y) = -yf(y), \quad (4.134)$$

$$\sqrt{1+y} \frac{d}{dy} \left( \frac{g(y)}{y} \right) = -\frac{r(y)}{3}, \quad (4.135)$$

and

$$\begin{aligned}
& -[(1+2y)yF'(y) + y(1+y)F''(y)]d(y) + \left[6F(y) + \frac{5}{2}yF'(y)\right]y\sqrt{1+y}f(y) \\
& + 3F(y)y^2\sqrt{1+y}f'(y) - \sqrt{1+y}\frac{d}{dy}\left(y^2\tilde{f}(y)\right) = \frac{3\tilde{d}(y)}{2} + \frac{4\tilde{r}(y)}{y} \\
& - \frac{3F(y)d(y)}{4} - \frac{4F(y)r(y)}{y}, \quad (4.136)
\end{aligned}$$

$$\sqrt{1+y}\frac{d}{dy}\tilde{d}(y) = -y\tilde{f}(y) - \sqrt{1+y}\frac{d}{dy}d(y), \quad (4.137)$$

$$\sqrt{1+y}\frac{d}{dy}\tilde{r}(y) = \frac{\kappa^2}{y}[\tilde{g}(y) + F(y)g(y)] - y\tilde{f}(y) - \sqrt{1+y}\frac{d}{dy}d(y), \quad (4.138)$$

$$\sqrt{1+y}\frac{d}{dy}\left(\frac{\tilde{g}(y)}{y}\right) = -\frac{\tilde{r}(y)}{3} + \sqrt{1+y}F(y)\frac{d}{dy}\left(\frac{g(y)}{y}\right). \quad (4.139)$$

In this notation, the initial conditions are

$$\begin{aligned}
d(y) &= r(y) \rightarrow y^2 \\
f(y) &\rightarrow -2 \\
g(y) &\rightarrow -\frac{y^4}{9}
\end{aligned}$$

For delta sector,

$$\begin{aligned}
\tilde{d}(y) &= \tilde{r}(y) \rightarrow -\frac{L_2C^{3/2}}{3}y^3 \\
\tilde{f}(y) &\rightarrow \sqrt{2}L_2C^{3/2}y \\
\tilde{g}(y) &\rightarrow \frac{L_2C^{3/2}}{2}y^5
\end{aligned}$$

From supernovae fit, we know that  $C \sim 10^{-4}$  and  $L \sim 0.45$  [53, 57], thus we can estimate that delta matter perturbation at the beginning of the Universe was much smaller than standard matter. For example, at  $y \sim 10^{-3}$  the ratio between components of the Universe is  $|\tilde{\delta}_\alpha/\delta_\alpha| \sim 10^{-10}$ . This does not mean that the intuitive fractional perturbation of delta matter  $\tilde{\delta}_{\alpha q}^{int} = \delta\tilde{\rho}_\alpha/(\tilde{\rho}_\alpha + \tilde{p})$  was much lower than the standard perturbations  $\delta_\alpha$  because

$$\tilde{\delta}_{\alpha q}(t) \propto (\tilde{\delta}_{\alpha q}^{int} - \delta_{\alpha q}) , \quad (4.140)$$

this implies that  $\tilde{\delta}_{\alpha q}^{int} \sim \delta_{\alpha q}$ .

We do not show numerical solutions here because the aim of this Thesis is to trace a guide for future work, in particular, in the numeric computation of multipole coefficients for temperature fluctuations in the CMB. However, in the next Chapter we will derive a formula to do that computation.

After finishing this Chapter, we must include the effect of taking  $R$  and  $\tilde{R} \neq 0$ , this could be included using a WKB approximation described in Appendix A, besides we also need to include another effect. Before the moment of last scattering the fluid of baryons and photons was damped due Thompson Scattering. This effect is known as the *Silk damping* [76, 77]. Then the full solutions for photons density perturbations are

$$\begin{aligned} \delta_{\gamma q} = & \frac{3\mathcal{R}_q^o}{5} [\mathcal{T}(\kappa)(1 + 3R) \\ & - (1 + R)^{-1/4} e^{-\int_0^t \Gamma dt} \mathcal{S}(\kappa) \cos \left( \int_0^t \frac{q dt}{\sqrt{3(1 + R(t))} a_{DG}(t)} + \Delta(\kappa) \right) ] , \end{aligned} \quad (4.141)$$

$$\begin{aligned} \delta u_{\gamma q} = & \frac{3\mathcal{R}_q^o}{5} \left[ -t\mathcal{T}(\kappa) + \frac{a_{DG}}{\sqrt{3}q(1 + R)^{3/4}} e^{-\int_0^t \Gamma dt} \mathcal{S}(\kappa) \right. \\ & \times \left. \sin \left( \int_0^t \frac{q dt}{\sqrt{3(1 + R(t))} a_{DG}(t)} + \Delta(\kappa) \right) \right] , \end{aligned} \quad (4.142)$$

where

$$\Gamma = \frac{q^2 t_\gamma}{6a_{DG}^2(1 + R)} \left[ \frac{16}{15} + \frac{R^2}{1 + R} \right] \quad (4.143)$$

Note that at this level we used  $a \sim a_{DG}$  which is true for  $t < t_{ls}$ . In particular we will see that those solutions at the moment of last scattering will play the crucial role when computing the temperature multipole coefficients of the CMB.



### 4.3 Summary and Conclusions

We have study the cosmological fluctuations in DG, to do that we perturbed the FLRW background of the theory and studied how the fields transform under an space-time coordinate transformation. We found that to fix gauge freedoms, DG extends the usual choices in GR, such as the Newtonian and Synchronous gauge. The extended Newtonian gauge fix all the degrees of freedom as usual, while Synchronous scenario left a remaining freedom that we can use it to set the velocity field of dark matter equal to zero, this mean that for us dark matter and its delta version evolves in rest with respect to the evolution of the Universe. This choice simplify the integration of the equations of this theory allowing us to get analytical solutions in the beginning of the Universe. When solving the matter-dominated era, we need to add some effects due the transition from  $R = 0$  to  $R \neq 0$ , in particular we can mediated this by the WKB approximation. Besides, the fluid of photons and baryons is damped by viscosity and heat conduction due Thompson scattering, so we need to include this effect.

One could use these perturbations to study of the very beginning of the Universe, such as inflationary scenarios, as for later effects, such as BAOs and others. However, in the next Chapter we will present the temperature fluctuations coming from the moment of last scattering  $t_{ls}$ , where we will present a formula for the scalar contribution to the CMB.



# Chapter 5

## Temperature Fluctuations

In this Chapter we present the derivation of temperature fluctuations coming from the moment of last scattering because we are interested in the CMB observations. However the analysis could be done for any photons coming from any source. The complete derivation should consider the evolution of Boltzmann equations for photons. Nevertheless, as photons follow geodesics in DG, we can study their propagation in the FLRW perturbed coordinates under the condition  $\mathbf{g}_{i0} = 0$ , because we are not considering angular deflections of photons when travelling to us.

### 5.1 Derivation of temperature fluctuations

As we saw in Section 4.1, photons moves in the metric (imposing  $\mathbf{g}_{i0} = 0$ )

$$\begin{aligned}\mathbf{g}_{00} &= -((1 + 3F(t))c^2 + E(\mathbf{x}, t) + \tilde{E}(\mathbf{x}, t)) \\ \mathbf{g}_{i0} &= 0 \\ \mathbf{g}_{ij} &= a^2(t)(1 + F(t))\delta_{ij} + h_{ij}(\mathbf{x}, t) + \tilde{h}_{ij}(\mathbf{x}, t) ,\end{aligned}\tag{5.1}$$

A ray of light propagating to the origin of the FRLW coordinate system , from a direction  $\hat{n}$ , will have a comoving radial coordinate  $r$  related with  $t$  by

$$\begin{aligned}
0 &= \bar{\mathbf{g}}_{\mu\nu} dx^\mu dx^\nu = -((1 + 3F(t))c^2 + E(r\hat{n}, t) + \tilde{E}(r\hat{n}, t))dt^2 \\
&+ (a^2(t)(1 + F(t)) + h_{rr}(r\hat{n}, t) + \tilde{h}_{rr}(r\hat{n}, t))dr^2,
\end{aligned} \tag{5.2}$$

in other words,

$$\begin{aligned}
\frac{dr}{dt} &= - \left( \frac{(1 + 3F(t))c^2 + E + \tilde{E}}{a^2(t)(1 + F(t)) + h_{rr} + \tilde{h}_{rr}} \right)^{1/2} \\
&\simeq - \frac{c}{a_{DG}(t)} + \frac{c(h_{rr} + \tilde{h}_{rr})}{2(1 + 3F(t))a_{DG}^3(t)} - \frac{E + \tilde{E}}{2(1 + 3F(t))ca_{DG}(t)},
\end{aligned} \tag{5.3}$$

where  $a_{DG}(t)$  is the modified scale factor defined in (3.34)

$$a_{DG}(t) = a(t) \sqrt{\frac{1 + F(t)}{1 + 3F(t)}}. \tag{5.4}$$

Now we will use the approximation of a sharp transition between opaque and transparent Universe at a moment  $t_{ls}$  of last scattering, at temperature  $T \simeq 3000$  K. With this approximation, the relevant term at first order in Eq. (5.3) is

$$r(t) = c \left[ s(t) + \int_{t_{ls}}^t \frac{dt'}{a_{DG}(t')} N(cs(t')\hat{n}, t') \right], \tag{5.5}$$

where

$$N(\mathbf{x}, t) \equiv \frac{1}{2(1 + 3F)} \left[ \frac{h_{rr}(\mathbf{x}, t) + \tilde{h}_{rr}(\mathbf{x}, t)}{a_{DG}^2} - \frac{E(\mathbf{x}, t)}{c^2} - \frac{\tilde{E}(\mathbf{x}, t)}{c^2} \right], \tag{5.6}$$

and  $s(t)$  is the zero order solution for the radial coordinate.  $s(t) = r_{ls}$  when  $t = t_{ls}$ :

$$s(t) = r_{ls} - \int_{t_{ls}}^t \frac{dt'}{a_{DG}(t')} = \int_t^{t_0} \frac{dt'}{a_{DG}(t')}. \tag{5.7}$$

If a ray of light arrives to  $r = 0$  at a time  $t_0$ , then Eq. (5.5) gives

$$0 = s(t_0) + \int_{t_{ls}}^t \frac{dt'}{a_{DG}(t')} N(cs(t')\hat{n}, t') = r_{ls} + \int_{t_{ls}}^{t_0} \frac{dt}{a_{DG}(t)} (N(cs(t)\hat{n}, t) - 1) . \quad (5.8)$$

A time interval  $\delta t_{ls}$ , between departure of successive rays of light at time  $t_{ls}$  of last scattering, produces an interval of time  $\delta t_0$ , between the arrival of the rays of light at  $t_0$ , given by the variation of Eq. (5.8):

$$\begin{aligned} 0 = \frac{\delta t_{ls}}{a_{DG}(t_{ls})} & \left[ 1 - N(cr_{ls}\hat{n}, t_{ls}) + c \int_{t_{ls}}^{t_0} \frac{dt}{a_{DG}(t)} \left( \frac{\partial N(r(t)\hat{n}, t)}{\partial r} \right)_{r=cs(t)} \right] \\ & + \delta t_{ls} (\partial u_\gamma^r(cr_{ls}\hat{n}, t_{ls}) + \partial \tilde{u}_\gamma^r(cr_{ls}\hat{n}, t_{ls})) + \frac{\delta t_0}{a_{DG}(t_0)} [-1 + N(0, t_0)] . \end{aligned} \quad (5.9)$$

The velocity terms of the photon-gas or photon-electron-nucleon arise because of the variation respect to the time of the radial coordinate  $r_{ls}$  described by the Eq. (5.8). The exchange rate of  $N(s(t)\hat{n}, t)$  is

$$\frac{d}{dt} N(s(t)\hat{n}, t) = \left( \frac{\partial}{\partial t} N(r\hat{n}, t) \right)_{r=cs(t)} - \frac{c}{a_{DG}(t)} \left( \frac{\partial N(r\hat{n}, t)}{\partial r} \right)_{r=cs(t)} ,$$

then,

$$\begin{aligned} 0 = \frac{\delta t_{ls}}{a_{DG}(t_{ls})} & \left[ 1 - N(0, t_{ls}) + \int_{t_{ls}}^{t_0} dt \left( \frac{\partial N(r\hat{n}, t)}{\partial t} \right)_{r=cs(t)} \right] \\ & + \delta t_{ls} (\partial u_\gamma^r(r_{ls}\hat{n}, t_{ls}) + \partial \tilde{u}_\gamma^r(r_{ls}\hat{n}, t_{ls})) + \frac{\delta t_0}{a_{DG}(t_0)} [-1 + N(0, t_0)] . \end{aligned} \quad (5.10)$$

This result gives the ratio between the time intervals between ray of lights that are emitted and received. However, we are interested in this ratio, but for the proper time, that in DG it is defined with the original metric  $g_{\mu\nu}$ :

$$\delta\tau_L = \sqrt{1 + \frac{E(r_{ls}, t_{ls})}{c^2}} \delta t_{ls} , \quad \delta\tau_0 = \sqrt{1 + \frac{E(0, t_0)}{c^2}} \delta t_0 , \quad (5.11)$$

At first order, it gives the ratio between a received frequency and an emitted one:

$$\frac{\nu_0}{\nu_L} = \frac{\delta\tau_L}{\delta\tau_0} = \frac{a_{DG}(t_{ls})}{a_{DG}(t_0)} \left[ 1 + \frac{1}{2c^2} (E(r_{ls}\hat{n}, t) - E(0, t_0)) - \int_{t_{ls}}^{t_0} \left( \frac{\partial}{\partial t} N(r\hat{n}, t) \right)_{r=cs(t)} dt - a_{DG}(t) (\delta u_\gamma^r(r_{ls}\hat{n}, t) + \delta \tilde{u}_\gamma^r(r_{ls}\hat{n}, t)) \right] \quad (5.12)$$

Eq. (5.12) extended the expression for the redshift in the perturbed background. The observed temperature at the present time  $t_0$  from direction  $\hat{n}$  is

$$T(\hat{n}) = \left( \frac{\nu_0}{\nu_L} \right) (\bar{T}(t_{ls}) + \delta T(cr_{ls}\hat{n}, t_{ls})) , \quad (5.13)$$

In absence of perturbations, the observed temperature in all directions should be

$$T_0 = \left( \frac{a_{DG}(t_{ls})}{a_{DG}(t_0)} \right) \bar{T}(t_{ls}) , \quad (5.14)$$

therefore, the ratio between the observed temperature shift that comes from direction  $\hat{n}$  and the unperturbed value is

$$\begin{aligned} \frac{\Delta T(\hat{n})}{T_0} &\equiv \frac{T(\hat{n}) - T_0}{T_0} = \frac{\nu_0 a_{DG}(t_0)}{\nu_L a_{DG}(t_{ls})} - 1 + \frac{\delta T(cr_{ls}\hat{n}, t_{ls})}{\bar{T}(t_{ls})} \\ &= \frac{1}{2c^2} (E(r_{ls}\hat{n}, t) - E(0, t_0)) - \int_{t_{ls}}^{t_0} dt \left( \frac{\partial}{\partial t} N(r\hat{n}, t) \right)_{r=cs(t)} \\ &\quad - a_{DG}(t) (\delta u_\gamma^r(r_{ls}\hat{n}, t) + \delta \tilde{u}_\gamma^r(r_{ls}\hat{n}, t)) + \frac{\delta T(cr_{ls}\hat{n}, t_{ls})}{\bar{T}(t_{ls})} . \end{aligned} \quad (5.15)$$

For scalar perturbations in any gauge with  $\mathbf{h}_{i0} = 0$ , the metric perturbations are

$$\begin{aligned}
h_{00} &= -E \quad , \quad h_{ij} = (1 + F)a^2 \left[ A\delta_{ij} + \frac{\partial^2 B}{\partial x^i \partial x^j} \right] , \\
\tilde{h}_{00} &= -\tilde{E} \quad , \quad \tilde{h}_{ij} = (1 + F)a^2 \left[ \tilde{A}\delta_{ij} + \frac{\partial^2 \tilde{B}}{\partial x^i \partial x^j} \right] .
\end{aligned} \tag{5.16}$$

Besides for scalar perturbations radial velocity of the photon fluid and the delta versions are given in terms of the velocity potentials  $\delta u_\gamma$  and  $\delta \tilde{u}_\gamma$ , respectively,

$$\begin{aligned}
\delta u_\gamma^r &= (\bar{g} + \tilde{g})^{r\mu} \frac{\partial \delta u_\gamma}{\partial x^\mu} = \frac{1}{(1 + F(t))a^2} \frac{\partial \delta u_\gamma}{\partial r} \\
\delta \tilde{u}_\gamma^r &= (\bar{g} + \tilde{g})^{r\mu} \frac{\partial \delta \tilde{u}_\gamma}{\partial x^\mu} = \frac{1}{(1 + F(t))a^2} \frac{\partial \delta \tilde{u}_\gamma}{\partial r} .
\end{aligned} \tag{5.17}$$

Then Eq. (5.15) gives the scalar contribution to temperature fluctuations

$$\begin{aligned}
\left( \frac{\Delta T(\hat{n})}{T_0} \right)^S &= \frac{1}{2c^2} (E(r_{ls}\hat{n}, t) - E(0, t_0)) - \int_{t_{ls}}^{t_0} dt \left( \frac{\partial}{\partial t} N(r\hat{n}, t) \right)_{r=cs(t)} \\
&- \frac{1}{(1 + 3F(t))a_{DG}} \left( \frac{\partial \delta u_\gamma(cr_{ls}\hat{n}, t)}{\partial r} + \frac{\partial \delta \tilde{u}_\gamma(cr_{ls}\hat{n}, t)}{\partial t} \right) \\
&+ \frac{\delta T(cr_{ls}\hat{n}, t_{ls})}{\bar{T}(t_{ls})} ,
\end{aligned} \tag{5.18}$$

where

$$N = \frac{1}{2} \left[ A + \frac{\partial^2 B}{\partial r^2} + \left( \tilde{A} + \frac{\partial^2 \tilde{B}}{\partial r^2} \right) - \frac{E}{1 + 3F} - \frac{\tilde{E}}{1 + 3F} \right] . \tag{5.19}$$

In the next step we will study the gauge transformations of these fluctuations. The following identity for the fields  $B$  and  $\tilde{B}$  will be useful:

$$\left(\frac{\partial^2 \dot{B}}{\partial r^2}\right)_{r=s(t)} = - \left( \frac{d}{dt} \left[ a_{DG} \frac{\partial \dot{B}}{\partial r} + a_{DG} \dot{a}_{DG} \dot{B} + a_{DG}^2 \ddot{B} \right] + \frac{\partial}{\partial t} \left[ a_{DG} \dot{a}_{DG} \dot{B} + a_{DG}^2 \ddot{B} \right] \right)_{r=s(t)}. \quad (5.20)$$

Then, the temperature fluctuations are described by

$$\left(\frac{\Delta T(\hat{n})}{T_0}\right)^S = \left(\frac{\Delta T(\hat{n})}{T_0}\right)_{early}^S + \left(\frac{\Delta T(\hat{n})}{T_0}\right)_{late}^S + \left(\frac{\Delta T(\hat{n})}{T_0}\right)_{ISW}^S \quad (5.21)$$

where

$$\begin{aligned} \left(\frac{\Delta T(\hat{n})}{T_0}\right)_{early}^S &= -\frac{1}{2}a_{DG}(t_{ls})\dot{a}_{DG}(t_{ls})\dot{B}(r_{ls}\hat{n}, t_{ls}) - \frac{1}{2}a_{DG}^2(t_{ls})\ddot{B}(r_{ls}\hat{n}, t_{ls}) + \frac{1}{2}E(r_{ls}\hat{n}, t_{ls}) + \frac{\delta T(r_{ls}\hat{n})}{\bar{T}(t_{ls})} \\ &- a_{DG}(t_{ls}) \left[ \frac{\partial}{\partial r} \left( \frac{1}{2}\dot{B}(r\hat{n}, t_{ls}) + \frac{1}{(1+3F(t_{ls}))a_{DG}^2(t_{ls})}\delta u_\gamma(r\hat{n}, t_{ls}) \right) \right]_{r=r_{ls}} \\ &- \left\{ \left( \frac{1}{2}a_{DG}(t_{ls})\dot{a}_{DG}(t_{ls})\dot{B}(r_{ls}\hat{n}, t_{ls}) + \frac{1}{2}a_{DG}^2(t_{ls})\ddot{B}(r_{ls}\hat{n}, t_{ls}) \right) \right. \\ &+ \left. a_{DG}(t_{ls}) \left[ \frac{\partial}{\partial r} \left( \frac{1}{2}\dot{B}(r\hat{n}, t_{ls}) + \frac{1}{(1+3F(t_{ls}))a_{DG}^2(t_{ls})}\delta \tilde{u}_\gamma(r\hat{n}, t_{ls}) \right) \right]_{r=r_{ls}} \right\} \end{aligned} \quad (5.22)$$

$$\begin{aligned} \left(\frac{\Delta T(\hat{n})}{T_0}\right)_{late}^S &= \frac{1}{2}a_{DG}(t_0)\dot{a}_{DG}(t_0)\dot{B}(0, t_0) + \frac{1}{2}a_{DG}^2(t_0)\ddot{B}(0, t_0) - \frac{1}{2}E(0, t_0) \\ &+ a_{DG}(t_0) \left[ \frac{\partial}{\partial r} \left( \frac{1}{2}\dot{B}(r\hat{n}, t_0) + \frac{1}{(1+3F(t_0))a_{DG}^2(t_0)}\delta u_\gamma(r\hat{n}, t_0) \right) \right]_{r=0} \\ &+ \left\{ \left( \frac{1}{2}a_{DG}(t_0)\dot{a}_{DG}(t_0)\dot{B}(0, t_0) + \frac{1}{2}a_{DG}^2(t_0)\ddot{B}(0, t_0) \right) \right. \\ &+ \left. a_{DG}(t_0) \left[ \frac{\partial}{\partial r} \left( \frac{1}{2}\dot{B}(r\hat{n}, t_0) + \frac{1}{(1+3F(t_0))a_{DG}^2(t_0)}\delta \tilde{u}_\gamma(r\hat{n}, t_0) \right) \right]_{r=r_{ls}} \right\} \end{aligned} \quad (5.23)$$



$$\begin{aligned}
\left(\frac{\Delta T(\hat{n})}{T_0}\right)_{ISW}^S &= -\frac{1}{2} \int_{t_{ls}}^{t_0} dt \left\{ \frac{\partial}{\partial t} \left[ a_{DG}^2(t) \ddot{B}(r\hat{n}, t) + a_{DG}(t) \dot{a}_{DG}(t) \dot{B}(r\hat{n}, t) + A(r\hat{n}, t) - \frac{E(r\hat{n}, t)}{1+3F(t)} \right. \right. \\
&\quad \left. \left. + \left( a_{DG}^2(t) \ddot{\tilde{B}}(r\hat{n}, t) + a_{DG}(t) \dot{a}_{DG}(t) \dot{\tilde{B}}(r\hat{n}, t) + \tilde{A}(r\hat{n}, t) - \frac{\tilde{E}(r\hat{n}, t)}{1+3F(t)} \right) \right] \right\} \quad (5.24)
\end{aligned}$$

The “late” term is the sum of independent direction terms and a term proportional to  $\hat{n}$ , which was added to represent the local anisotropies of the gravitational field and the local fluid. In GR, these terms only contribute to the multipole expansion for  $l = 0$  and  $l = 1$ . Thus we will ignore their contribution to DG. The acronym ISW refers to the integrate Sachs-Wolve effect[78, 79] and involved the evolution of perturbations from the moment of last scattering  $t_{ls}$  until the present. We will refer to this effect in the next section.

### 5.1.1 Gauge transformations

We need to study the gauge transformations for photons propagating in the metric  $\mathbf{g}_{\mu\nu}$  with a parameter  $\epsilon_\mu$ . The transformations are

$$\begin{aligned}
\Delta A &= \frac{2\dot{a}}{(1+F)a} \frac{\epsilon_0}{1+3F}, \quad \Delta B = -\frac{2}{1+F} \frac{\epsilon^S}{(1+F)a^2}, \\
\Delta C_i &= -\frac{1}{1+F} \frac{\epsilon_i^V}{(1+F)a^2}, \quad \Delta D_{ij} = 0, \quad \Delta E = 2 \frac{\partial}{\partial t} \left( \frac{\epsilon_0}{1+3F} \right), \\
\Delta H &= -\frac{1}{\sqrt{1+F}a} \left[ a^2 \frac{\partial}{\partial t} \left( \frac{\epsilon^S}{(1+F)a^2} \right) + \frac{\epsilon_0}{(1+3F)} \right], \quad \Delta G_i = -\frac{a}{\sqrt{1+F}} \frac{\partial}{\partial t} \left( \frac{\epsilon_i^V}{(1+F)a^2} \right).
\end{aligned} \quad (5.25)$$

and

$$\begin{aligned}
\Delta\tilde{A} &= \frac{1}{(1+F)a^2} \left[ \frac{\partial}{\partial t} (Fa^2) \frac{\boldsymbol{\epsilon}_0}{1+3F} \right], & \Delta\tilde{B} &= -\frac{1}{(1+F)a^2} \left[ \frac{2F}{1+F} \boldsymbol{\epsilon}^S \right], \\
\Delta\tilde{C}_i &= -\frac{F}{1+F} \frac{\boldsymbol{\epsilon}_i^V}{(1+F)a^2}, & \Delta\tilde{D}_{ij} &= 0, & \Delta\tilde{E} &= 6F \frac{\partial}{\partial t} \left( \frac{\boldsymbol{\epsilon}_0}{1+3F} \right) + \frac{3\dot{F}}{1+3F} \boldsymbol{\epsilon}_0 \\
\Delta\tilde{H} &= -\frac{1}{\sqrt{1+Fa}} \left[ Fa^2 \frac{\partial}{\partial t} \left( \frac{\boldsymbol{\epsilon}^S}{(1+F)a^2} \right) + \frac{3F\boldsymbol{\epsilon}_0}{(1+3F)} \right], \\
\Delta\tilde{G}_i &= -\frac{1}{\sqrt{1+Fa}} \left[ Fa^2 \frac{\partial}{\partial t} \left( \frac{\boldsymbol{\epsilon}_i^V}{(1+F)a^2} \right) \right].
\end{aligned} \tag{5.26}$$

Considering the sum of the perturbations we get

$$\Delta A + \Delta\tilde{A} = \frac{1}{(1+F)a^2} \frac{\partial}{\partial t} [(1+F)a^2] \frac{\boldsymbol{\epsilon}_0}{1+3F}, \tag{5.27}$$

$$\Delta B + \Delta\tilde{B} = -\frac{2\boldsymbol{\epsilon}^S}{(1+F)a^2}, \tag{5.28}$$

$$\Delta E + \Delta\tilde{E} = 2(1+3F) \frac{\partial}{\partial t} \left( \frac{\boldsymbol{\epsilon}_0}{1+3F} \right) + \frac{3\dot{F}}{1+3F} \boldsymbol{\epsilon}_0, \tag{5.29}$$

$$\Delta H + \Delta\tilde{H} = -\frac{1}{\sqrt{1+Fa}} \left[ (1+F)a^2 \frac{\partial}{\partial t} \left( \frac{\boldsymbol{\epsilon}^S}{(1+F)a^2} \right) + \boldsymbol{\epsilon}_0 \right], \tag{5.30}$$

$$\Delta C_i + \Delta\tilde{C}_i = -\frac{\boldsymbol{\epsilon}_i^V}{(1+F)a^2}, \tag{5.31}$$

$$\Delta G_i + \Delta\tilde{G}_i = -\frac{1}{\sqrt{1+Fa}} \left[ (1+F)a^2 \frac{\partial}{\partial t} \left( \frac{\boldsymbol{\epsilon}_i^V}{(1+F)a^2} \right) \right]. \tag{5.32}$$

We are interested in gauge transformations that preserve the condition  $\mathbf{g}_{i0} = g_{i0} + \tilde{g}_{i0} = 0$ . This means that  $\Delta H + \Delta\tilde{H} = 0$ . This gives a solution for  $\boldsymbol{\epsilon}_0$  given by

$$\boldsymbol{\epsilon}_0 = -(1+F)a^2 \frac{\partial}{\partial t} \left( \frac{\boldsymbol{\epsilon}^S}{(1+F)a^2} \right) \tag{5.33}$$

When we study how “ISW” term transform under this type of transformations, we found that  $\Delta ISW = 0$ . While for the “early” term we should note that temperature perturbations transforms as

$$\Delta\delta T(r_{ls}\hat{n}, t) = \dot{\bar{T}}(t) \frac{\epsilon_0}{1 + 3F}, \quad (5.34)$$

With this expression and  $\bar{T}a_{DG} = cte$ , we finally obtain

$$\frac{\Delta\delta T(r_{ls}\hat{n}, t)}{\bar{T}(t_{ls})} = -\frac{\dot{a}_{DG}}{a_{DG}} \frac{\epsilon_0}{1 + 3F}. \quad (5.35)$$

This result implies that the “early” term is invariant under this gauge transformation  $\Delta_{early} = 0$ . Note that this gauge transformation is equivalent to the previously discussed in Section 4.1.1, because we can always take  $\epsilon$  as a combination of  $\epsilon$  and  $\tilde{\epsilon}$ . Then we remark that the three terms of temperature fluctuations are gauge invariant under scalar transformations that leave  $\mathbf{g}_{i0} = 0$ .

### 5.1.2 Single modes

We will assume that since the last scattering until now all the scalar contributions are dominated by a unique mode, such that any perturbation  $X(\mathbf{x}, t)$  could be written as

$$X(\mathbf{x}, t) = \int d^3q \alpha(\mathbf{q}) e^{i\mathbf{q}\cdot\mathbf{x}} X_q(t), \quad (5.36)$$

where  $\alpha(\mathbf{q})$  an stochastic variable, normalized such that

$$\langle \alpha(\mathbf{q}) \alpha^*(\mathbf{q}') \rangle = \delta^3(\mathbf{q} - \mathbf{q}'). \quad (5.37)$$

Then Eqs (5.22) and (5.24) become

$$\left( \frac{\Delta T(\hat{n})}{T_0} \right)_{early}^S = \int d^3q \alpha(\mathbf{q}) e^{i\mathbf{q}\cdot\hat{n}r(t_{ls})} \left( \mathcal{F}(q) + \tilde{\mathcal{F}}(q) + i\hat{q} \cdot \hat{n} (\mathcal{G}(q) + \tilde{\mathcal{G}}(q)) \right), \quad (5.38)$$

$$\begin{aligned} \left( \frac{\Delta T(\hat{n})}{T_0} \right)_{ISW}^S &= -\frac{1}{2} \int_{t_0}^{t_1} dt \int d^3q \alpha(\mathbf{q}) e^{i\mathbf{q}\cdot\hat{n}s(t)} \frac{d}{dt} \left[ a_{DG}^2(t) \ddot{B}_q(t) + a_{DG}(t) \dot{a}_{DG}(t) \dot{B}_q(t) + A_q(t) \right. \\ &\quad \left. - \frac{E_q(t)}{1 + 3F(t)} + \left( a_{DG}^2(t) \ddot{B}_q(t) + a_{DG}(t) \dot{a}_{DG}(t) \dot{B}_q(t) + \tilde{A}_q(t) - \frac{\tilde{E}_q(t)}{1 + 3F(t)} \right) \right], \end{aligned} \quad (5.39)$$

where

$$\mathcal{F}(q) = -\frac{1}{2}a_{DG}^2(t)\ddot{B}_q(t_{ls}) - \frac{1}{2}a_{DG}(t)\dot{a}_{DG}(t_{ls})\dot{B}_q(t_{ls}) + \frac{1}{2}E_q(t_{ls}) + \frac{\delta T_q(t_{ls})}{\bar{T}(t_{ls})}, \quad (5.40)$$

$$\tilde{\mathcal{F}}(q) = -\frac{1}{2}a_{DG}^2(t)\ddot{B}_q(t_{ls}) - \frac{1}{2}a_{DG}(t_{ls})\dot{a}_{DG}(t_{ls})\dot{B}_q(t_{ls}), \quad (5.41)$$

$$\mathcal{G}(q) = -q \left( \frac{1}{2}a_{DG}(t_{ls})\dot{B}_q(t_{ls}) + \frac{1}{(1+3F(t_{ls}))a_{DG}(t_{ls})}\delta u_\gamma(t_{ls}) \right), \quad (5.42)$$

$$\tilde{\mathcal{G}}(q) = -q \left( \frac{1}{2}a_{DG}(t_{ls})\dot{B}_q(t_{ls}) + \frac{1}{(1+3F(t_{ls}))a_{DG}(t_{ls})}\delta \tilde{u}_\gamma(t_{ls}) \right). \quad (5.43)$$

These functions are called form factors. We emphasize that combination given by  $\mathcal{F}(q)+\tilde{\mathcal{F}}(q)$  and  $\mathcal{G}(q)+\tilde{\mathcal{G}}(q)$ , and the expression inside the integral are gauge invariants under gauge transformations that preserve  $\mathbf{g}_{i0}$  equal to zero.

In the next section we present the scalar contribution to the coefficients of multipole temperature expansion. In these computation we only consider the early contribution to the temperature fluctuations, because the integrate Sachs-Wolfe term (5.39) incorporate the evolution of the gravitational fields from the last scattering to the present. In GR, its contribution is dominant from relative low  $l$ , say  $10 < l < 50$ . As we are interested in an estimation of the scalar contribution we will neglect this effect in our analysis. Moreover, our solutions are valid up to the last scattering time  $t_{ls}$ , so we are not able to do a proper analysis of ISW contribution.

## 5.2 Coefficients of multipole temperature expansion: Scalar modes

As an application of the previous results, we will study the contribution of the scalar modes for temperature-temperature correlation, given by:

$$C_{TT,l} = \frac{1}{4\pi} \int d^2\hat{n} \int d^2\hat{n}' P_l(\hat{n} \cdot \hat{n}') \langle \Delta T(\hat{n}) \Delta T(\hat{n}') \rangle, \quad (5.44)$$

where  $\Delta T(\hat{n})$  is the stochastic variable which gives the deviation of the average of observed temperature in direction  $\hat{n}$ , and  $\langle \dots \rangle$  denotes the average over the position of the observer. However, the observed quantity is

$$C_{TT,l}^{obs} = \frac{1}{4\pi} \int d^2\hat{n} \int d^2\hat{n}' P_l(\hat{n} \cdot \hat{n}') \Delta T(\hat{n}) \Delta T(\hat{n}'), \quad (5.45)$$

nevertheless, the mean square fractional difference between this equation and Eq. (5.44) is  $2/(2l+1)$ , and therefore it may be neglected for  $l \gg 1$  (say  $l > 200$ ).

In order to calculate this coefficients we use the following expansion in spherical harmonics

$$e^{i\hat{q} \cdot \hat{n} \rho} = 4\pi \sum_{l=0}^{\infty} \sum_{m=-l}^{m=l} i^l j_l(\rho) Y_l^m(\hat{n}) Y_l^{m*}(\hat{q}), \quad (5.46)$$

where  $j_l(\rho)$  are the spherical Bessel's functions. Using this expression in Eq. (5.38), and replacing the factor  $i\hat{q} \cdot \hat{n}$  for time derivatives of Bessel's functions, the scalar contribution of the observed T-T fluctuations in direction  $\hat{n}$  are

$$(\Delta T(\hat{n}))^S = \sum_{lm} a_{T,lm}^S Y_l^m(\hat{n}), \quad (5.47)$$

where

$$a_{T,lm}^S = 4\pi i^l T_0 \int d^3q \alpha(\mathbf{q}) Y_l^{l*}(\hat{q}) \left[ j_l(qr_{ls})(\mathcal{F}(q) + \tilde{\mathcal{F}}(q)) + j'_l(qr_{ls})(\mathcal{G}(q) + \tilde{\mathcal{G}}(q)) \right], \quad (5.48)$$

and  $\alpha(\mathbf{q})$  is a stochastic parameter for the dominant scalar mode. It is normalized such that

$$\langle \alpha(\mathbf{q}) \alpha^*(\mathbf{q}') \rangle = \delta^3(\mathbf{q} - \mathbf{q}'). \quad (5.49)$$

Inserting this expression in Eq. (5.44) we get

$$C_{TT,l}^S = 16\pi^2 T_0^2 \int_0^\infty q^2 dq \left[ j_l(qr_{ls})(\mathcal{F}(q) + \tilde{\mathcal{F}}(q)) + j'_l(qr_{ls})(\mathcal{G}(q) + \tilde{\mathcal{G}}(q)) \right]^2 \quad (5.50)$$

Now we will consider the case  $l \gg 1$ . In this limit we can use the following approximation for Bessel's functions<sup>1</sup>:

$$j_l(\rho) \rightarrow \begin{cases} \cos(b) \cos[\nu(\tan b - b) - \pi/4] / (\nu \sqrt{\sin b}) & \rho > \nu, \\ 0 & \rho < \nu, \end{cases} \quad (5.51)$$

where  $\nu \equiv l + 1/2$ , and  $\cos b \equiv \nu/\rho$ , with  $0 \leq b \leq \pi/2$ . Besides, for  $\rho > \nu \gg 1$  the phase  $\nu(\tan b - b)$  is a function of  $\rho$  that grows very fast, then the derivatives of Bessel's functions only acts in its phase:

$$j'_l(\rho) \rightarrow \begin{cases} -\cos(b) \sqrt{\sin b} \sin[\nu(\tan b - b) - \pi/4] / \nu & \rho > \nu \\ 0 & \rho < \nu. \end{cases} \quad (5.52)$$

Using these approximations in Eq. (5.50) and changing the variable from  $q$  to  $b = \cos^{-1}(\nu/\rho r_{ls})$ , we obtain

$$\begin{aligned} C_{TT,l}^S &= \frac{16\pi^2 T_0^2 \nu}{r_{ls}^3} \int_0^{\pi/2} \frac{db}{\cos^2 b} \\ &\times \left[ \left( \mathcal{F} \left( \frac{\nu}{r_{ls} \cos b} \right) + \tilde{\mathcal{F}} \left( \frac{\nu}{r_{ls} \cos b} \right) \right) \cos[\nu(\tan b - b) - \pi/4] \right. \\ &\left. - \sin b \left( \mathcal{G} \left( \frac{\nu}{r_{ls} \cos b} \right) + \tilde{\mathcal{G}} \left( \frac{\nu}{r_{ls} \cos b} \right) \right) \sin[\nu(\tan b - b) - \pi/4] \right]^2. \end{aligned} \quad (5.53)$$

When  $\nu \gg 1$ , the functions  $\cos[\nu(\tan b - b) - \pi/4]$  and  $\sin[\nu(\tan b - b) - \pi/4]$  oscillate very rapidly, then the squared average of its values are  $1/2$ , while the averaged cross terms are zero. Using  $l \approx \nu$ , and changing the integration variable from  $b$  to  $\beta = 1/\cos b$ , the Eq. (5.53) becomes

---

<sup>1</sup>See, e.g. I. S. Gradshteyn & I. M. Ryzhik, *Table of Integral, Series, and Products*, translated, corrected and enlarged by A. Jeffrey (Academic Press, New York, 1980): formula 8.453.1.

$$l(l+1)C_{TT,l}^S = \frac{8\pi^2 T_0^2 l^3}{r_{ls}^3} \int_1^\infty \frac{\beta d\beta}{\sqrt{\beta^2 - 1}} \times \left[ \left( \mathcal{F}\left(\frac{l\beta}{r_{ls}}\right) + \tilde{\mathcal{F}}\left(\frac{l\beta}{r_{ls}}\right) \right)^2 + \frac{\beta^2 - 1}{\beta^2} \left( \mathcal{G}\left(\frac{l\beta}{r_{ls}}\right) + \tilde{\mathcal{G}}\left(\frac{l\beta}{r_{ls}}\right) \right)^2 \right] \quad (5.54)$$

Note that  $d_A = r_{ls}\tilde{R}_{ls}$  is the angular diameter distance of the last scattering surface. To calculate the CMB power spectrum, we need to know the value of  $\dot{\tilde{B}}_q$ . We use the off diagonal equation from Delta sector to obtain it. This gives:

$$\dot{\tilde{A}}_q = \dot{A}_q F + A_q \dot{F} - 2a^2(\rho + p)\delta u_q - a^2(\tilde{\rho} + \tilde{p})\delta u_q - (\rho + p)\delta \tilde{u}_q, \quad (5.55)$$

so if we use this equation with the definition of  $\tilde{\Psi}$

$$\dot{\tilde{\Psi}}_q = \frac{1}{2}(3\dot{\tilde{A}}_q - q^2\dot{\tilde{B}}_q), \quad (5.56)$$

it allow us to find  $\dot{\tilde{B}}$ . As we used the approximation of that perturbations of gravitational field were dominated by perturbations of dark matter density at matter-dominated era. at this regime  $\dot{A}_q(t_{ls}) = 0$  and in the synchronous gauge, the velocity perturbations for Dark matter are zero, then

$$\dot{\tilde{A}}_q(t_{ls}) = A_q(t_{ls})\dot{F}(t_{ls}), \quad (5.57)$$

and

$$\dot{\tilde{B}}_q(t_{ls}) = \frac{3}{q^2}A_q(t_{ls})\dot{F}(t_{ls}) - \frac{2\dot{\tilde{\Psi}}_q(t_{ls})}{q^2} \Rightarrow \ddot{\tilde{B}}_q(t_{ls}) = \frac{3}{q^2}A_q(t_{ls})\ddot{F}(t_{ls}) - \frac{2\ddot{\tilde{\Psi}}_q(t_{ls})}{q^2}, \quad (5.58)$$

where

$$\begin{aligned}
q^2 A_q &= 8\pi G a^2 \delta \rho_{Dq} - 2H a^2 \dot{\Psi}_q \\
&= 3H^2 a^2 \delta_{Dq} - 2H a^2 \dot{\Psi}_q .
\end{aligned} \tag{5.59}$$

In GR  $\ddot{B}_q = -2\dot{\Psi}_q/q^2$ , and  $\dot{\Psi}_q \propto t^{-1/3}$  implies  $\ddot{B}_q = 2\dot{\Psi}_q/3tq^2$ . Therefore, the usual form factors are:

$$\mathcal{F}(q) = \frac{1}{3} \delta_{\gamma q}(t_{ls}) + \frac{\dot{\Psi}_q(t_{ls})}{q^2} \left( a_{DG}(t_{ls}) \dot{a}_{DG}(t_{ls}) - \frac{2}{3} \frac{a_{DG}^2(t_{ls})}{t_{ls}} \right) \tag{5.60}$$

$$\mathcal{G}(q) = -q \frac{\delta u_{\gamma q}(t_{ls})}{(1 + 3F(t_{ls})) a_{DG}(t_{ls})} + \frac{a_{DG}(t_{ls}) \dot{\Psi}_q(t_{ls})}{q} . \tag{5.61}$$

where we have used  $\delta T_q/\bar{T} = \delta \rho_{\gamma q}/4\bar{\rho}_\gamma = \delta_{\gamma q}/3$ . Nevertheless, for the “delta” contribution,  $\dot{\tilde{\Psi}}_q$  and  $\ddot{\tilde{\Psi}}_q$  satisfy the same relation than the standard case. Due to our decomposition, the tilde expressions are

$$\begin{aligned}
\tilde{\mathcal{F}}(q) &= -\frac{3}{2} \frac{A_q(t_{ls})}{q^2} (a_{DG}^2(t_{ls}) \ddot{F}(t_{ls}) + a_{DG}(t_{ls}) \dot{a}_{DG}(t_{ls}) \dot{F}(t_{ls})) \\
&\quad + \frac{\dot{\tilde{\Psi}}_q(t_{ls})}{q^2} \left( a_{DG}(t_{ls}) \dot{a}_{DG}(t_{ls}) - \frac{2}{3} \frac{a_{DG}^2(t_{ls})}{t_{ls}} \right)
\end{aligned} \tag{5.62}$$

$$\tilde{\mathcal{G}}(q) = -q \frac{\delta \tilde{u}_{\gamma q}(t_{ls})}{(1 + 3F(t_{ls})) a_{DG}(t_{ls})} + \frac{a_{DG}(t_{ls}) \dot{\tilde{\Psi}}_q(t_{ls})}{q} . \tag{5.63}$$

Unfortunately, due to all the approximations we have used, we need to add one more correction to the solutions of the GR sector, as Weinberg does. We considered a sharp transition from the moment when the Universe was opaque to transparent. However, this was actually not instantaneous yet it could be considered Gaussian. This effect is known as Landau damping[80] and is described in Appendix A.2. With these considerations, the solutions of perturbations are given by:



$$\dot{\Psi}_q(t_{ls}) = -\frac{3q^2 t_{ls} \mathcal{R}_q^o \mathcal{T}(\kappa)}{5a_{DG}^2(t_{ls})}, \quad (5.64)$$

$$\begin{aligned} \delta_{\gamma q}(t_{ls}) &= \frac{3\mathcal{R}_q^o}{5} \left[ \mathcal{T}(\kappa)(1 + 3R_{ls}) - (1 + R_{ls})^{-1/4} e^{-q^2 d_D^2 / a_{DG}^2(t_{ls})} \right. \\ &\quad \times \left. \mathcal{S}(\kappa) \cos \left( q \int_0^{t_{ls}} \frac{dt}{\sqrt{3(1 + R(t))} a_{DG}(t)} + \Delta(\kappa) \right) \right], \end{aligned} \quad (5.65)$$

$$\begin{aligned} \delta u_{\gamma q}(t_{ls}) &= \frac{3\mathcal{R}_q^o}{5} \left[ -t_{ls} \mathcal{T}(\kappa) + \frac{a_{DG}(t_{ls})}{\sqrt{3} q (1 + R_{ls})^{3/4}} e^{-q^2 d_D^2 / a_{DG}^2(t_{ls})} \right. \\ &\quad \times \left. \mathcal{S}(\kappa) \sin \left( q \int_0^{t_{ls}} \frac{dt}{\sqrt{3(1 + R(t))} a_{DG}(t)} + \Delta(\kappa) \right) \right], \end{aligned} \quad (5.66)$$

where

$$d_D^2 = d_{Silk}^2 + d_{Landau}^2, \quad (5.67)$$

$$d_{Silk}^2 = Y_{DG}^2(t_{ls}) \int_0^{t_{ls}} \frac{t_\gamma}{6Y_{DG}^2(1 + R)} \left\{ \frac{16}{15} + \frac{R^2}{(1 + R)} \right\} dt, \quad (5.68)$$

$$d_{Landau}^2 = \frac{\sigma_t^2}{6(1 + R_{ls})}, \quad (5.69)$$

where  $t_\gamma$  is the mean free time for photons and  $R = 3\bar{\rho}_B/4\bar{\rho}_\gamma = 3\Omega_B Y_{DG}/4\Omega_\gamma$ .

In order to evaluate the Silk damping, we have

$$t_\gamma = \frac{1}{n_e \sigma_T c} \quad (5.70)$$

where  $n_e$  is the number density of electrons and  $\sigma_T$  is the Thomson cross section.

On the other hand

$$\begin{aligned} q \int_0^{r_{ls}} c_s dr &= q \int_0^{t_{ls}} \frac{dt}{\sqrt{3(1 + R(t))} a_{DG}(t)} \equiv q r_{ls}^{SH} \\ &= \frac{q}{a_{DG}(t_{ls})} \cdot (a_{DG}(t_{ls}) r_{ls}^{SH}) = \frac{q}{a_{DG}(t_{ls})} \cdot d_H(t_{ls}) \end{aligned} \quad (5.71)$$

where  $c_s$  is the speed of sound,  $r_{ls}^{SH}$  is the sound horizon radial coordinate and  $d_H$  is the horizon distance.

With all these approximations, the transfers functions are simplified to the following expressions:

$$\mathcal{F}(q) = \frac{1}{3}\delta_{\gamma q}(t_{ls}) + \frac{a_{DG}^2(t_{ls})\dot{\Psi}_q(t_{ls})}{3q^2 t_{ls}}, \quad (5.72)$$

$$\mathcal{G}(q) = -q \frac{\delta u_{\gamma q}(t_{ls})}{(1 + 3F(t_{ls}))a_{DG}(t_{ls})} + \frac{a_{DG}(t_{ls})\dot{\Psi}_q(t_{ls})}{q}, \quad (5.73)$$

where  $A_q(t_{ls}) = \mathcal{R}_q^o \mathcal{T}(\kappa)$ . Then, we replaced the GR solutions and we get

$$\begin{aligned} \mathcal{F}(q) &= \frac{\mathcal{R}_q^o}{5} \left[ 3\mathcal{T}(qd_T/a_{DG}(t_{ls}))R_{ls} - (1 + R_{ls})^{-1/4} e^{-q^2 d_D^2/a_{DG}^2(t_{ls})} \right. \\ &\times \left. \mathcal{S}(qd_T/a_{DG}(t_{ls})) \cos(qd_H/a_{DG}(t_{ls}) + \Delta(qd_T/a_{DG}(t_{ls}))) \right], \end{aligned} \quad (5.74)$$

$$\begin{aligned} \mathcal{G}(q) &= \frac{\sqrt{3}\mathcal{R}_q^o}{5(1 + R_{ls})^{3/4}} e^{-q^2 d_D^2/a_{DG}^2(t_{ls})} \\ &\times \mathcal{S}(qd_T/a_{DG}(t_{ls})) \sin(qd_H/a_{DG}(t_{ls}) + \Delta(qd_T/a_{DG}(t_{ls}))), \end{aligned} \quad (5.75)$$

where  $\kappa = qd_T/a_{ls}$  (defined in eq. (4.130)) and

$$d_T(t_{ls}) \equiv c \frac{\sqrt{2}a_{DG}(t_{ls})}{a_{EQ}H_{EQ}} = c \frac{a_{DG}(t_{ls})\sqrt{\Omega_R}}{H_0\Omega_M} = c \frac{a_{DG}(t_{ls})}{100h} \sqrt{C(C+1)} \quad (5.76)$$

The final consideration that we must include is that due to the reionization of hydrogen at  $z_{reion} \sim 10$  by ultraviolet light coming from the first generation of massive stars, photons of the CMB have a probability of being scattered  $1 - \exp(-\tau_{reion})$ . CMB has two contributions. The non-scattered photons provide the first contribution, where we have to correct by a factor given by  $\exp(-\tau_{reion})$ . The scattered photons provide the second contribution, but the reionization occurs at  $z \ll z_L$  affecting only low  $ls$ . We are not interested in this effect, and therefore we will not include it. Measurements shows that in GR  $\exp(-2\tau_{reion}) \approx 0.8$ .

On the other hand, we will use a standard parametrization of  $\mathcal{R}_q^0$  given by

$$|\mathcal{R}_q^0|^2 = N^2 q^{-3} \left( \frac{q/R_0}{\kappa_{\mathcal{R}}} \right)^{n_s-1}, \quad (5.77)$$

where  $n_s$  could vary with the wave number. It is usual to take  $\kappa_{\mathcal{R}} = 0.05 \text{ Mpc}^{-1}$ .

Note that  $d_A(t_{ls}) = r_{ls} a_{DG}(t_{ls})$  is the angular diameter distance of the last scattering surface.

$$d_A(t_{ls}) = c a_{DG}(t_{ls}) \int_{t_{ls}}^{t_0} \frac{dt'}{a_{DG}(t')} = c \frac{a_{DG}(t_0)}{1+z_{ls}} \int_{t_{ls}}^{t_0} \frac{dt'}{a_{DG}(t')} = c \frac{1}{1+z_{ls}} \int_{t_{ls}}^{t_0} \frac{dt'}{Y_{DG}(t')} \quad (5.78)$$

$$= c \frac{1}{1+z_{ls}} \int_{Y_{ls}}^1 \frac{dY'}{Y_{DG}(Y')} \frac{dt}{dY'} = \frac{d_L(t_{ls})}{(1+z_{ls})^2} \quad (5.79)$$

This is consistent with the luminosity distance definition[54]. Then, when we set  $q = \beta l / r_{ls}$  we get

$$\begin{aligned} |\mathcal{R}_{\beta l / r_{ls}}^0|^2 &= N^2 \left( \frac{\beta l}{r_{ls}} \right)^{-3} \left( \frac{\beta l}{\kappa_{\mathcal{R}} r_{ls}} \right)^{n_s-1} = N^2 \left( \frac{\beta l}{r_{ls}} \right)^{-3} \left( \frac{\beta l a_{DG}(t_{ls})}{\kappa_{\mathcal{R}} r_{ls} a_{DG}(t_{ls})} \right)^{n_s-1} \\ &= N^2 \left( \frac{\beta l}{r_{ls}} \right)^{-3} \left( \frac{\beta l a_{DG}(t_{ls})}{\kappa_{\mathcal{R}} d_A(t_{ls})} \right)^{n_s-1} \equiv N^2 \left( \frac{\beta l}{r_{ls}} \right)^{-3} \left( \frac{\beta l}{l_R} \right)^{n_s-1} \end{aligned}$$

Using a similar computations for the other distances, the final form of the form factors are given by

$$\begin{aligned} \mathcal{F}(q) &= \frac{\mathcal{R}_q^o}{5} \left[ 3\mathcal{T}(\beta l / l_T) R_{ls} - (1 + R_{ls})^{-1/4} e^{-\beta^2 l^2 / l_D^2} \mathcal{S}(\beta l / l_T) \cos(\beta l / l_H + \Delta(\beta l / l_T)) \right] \quad (5.80) \\ \mathcal{G}(q) &= \frac{\sqrt{3} \mathcal{R}_q^o}{5(1 + R_{ls})^{3/4}} e^{-\beta^2 l^2 / l_D^2} \mathcal{S}(\beta l / l_T) \sin(\beta l / l_H + \Delta(\beta l / l_T)), \quad (5.81) \end{aligned}$$

where

$$l_R = \frac{\kappa_{\mathcal{R}} d_A(t_{ls})}{a_{DG}(t_{ls})}, \quad l_H = \frac{d_A(t_{ls})}{d_H(t_{ls})}, \quad l_T = \frac{d_A(t_{ls})}{d_T(t_{ls})}, \quad l_D = \frac{d_A(t_{ls})}{d_D(t_{ls})}. \quad (5.82)$$

To summarize, for reasonably large values of  $l$  (say  $l > 150$ ), CMB multipoles are given by

$$\begin{aligned} \frac{l(l+1)C_{TT,l}^S}{2\pi} &= \frac{4\pi T_0^2 l^3 \exp(-2\tau_{reion})}{r_{ls}^3} \int_1^\infty \frac{\beta d\beta}{\sqrt{\beta^2 - 1}} \\ &\times \left[ \left( F\left(\frac{l\beta}{r_{ls}}\right) + \tilde{F}\left(\frac{l\beta}{r_{ls}}\right) \right)^2 + \frac{\beta^2 - 1}{\beta^2} \left( G\left(\frac{l\beta}{r_{ls}}\right) + \tilde{G}\left(\frac{l\beta}{r_{ls}}\right) \right)^2 \right] \end{aligned} \quad (5.83)$$

Numerical solutions and other considerations to the delta sector need to be included to compute the solution for the perturbations; however, this is not the aim of this Thesis. It is remarkable the structure of eq. (5.83), where the delta sector contributes additively inside the integral. If we set all delta sector equal to zero, we recover the result directly for scalar temperature-temperature multipole coefficients in GR given by Weinberg[62].

### 5.3 Summary and Conclusions

We studied the propagation of photons from the moment of the last scattering until reaching us in a perturbed FLRW universe. We did not consider angular deflections in our analysis which is in agreement with our choice of working in the synchronous gauge. When studying temperature fluctuations we can split them into three independent terms: an early term which only depends on the moment of the last scattering  $t_{ls}$ . An ISW term that includes the evolution of gravitational fields from the last scattering to the present and a late-term which depends on the actual value for those fields. We compute the gauge transformations which leaves  $\mathbf{g}_{i0} = 0$ , and we found that those three terms are separately gauge invariants. This is a very important test for DG because those fluctuations are physical. In order to compute the scalar contribution to the multipole temperature expansion, we only consider the early term (5.22) in our analysis because it has the greatest contribution compared with the other two, where the late-term (5.23) only contribute to the first  $ls$ , and the ISW term (5.24) was not considered because we have not studied solutions valid in all the time after the last scattering moment  $t_{ls}$ . After computing the multipole coefficients we found that DG extends solutions in a way that the delta sector acts additively, so the limit to GR is naturally recovered when setting all delta fields equal to zero. Moreover, the sharp transition from opaque to transparent Universe is relaxed to be a gaussian. Finally, we recall that the delta sector can be obtained numerically with GR solutions as an external force but this work will be reported in a forthcoming publication.

# Chapter 6

## Discussion and conclusions

This Thesis was divided in two parts. In the first part we study the minimal geometric deformation (MGD) approach in order to extend isotropic solutions to anisotropic configurations, which are more likely to pass astrophysical tests. The crucial point of this approach is the linearity of Einstein's equation when deforming Schwarzschild metric in the temporal and radial component, allowing to get exact solutions to deformations which are not perturbations of GR. We presented a detailed guideline of how to find anisotropic solutions for Durgapal-Fuloria stars and a possibly way of detection of anisotropic distributions.

By the other side, we studied the cosmological scenario of Delta Gravity (DG), a theory which extend General Relativity by a  $\tilde{\delta}$  symmetry[55] in a way that new fields are added to GR, and induce modifications of the metric that particles follow. We presented and solved the cosmological perturbations of DG in the synchronous gauge following Weinberg's prescription[62]. We found that DG extend gauge symmetries, however we can fix consistently those degrees of freedom. After that, we analysed the temperature fluctuations coming from the moment of last scattering to the present and presented a formula for the scalar contribution to the temperature multipole coefficients of the CMB, where we found that DG affects additively, which could have an observational effect that could be compared with Planck results and give a physical meaning for the so-called delta matter.

With the full scalar expression for the CMB Power Spectrum coefficients, we can find the shape of the spectrum. In order to achieve it, we have to determine the best cosmological parameters that can describe the observational spectrum given by Planck [38]. The determination of the cosmological parameters could be demanding (from a computational point of view), but if we constraints the cosmological parameters with the SNe-Ia analysis [57]

the determination of the CMB Power Spectrum in DG could be more comfortable. In the context of the controversy about the  $H_0$  value [34] and other problems as the curvature measurements [36] or the possibility of a Universe with less Dark Energy [46], this work could provide an alternative to solve the today cosmological puzzle. Future work in this line is being carried out in collaboration with Marco San Martín which will include the numerical analysis of the solutions presented in this Thesis.

The perturbation theory and the temperature fluctuations of the CMB are included in the article *Cosmological Fluctuations in Delta Gravity*, written with Jorge Alfaro and Marco San Martín.

The numerical analysis, and the fit of the CMB with SNe-Ia is part of the article *CMB and SNe constraints in Delta Gravity*, also written with Jorge Alfaro and Marco San Martín.

Both articles are in preparation to be submitted in coming days.

Before finishing, we have to point out some aspects of this work:

- Despite both parts of this Thesis are not correlated, both shared some similar considerations.
  - Both MGD and DG include modifications on the metric of a non-perturbative nature.
  - This modification of the metric allow both theories to have physical solutions. In MGD we get anisotropic configurations and in DG we could provide a solution of the actual controversy about the Hubble constant  $H_0$  (or  $H_{DG0}$  in DG).
  - In MGD we can not get solutions before applying a mimic condition. While in DG we need to fix the harmonic gauge to reduce the system in a FLRW Universe or fix a gauge to drop new coordinate system when studying test particles.
- The fundamentals of DG still need to be study, in special the quantum theory. For now, we can interpret DG as an effective theory that interpolates successfully the early with the late behaviour of the Universe. The advantage of DG is that it modifies GR in a subtle way that preserves all tests of Special Relativity and GR in the local solar system[52, 53].
- In principle, due the non-linearity of Einstein's equations MGD is only applicable in particular backgrounds and could not be applied to the cosmological FLRW metric,

unless we only consider deformations of the temporal component of the metric. We studied anisotropic solution for Durgapal-Fuloria stars so our motivations was to deform the radial component of Schwarzschild background. In the cosmological case, we require an isotropic and homogeneous universe so deformation in spacial coordinate are not allowed, nevertheless, we could explore deformations in the temporal component and see its implications. This is a future approach that definitively we need to explore.

- Despite DG adds new fields to the theory, is thermodynamic who establish the interpretation of physical quantities over mathematical symbols. So the hypothesis of applying MGD to FLRW has the advantage of we are not outside of GR, then interpretations of GR are consistent with thermodynamics.





# Chapter 7

## Afterword

Personally, I enjoyed so much my stay in the doctorate. I learned a lot about Gravitation and Cosmology yet I feel so represented with the Newton quote of the beginning of this manuscript: “I do not know what I may appear to the world, but to myself, I seem to have been only like a boy playing on the seashore, and diverting myself in now and then finding a smoother pebble or a prettier shell than ordinary, whilst the great ocean of truth lay all undiscovered before me.” So I thank again Jorge Alfaro for being my advisor and for letting me play in this seashore with beautiful pebbles and shells.



# Appendix A

## A.1 $R$ and $\tilde{R} \neq 0$

Up to now, we showed the way to solved the complete system in both radiation and matter era. However for the second era we use  $R$  and  $\tilde{R}$  to be equal to zero, which is no true while going deeper on this era. So we need to add this consideration to the solutions (4.127). We only need to focus on GR solutions because delta sector is obtained using those solutions as an external force. Lets consider again the system (4.116)-(4.119) in the matter era without setting  $R = 0$

$$\frac{d}{dt} (a^2 \Psi_q) = -4\pi G \bar{\rho}_D a^2 \delta_{Dq}, \quad (\text{A.1})$$

$$\dot{\delta}_{Dq} = -\Psi_q, \quad (\text{A.2})$$

$$\frac{d}{dt} \left( \frac{(1+R)\delta u_{\gamma q}}{a} \right) = -\frac{1}{3a} \delta_{\gamma q}, \quad (\text{A.3})$$

$$\frac{d}{dt} \left( \frac{\delta u_{\nu q}}{a} \right) = -\frac{1}{3a} \delta_{\nu q}. \quad (\text{A.4})$$

where  $R \equiv 3\bar{\rho}_B/4\bar{\rho}_R \propto a$ . Inspection of system show that Dark Matter  $\delta_{Dq}$  is decoupled with the gravitational field  $\dot{\Psi}_q$  which solutions are given by (4.126) and (4.127), and this one acts as a forcing term for photons. The particular solution is

$$\delta_{\gamma q}^{(1)} = \frac{3q^2 t^2 (1+3R) \mathcal{R}_q^o}{5a^2 (t^2 q^2 / a^2 + 2R)}, \quad \delta u_{\gamma q}^{(1)} = -\frac{3t^3 q^2 \mathcal{R}_q^o}{5a^2 (t^2 q^2 / a^2 + 2R)}. \quad (\text{A.5})$$

To this particular solution we need to add the solution of the homogeneous version of eqs (A.3)-(A.4).

$$\dot{\delta}_{\gamma q}^{(2)} = \frac{q^2}{a^2} \delta u_{\gamma q}^{(2)}, \quad \frac{d}{dt} (t^{2/3} (1+R) \delta u_{\gamma q}^{(2)}) = -\frac{1}{3} t^{-2/3} \delta_{\gamma q}^{(2)} \quad (\text{A.6})$$

or, equivalently

$$\frac{d}{dt} \left( t^{-2/3} (1+R) a^2 \frac{d}{dt} \delta_{\gamma q}^{(2)} \right) + \frac{q^2}{3} t^{-2/3} \delta_{\gamma q}^{(2)} = 0 \quad (\text{A.7})$$

Using the fact that in the matter era  $R \propto a \propto t^{2/3}$  there are a general solution of this system given as a linear combination of

$$\begin{aligned} & F \left( \frac{1}{4} - \frac{1}{4} \sqrt{1-16\eta}, \frac{1}{4} + \frac{1}{4} \sqrt{1-16\eta}, \frac{1}{2}, -R \right), \\ & \sqrt{R} F \left( \frac{3}{4} - \frac{1}{4} \sqrt{1-16\eta}, \frac{3}{4} + \frac{1}{4} \sqrt{1-16\eta}, \frac{3}{2}, -R \right), \end{aligned}$$

where  $F$  is the Gauss hypergeometric function, and  $\eta$  is

$$\eta \equiv \frac{3q^2 t^2}{4a^2 R}$$

which is time-independent during the matter era. In order to get an insight about the behaviour of those solutions, let's consider that the wavelength of these perturbations are moderately long, in the sense that  $\eta \gg 1$ . Before using this condition, eq. (A.7) has an exact solution when  $R \ll 1$

$$\begin{aligned} \delta_{\gamma q}^{(2)} &= c_q \cos(\sqrt{3}qt/a) + d_q \sin(\sqrt{3}qt/a) \\ \delta u_{\gamma q}^{(2)} &= \frac{a}{\sqrt{3}q} \left[ -c_q \sin(\sqrt{3}qt/a) + d_q \cos(\sqrt{3}qt/a) \right] \end{aligned}$$

To this, we need to add the particular solution (A.6), which in the limit  $R \ll q^2 t^2 / a^2$  (or, equivalently  $\eta \gg 1$ )

$$\delta_{\gamma q}^{(1)} = \frac{3(1+3R)\mathcal{R}_q^o}{5}, \quad \delta u_{\gamma q}^{(1)} = -\frac{3t\mathcal{R}_q^o}{5}, \quad (\text{A.8})$$

We can evaluate the constants  $c_q$  and  $d_q$  by requiring that  $qt/a \ll 1$  (which also implies  $R \ll 1$ ), the total photon density perturbation  $\delta_{\gamma q}^{(1)} + \delta_{\gamma q}^{(2)}$  must approach to  $\delta_D \rightarrow 9q^2 t \mathcal{R}_q^o / 10a^2$ . This give us

$$c_q = -\frac{3\mathcal{R}_q^o}{5} \quad d_q = 0 . \quad (\text{A.9})$$

so that, while  $R \ll 1$

$$\delta_{\gamma q}^{(2)} = -\frac{3\mathcal{R}_q^o}{5} \cos(\sqrt{3}qt/a) \quad (\text{A.10})$$

Eventually  $R$  becomes non-negligible, but under the assumption  $\eta \gg 1$  one can solve the homogeneous equation A.7 using WKB approximation. In the limit  $qt/a \gg 1$  the density fluctuation will oscillate rapidly with phase

$$\phi \equiv \int_0^t \frac{qdt}{a\sqrt{3(1+R)}} = \frac{\sqrt{3}qt}{a\sqrt{R}} \log(\sqrt{R} + \sqrt{1+R}) . \quad (\text{A.11})$$

Using  $\phi$  as the independent variable eq. (A.7) becomes

$$\frac{d^2}{d\phi^2} \delta_{\gamma q} + \frac{1}{2} \left( \frac{d \log(1+R)}{d\phi} \right) \frac{d}{d\phi} \delta_{\gamma q} + \delta_{\gamma q} = 0 . \quad (\text{A.12})$$

If we try a solution of the form  $\mathcal{A}e^{\pm i\phi}$ . With  $\mathcal{A}$  varying slowly with respect to  $\phi$ , we get a solution

$$\delta_{\gamma q}^{(2\pm)} \propto (1+R)^{-1/4} \exp(\pm i\phi) . \quad (\text{A.13})$$

We can see that the linear combination of these solutions merge smoothly with the result of  $R \ll 1$  is obtained by replacing the argument of the cosine in (A.10) with  $\phi$ , and multiplying with  $(1+R)^{-1/4}$ . Adding the inhomogeneous solution (A.8), the total photon and baryon density perturbations for moderately long wavelength in the matter dominated era are

$$\delta_{\gamma q} = \delta_{Bq} = \frac{3\mathcal{R}_q^o}{5} [1 + 3R - (1+R)^{-1/4} \cos(\phi)] \quad (\text{A.14})$$

And the velocity potential

$$\delta u_{\gamma q} = \frac{3t\mathcal{R}_q^o}{5} \left[ -1 + \frac{a}{\sqrt{3}qt(1+R)^{3/4}} \sin(\phi) \right] \quad (\text{A.15})$$

The solutions (A.14) and (A.15) apply only up to the time of last scattering. After that moment  $R$  becomes larger than one and we should use the full solutions given by the Gauss hypergeometric functions.

## A.2 Landau Damping

In the analysis we assume that the transition of a opaque to transparent Universe was instantaneous, but we know that the transition took some finite interval of time, over which the form factors must be averaged.

Since the probability of last scattering is a sharply peaked function of time, we can approximate it to a gaussian: the probability that last scattering occurs between a time  $t$  and  $t + dt$  will take the form

$$P(t)dt = \frac{\exp(-(t - t_{ls})^2/2\sigma_t^2)}{\sigma_t\sqrt{2\pi}}dt, \quad (\text{A.16})$$

so in the sinusoidal solutions of photon density and velocity perturbations we need to make the replacement:

$$\left\{ \begin{array}{c} \cos \left( \int_0^{t_{ls}} \omega dt + \Delta \right) \\ \sin \left( \int_0^{t_{ls}} \omega dt + \Delta \right) \end{array} \right\} \rightarrow \int_{-\infty}^{\infty} P(t)dt \left\{ \begin{array}{c} \cos \left( \int_0^t \omega dt + \Delta \right) \\ \sin \left( \int_0^t \omega dt + \Delta \right) \end{array} \right\}, \quad (\text{A.17})$$

where  $\omega = q/a_{DG}\sqrt{3(1+R)}$ . We can do those integral expanding the argument of sines and cosines to first order in  $t - t_{ls}$ :

$$\int_0^t \omega dt \simeq \int_0^{t_{ls}} \omega dt + \omega_{ls}(t - t_{ls})$$

then the integrals (A.17) can be now done

$$\int_{-\infty}^{\infty} P(t)dt \left\{ \begin{array}{c} \cos \left( \int_0^t \omega dt + \Delta \right) \\ \sin \left( \int_0^t \omega dt + \Delta \right) \end{array} \right\} \simeq \exp \left( -\frac{\omega_{ls}^2 \sigma_t^2}{2} \right) \left\{ \begin{array}{c} \cos \left( \int_0^{t_{ls}} \omega dt + \Delta \right) \\ \sin \left( \int_0^{t_{ls}} \omega dt + \Delta \right) \end{array} \right\}. \quad (\text{A.18})$$

Thus, the whole effect of this averaging is to introduce an additional damping factor  $\exp(-\omega_{ls}^2 \sigma_t^2/2)$  in the sines and cosines of the form factor. Both Silk and Landau damping are proportional to  $q^2$ , so we can write

$$\int_0^{t_{ls}} \Gamma dt + \frac{\omega_{ls}^2 \sigma_t^2}{2} = q^2 \frac{d_D^2}{a_{DG}^2(t_{ls})}, \quad (\text{A.19})$$

where  $d_D$  is the damping length defined by

$$d_D^2 = d_{Silk}^2 + d_{Landau}^2,$$

where

$$d_{Silk}^2 = a_{DG}^2(t_{ls}) \int_0^{t_{ls}} \frac{t_\gamma}{6a_{DG}^2(1+R)} \left[ \frac{16}{15} + \frac{R^2}{1+R} \right], \quad (\text{A.20})$$

$$d_{Landau}^2 = \frac{\sigma_t^2}{6(1+R_{ls})}. \quad (\text{A.21})$$

The evaluation of the damping length is outside of this Thesis. But is a part of a future publication in preparation.





# Bibliography

- [1] Clifford M. Will. The confrontation between general relativity and experiment. *Living Reviews in Relativity*, 9(1):3, Mar 2006. ISSN 1433-8351. doi: 10.12942/lrr-2006-3. URL <https://doi.org/10.12942/lrr-2006-3>.
- [2] S G Turyshev. Experimental tests of general relativity: recent progress and future directions. *Physics-Uspekhi*, 52(1):1–27, Jan 2009. ISSN 1468-4780. doi: 10.3367/ufne.0179.200901a.0003. URL <http://dx.doi.org/10.3367/UFNe.0179.200901a.0003>.
- [3] H. Stephani, D. Kramer, M. MacCallum, C. Hoenselaers, and E. Herlt. *Exact solutions of Einstein's field equations*. Cambridge monographs on mathematical physics (Cambridge University Press, 1 edition, 2003).
- [4] M.S.R. Delgaty and Kayll Lake. Physical acceptability of isolated, static, spherically symmetric, perfect fluid solutions of Einstein's equations. *Comput. Phys. Commun.*, 115:395–415, 1998. doi: 10.1016/S0010-4655(98)00130-1.
- [5] İBRAHİM SEMİZ. All "static" spherically symmetric perfect fluid solutions of einstein's equations with constant equation of state parameter and finite polynomial "mass function". *Reviews in Mathematical Physics*, 23(08):865–882, 2011. doi: 10.1142/S0129055X1100445X. URL <https://doi.org/10.1142/S0129055X1100445X>.
- [6] P.S. Negi. Exact solutions of Einstein's field equations. *Int. J. Theor. Phys.*, 45:1684–1702, 2006. doi: 10.1007/s10773-006-9104-5.
- [7] L. Herrera and N.O. Santos. Local anisotropy in self-gravitating systems. *Physics Reports*, 286(2):53 – 130, 1997. ISSN 0370-1573. doi: [https://doi.org/10.1016/S0370-1573\(96\)00042-7](https://doi.org/10.1016/S0370-1573(96)00042-7). URL <http://www.sciencedirect.com/science/article/pii/S0370157396000427>.

- [8] M. Ruderman. Pulsars: Structure and dynamics. *Annual Review of Astronomy and Astrophysics*, 10(1):427–476, 1972. doi: 10.1146/annurev.aa.10.090172.002235. URL <https://doi.org/10.1146/annurev.aa.10.090172.002235>.
- [9] M.K. Mak and T. Harko. Anisotropic stars in general relativity. *Proceedings of the Royal Society of London. Series A: Mathematical, Physical and Engineering Sciences*, 459(2030):393–408, Feb 2003. ISSN 1471-2946. doi: 10.1098/rspa.2002.1014. URL <http://dx.doi.org/10.1098/rspa.2002.1014>.
- [10] A. I. Sokolov. Phase transitions in a superfluid neutron liquid. *Soviet Physics - JETP*, 52(4):575–576, 1980. URL [http://inis.iaea.org/search/search.aspx?orig\\_q=RN:13667729](http://inis.iaea.org/search/search.aspx?orig_q=RN:13667729).
- [11] R. F. Sawyer. Condensed  $\pi^-$  phase in neutron-star matter. *Phys. Rev. Lett.*, 29:382–385, Aug 1972. doi: 10.1103/PhysRevLett.29.382. URL <https://link.aps.org/doi/10.1103/PhysRevLett.29.382>.
- [12] S. K. Maurya, M. K. Jasim, Y. K. Gupta, and T. T. Smitha. A new model for charged anisotropic compact star. *Astrophysics and Space Science*, 361(5), Apr 2016. ISSN 1572-946X. doi: 10.1007/s10509-016-2747-7. URL <http://dx.doi.org/10.1007/s10509-016-2747-7>.
- [13] Inyong Cho and Hyeong-Chan Kim. Simple black holes with anisotropic fluid, 2017.
- [14] Cristiano Germani and Roy Maartens. Stars in the braneworld. *Physical Review D*, 64(12), Nov 2001. ISSN 1089-4918. doi: 10.1103/physrevd.64.124010. URL <http://dx.doi.org/10.1103/PhysRevD.64.124010>.
- [15] J. OVALLE. Searching exact solutions for compact stars in braneworld: A conjecture. *Modern Physics Letters A*, 23(38):3247–3263, Dec 2008. ISSN 1793-6632. doi: 10.1142/S0217732308027011. URL <http://dx.doi.org/10.1142/S0217732308027011>.
- [16] Jorge Ovalle, László Á Gergely, and Roberto Casadio. Brane-world stars with a solid crust and vacuum exterior. *Classical and Quantum Gravity*, 32(4):045015, Jan 2015. ISSN 1361-6382. doi: 10.1088/0264-9381/32/4/045015. URL <http://dx.doi.org/10.1088/0264-9381/32/4/045015>.
- [17] Jorge Ovalle. Decoupling gravitational sources in general relativity: From perfect to anisotropic fluids. *Phys. Rev. D*, 95:104019, May 2017. doi: 10.1103/PhysRevD.95.104019. URL <https://link.aps.org/doi/10.1103/PhysRevD.95.104019>.

- [18] J. Ovalle, R. Casadio, R. da Rocha, and A. Sotomayor. Anisotropic solutions by gravitational decoupling. *The European Physical Journal C*, 78(2), Feb 2018. ISSN 1434-6052. doi: 10.1140/epjc/s10052-018-5606-6. URL <http://dx.doi.org/10.1140/epjc/s10052-018-5606-6>.
- [19] Lisa Randall and Raman Sundrum. Large mass hierarchy from a small extra dimension. *Phys. Rev. Lett.*, 83:3370–3373, Oct 1999. doi: 10.1103/PhysRevLett.83.3370. URL <https://link.aps.org/doi/10.1103/PhysRevLett.83.3370>.
- [20] Lisa Randall and Raman Sundrum. An alternative to compactification. *Phys. Rev. Lett.*, 83:4690–4693, Dec 1999. doi: 10.1103/PhysRevLett.83.4690. URL <https://link.aps.org/doi/10.1103/PhysRevLett.83.4690>.
- [21] R. Casadio, Jorge Ovalle, and Roldão da Rocha. The minimal geometric deformation approach extended. *Classical and Quantum Gravity*, 32:215020, 10 2015. doi: 10.1088/0264-9381/32/21/215020.
- [22] Jorge Ovalle. Extending the geometric deformation: New black hole solutions. *International Journal of Modern Physics: Conference Series*, 41:1660132, Jan 2016. ISSN 2010-1945. doi: 10.1142/s2010194516601320. URL <http://dx.doi.org/10.1142/S2010194516601320>.
- [23] M. C. Durgapal and R. S. Fuloria. Analytic relativistic model for a superdense star. *General Relativity and Gravitation*, 17(7):671–681, Jul 1985. ISSN 1572-9532. doi: 10.1007/BF00763028. URL <https://doi.org/10.1007/BF00763028>.
- [24] S. K. Maurya, Y. K. Gupta, Saibal Ray, and Baiju Dayanandan. Anisotropic models for compact stars. *The European Physical Journal C*, 75(5), May 2015. ISSN 1434-6052. doi: 10.1140/epjc/s10052-015-3456-z. URL <http://dx.doi.org/10.1140/epjc/s10052-015-3456-z>.
- [25] J. OVALLE. Nonuniform braneworld stars: An exact solution. *International Journal of Modern Physics D*, 18(05):837–852, May 2009. ISSN 1793-6594. doi: 10.1142/s0218271809014790. URL <http://dx.doi.org/10.1142/S0218271809014790>.
- [26] Antonio De Felice and Shinji Tsujikawa.  $f(r)$  theories. *Living Reviews in Relativity*, 13(1), Jun 2010. ISSN 1433-8351. doi: 10.12942/lrr-2010-3. URL <http://dx.doi.org/10.12942/lrr-2010-3>.

- [27] Luisa G. Jaime, Leonardo Patiño, and Marcelo Salgado. Robust approach to  $f(R)$  gravity. *Physical Review D*, 83(2), Jan 2011. ISSN 1550-2368. doi: 10.1103/PhysRevD.83.024039. URL <http://dx.doi.org/10.1103/PhysRevD.83.024039>.
- [28] Daniele Vernieri and Sante Carloni. On the anisotropic interior solutions in horava gravity and einstein-æther theory. *EPL (Europhysics Letters)*, 121(3):30002, Feb 2018. ISSN 1286-4854. doi: 10.1209/0295-5075/121/30002. URL <http://dx.doi.org/10.1209/0295-5075/121/30002>.
- [29] Jorge Alfaro, Domènec Espriu, and Luciano Gabbanelli. Bose–einstein graviton condensate in a schwarzschild black hole. *Classical and Quantum Gravity*, 35(1):015001, Nov 2017. ISSN 1361-6382. doi: 10.1088/1361-6382/aa9771. URL <http://dx.doi.org/10.1088/1361-6382/aa9771>.
- [30] Gia Dvali and Cesar Gomez. Black holes  $1/n$  hair. *Physics Letters B*, 719(4-5):419–423, Feb 2013. ISSN 0370-2693. doi: 10.1016/j.physletb.2013.01.020. URL <http://dx.doi.org/10.1016/j.physletb.2013.01.020>.
- [31] Roberto Casadio and Roldão da Rocha. Stability of the graviton bose–einstein condensate in the brane-world. *Physics Letters B*, 763:434–438, Dec 2016. ISSN 0370-2693. doi: 10.1016/j.physletb.2016.10.072. URL <http://dx.doi.org/10.1016/j.physletb.2016.10.072>.
- [32] Luciano Gabbanelli, Ángel Rincón, and Carlos Rubio. Gravitational decoupled anisotropies in compact stars. *The European Physical Journal C*, 78(5), May 2018. ISSN 1434-6052. doi: 10.1140/epjc/s10052-018-5865-2. URL <http://dx.doi.org/10.1140/epjc/s10052-018-5865-2>.
- [33] G. E. Addison, D. J. Watts, C. L. Bennett, M. Halpern, G. Hinshaw, and J. L. Weiland. Elucidating  $\Lambda$ CDM: Impact of baryon acoustic oscillation measurements on the hubble constant discrepancy. *The Astrophysical Journal*, 853(2):119, Jan 2018. ISSN 1538-4357. doi: 10.3847/1538-4357/aaa1ed. URL <http://dx.doi.org/10.3847/1538-4357/aaa1ed>.
- [34] Adam G. Riess, Stefano Casertano, Wenlong Yuan, Lucas Macri, Jay Anderson, John W. MacKenty, J. Bradley Bowers, Kelsey I. Clubb, Alexei V. Filippenko, David O. Jones, and Brad E. Tucker. New parallaxes of galactic cepheids from spatially scanning the hubble space telescope : Implications for the hubble constant. *The Astrophysical Journal*, 855(2):136, 2018. URL <http://stacks.iop.org/0004-637X/855/i=2/a=136>.

- [35] Adam G. Riess, Stefano Casertano, Wenlong Yuan, Lucas M. Macri, and Dan Scolnic. Large magellanic cloud cepheid standards provide a 1% foundation for the determination of the hubble constant and stronger evidence for physics beyond  $\Lambda$ CDM. *The Astrophysical Journal*, 876(1):85, may 2019. doi: 10.3847/1538-4357/ab1422. URL <https://doi.org/10.3847%2F1538-4357%2Fab1422>.
- [36] Eleonora Di Valentino, Alessandro Melchiorri, and Joseph Silk. Planck evidence for a closed Universe and a possible crisis for cosmology. *Nature Astronomy*, 4:196,203, February 2020. doi: 10.1038/s41550-019-0906-9.
- [37] Richard A. Battye, Tom Charnock, and Adam Moss. Tension between the power spectrum of density perturbations measured on large and small scales. *Phys. Rev. D*, 91: 103508, May 2015. doi: 10.1103/PhysRevD.91.103508. URL <https://link.aps.org/doi/10.1103/PhysRevD.91.103508>.
- [38] Planck Collaboration, N. Aghanim, Y. Akrami, M. Ashdown, J. Aumont, C. Baccigalupi, M. Ballardini, A. J. Banday, R. B. Barreiro, N. Bartolo, S. Basak, R. Battye, K. Benabed, J. P. Bernard, M. Bersanelli, P. Bielewicz, J. J. Bock, J. R. Bond, J. Borrill, F. R. Bouchet, F. Boulanger, M. Bucher, C. Burigana, R. C. Butler, E. Calabrese, J. F. Cardoso, J. Carron, A. Challinor, H. C. Chiang, J. Chluba, L. P. L. Colombo, C. Combet, D. Contreras, B. P. Crill, F. Cuttaia, P. de Bernardis, G. de Zotti, J. Delabrouille, J. M. Delouis, E. Di Valentino, J. M. Diego, O. Doré, M. Douspis, A. Ducout, X. Dupac, S. Dusini, G. Efstathiou, F. Elsner, T. A. Enßlin, H. K. Eriksen, Y. Fantaye, M. Farhang, J. Fergusson, R. Fernandez-Cobos, F. Finelli, F. Forastieri, M. Frailis, A. A. Fraisse, E. Franceschi, A. Frolov, S. Galeotta, S. Galli, K. Ganga, R. T. Génova-Santos, M. Gerbino, T. Ghosh, J. González-Nuevo, K. M. Górski, S. Gratton, A. Gruppuso, J. E. Gudmundsson, J. Hamann, W. Handley, F. K. Hansen, D. Herranz, S. R. Hildebrandt, E. Hivon, Z. Huang, A. H. Jaffe, W. C. Jones, A. Karakci, E. Keihänen, R. Keskitalo, K. Kiiveri, J. Kim, T. S. Kisner, L. Knox, N. Krachmalnicoff, M. Kunz, H. Kurki-Suonio, G. Lagache, J. M. Lamarre, A. Lasenby, M. Lattanzi, C. R. Lawrence, M. Le Jeune, P. Lemos, J. Lesgourgues, F. Levrier, A. Lewis, M. Liguori, P. B. Lilje, M. Lilley, V. Lindholm, M. López-Caniego, P. M. Lubin, Y. Z. Ma, J. F. Macías-Pérez, G. Maggio, D. Maino, N. Mandolesi, A. Mangilli, A. Marcos-Caballero, M. Maris, P. G. Martin, M. Martinelli, E. Martínez-González, S. Matarrese, N. Mauri, J. D. McEwen, P. R. Meinhold, A. Melchiorri, A. Mennella, M. Migliaccio, M. Millea, S. Mitra, M. A. Miville-Deschênes, D. Molinari, L. Montier, G. Morgante, A. Moss, P. Natoli, H. U.

- Nørgaard-Nielsen, L. Pagano, D. Paoletti, B. Partridge, G. Patanchon, H. V. Peiris, F. Perrotta, V. Pettorino, F. Piacentini, L. Polastri, G. Polenta, J. L. Puget, J. P. Rachen, M. Reinecke, M. Remazeilles, A. Renzi, G. Rocha, C. Rosset, G. Roudier, J. A. Rubiño-Martín, B. Ruiz-Granados, L. Salvati, M. Sandri, M. Savelainen, D. Scott, E. P. S. Shellard, C. Sirignano, G. Sirri, L. D. Spencer, R. Sunyaev, A. S. Suur-Uski, J. A. Tauber, D. Tavagnacco, M. Tenti, L. Toffolatti, M. Tomasi, T. Trombetti, L. Valenziano, J. Valiviita, B. Van Tent, L. Vibert, P. Vielva, F. Villa, N. Vittorio, B. D. Wandelt, I. K. Wehus, M. White, S. D. M. White, A. Zacchei, and A. Zonca. Planck 2018 results. vi. cosmological parameters, 2018.
- [39] S Birrer, T Treu, C E Rusu, V Bonvin, C D Fassnacht, J H H Chan, A Agnello, A J Shajib, G C-F Chen, M Auger, F Courbin, S Hilbert, D Sluse, S H Suyu, K C Wong, P Marshall, B C Lemaux, and G Meylan. H0LiCOW – IX. Cosmographic analysis of the doubly imaged quasar SDSS 1206+4332 and a new measurement of the Hubble constant. *Monthly Notices of the Royal Astronomical Society*, 484(4):4726–4753, 01 2019. ISSN 0035-8711. doi: 10.1093/mnras/stz200. URL <https://doi.org/10.1093/mnras/stz200>.
- [40] Radosław Wojtak, Alexander Knebe, William A. Watson, Ilian T. Iliev, Steffen Heß, David Rapetti, Gustavo Yepes, and Stefan Gottlöber. Cosmic variance of the local Hubble flow in large-scale cosmological simulations. *Monthly Notices of the Royal Astronomical Society*, 438(2):1805–1812, 12 2013. ISSN 0035-8711. doi: 10.1093/mnras/stt2321. URL <https://doi.org/10.1093/mnras/stt2321>.
- [41] Adam G. Riess et al. A 2.4% Determination of the Local Value of the Hubble Constant. *Astrophys. J.*, 826(1):56, 2016. doi: 10.3847/0004-637X/826/1/56.
- [42] Adam G. Riess, Wenlong Yuan, Stefano Casertano, Lucas M. Macri, and Dan Scolnic. The accuracy of the hubble constant measurement verified through cepheid amplitudes. *The Astrophysical Journal*, 896(2):L43, jun 2020. doi: 10.3847/2041-8213/ab9900. URL <https://doi.org/10.3847/2041-8213/ab9900>.
- [43] J. S. Wang and F. Y. Wang. Probing the anisotropic expansion from supernovae and grbs in a model-independent way. *Monthly Notices of the Royal Astronomical Society*, 443(2):1680–1687, 2014.

- [44] Colin, Jacques, Mohayaee, Roya, Rameez, Mohamed, and Sarkar, Subir. Evidence for anisotropy of cosmic acceleration. *A&A*, 631:L13, 2019. doi: 10.1051/0004-6361/201936373. URL <https://doi.org/10.1051/0004-6361/201936373>.
- [45] Z. Q. Sun and F. Y. Wang. Probing the isotropy of cosmic acceleration using different supernova samples. *The European Physical Journal C*, 79(9), September 2019. doi: 10.1140/epjc/s10052-019-7293-3. URL <https://doi.org/10.1140/epjc/s10052-019-7293-3>.
- [46] Yijung Kang, Young-Wook Lee, Young-Lo Kim, Chul Chung, and Chang Hee Ree. Early-type host galaxies of type ia supernovae. II. evidence for luminosity evolution in supernova cosmology. *The Astrophysical Journal*, 889(1):8, jan 2020. doi: 10.3847/1538-4357/ab5afc. URL <https://doi.org/10.3847/1538-4357/ab5afc>.
- [47] W. D’Arcy Kenworthy, Dan Scolnic, and Adam Riess. The local perspective on the hubble tension: Local structure does not impact measurement of the hubble constant. *The Astrophysical Journal*, 875(2):145, apr 2019. doi: 10.3847/1538-4357/ab0ebf. URL <https://doi.org/10.3847/1538-4357/ab0ebf>.
- [48] T de Jaeger, B E Stahl, W Zheng, A V Filippenko, A G Riess, and L Galbany. A measurement of the Hubble constant from Type II supernovae. *Monthly Notices of the Royal Astronomical Society*, 06 2020. ISSN 0035-8711. doi: 10.1093/mnras/staa1801. URL <https://doi.org/10.1093/mnras/staa1801>. staa1801.
- [49] Eleonora Di Valentino, Alessandro Melchiorri, and Olga Mena. Can interacting dark energy solve the  $H_0$  tension? *Phys. Rev. D*, 96:043503, Aug 2017. doi: 10.1103/PhysRevD.96.043503. URL <https://link.aps.org/doi/10.1103/PhysRevD.96.043503>.
- [50] Kanhaiya L. Pandey, Tanvi Karwal, and Subinoy Das. Alleviating the  $h_0$  and 8 anomalies with a decaying dark matter model. *Journal of Cosmology and Astroparticle Physics*, 2020(07):026–026, Jul 2020. ISSN 1475-7516. doi: 10.1088/1475-7516/2020/07/026. URL <http://dx.doi.org/10.1088/1475-7516/2020/07/026>.
- [51] Richard A. Battye, Tom Charnock, and Adam Moss. Tension between the power spectrum of density perturbations measured on large and small scales. *Phys. Rev. D*, 91: 103508, May 2015. doi: 10.1103/PhysRevD.91.103508. URL <https://link.aps.org/doi/10.1103/PhysRevD.91.103508>.



- [52] J. Alfaro. Delta-gravity and dark energy. *Physics Letters B*, 709(1):101 – 105, 2012. ISSN 0370-2693. doi: <https://doi.org/10.1016/j.physletb.2012.01.067>. URL <http://www.sciencedirect.com/science/article/pii/S0370269312001086>.
- [53] Jorge Alfaro and Pablo Gonzalez. Cosmology in Delta-Gravity. *Class. Quant. Grav.*, 30:085002, 2013. doi: 10.1088/0264-9381/30/8/085002.
- [54] Jorge Alfaro and Pablo González.  $\delta$  Gravity: Dark Sector, Post-Newtonian Limit and Schwarzschild Solution. *Universe*, 5(5):96, 2019. doi: 10.3390/universe5050096.
- [55] Jorge Alfaro. Bv gauge theories, 1997.
- [56] Jorge Alfaro and Pedro Labraña. Semiclassical gauge theories. *Physical Review D*, 65(4), Jan 2002. ISSN 1089-4918. doi: 10.1103/physrevd.65.045002. URL <http://dx.doi.org/10.1103/PhysRevD.65.045002>.
- [57] Jorge Alfaro, Marco San Martín, and Joaquín Sureda. An accelerating universe without lambda: Delta gravity using monte carlo. *Universe*, 5(2), 2019. ISSN 2218-1997. doi: 10.3390/universe5020051. URL <https://www.mdpi.com/2218-1997/5/2/51>.
- [58] Uros Seljak and Matias Zaldarriaga. A line-of-sight integration approach to cosmic microwave background anisotropies. *ApJ*, 469:437, October 1996. doi: 10.1086/177793.
- [59] Matias Zaldarriaga, Uroš Seljak, and Edmund Bertschinger. Integral solution for the microwave background anisotropies in nonflat universes. *ApJ*, 494(2):491–502, February 1998. doi: 10.1086/305223.
- [60] Antony Lewis, Anthony Challinor, and Anthony Lasenby. Efficient computation of cosmic microwave background anisotropies in closed friedmann-robertson-walker models. *The Astrophysical Journal*, 538(2):473–476, aug 2000. doi: 10.1086/309179. URL <https://doi.org/10.1086%2F309179>.
- [61] V. Mukhanov. “CMB-Slow” or How to Determine Cosmological Parameters by Hand? *International Journal of Theoretical Physics*, 43:623,668, March 2004. doi: 10.1023/B:IJTP.0000048168.90282.db.
- [62] S. Weinberg. *Cosmology*. Cosmology. OUP Oxford, 2008. ISBN 9780191523601. URL <https://books.google.cl/books?id=nqQZdg020fsC>.



- [63] Karl Schwarzschild. Über das Gravitationsfeld einer Kugel aus inkompressibler Flüssigkeit nach der Einsteinschen Theorie. In *Sitzungsberichte der Königlich Preussischen Akademie der Wissenschaften zu Berlin*, pages 424–434, March 1916.
- [64] G. Lemaitre. The expanding universe. *Gen. Rel. Grav.*, 29:641–680, 1997. doi: 10.1023/A:1018855621348.
- [65] B. V. Ivanov. Analytical study of anisotropic compact star models. *The European Physical Journal C*, 77(11), Nov 2017. ISSN 1434-6052. doi: 10.1140/epjc/s10052-017-5322-7. URL <http://dx.doi.org/10.1140/epjc/s10052-017-5322-7>.
- [66] Y. K. Gupta and Sunil Kumar Maurya. A class of charged analogues of durgapal and fuloria superdense star. *Astrophysics and Space Science*, 331(1):135–144, Jan 2011. ISSN 1572-946X. doi: 10.1007/s10509-010-0445-4. URL <https://doi.org/10.1007/s10509-010-0445-4>.
- [67] Piyabut Burikham, Tiberiu Harko, and Matthew J. Lake. Mass bounds for compact spherically symmetric objects in generalized gravity theories. *Physical Review D*, 94(6), Sep 2016. ISSN 2470-0029. doi: 10.1103/physrevd.94.064070. URL <http://dx.doi.org/10.1103/PhysRevD.94.064070>.
- [68] J. Ovalle, R. Casadio, and A. Sotomayor. The minimal geometric deformation approach: A brief introduction. *Advances in High Energy Physics*, 2017:1–9, 2017. ISSN 1687-7365. doi: 10.1155/2017/9756914. URL <http://dx.doi.org/10.1155/2017/9756914>.
- [69] J. Ovalle, R. Casadio, and A. Sotomayor. Searching for modified gravity: a conformal sector? *Journal of Physics: Conference Series*, 883:012004, Aug 2017. ISSN 1742-6596. doi: 10.1088/1742-6596/883/1/012004. URL <http://dx.doi.org/10.1088/1742-6596/883/1/012004>.
- [70] W. Israel. Singular hypersurfaces and thin shells in general relativity. *Il Nuovo Cimento B (1965-1970)*, 44(1):1–14, Jul 1966. ISSN 1826-9877. doi: 10.1007/BF02710419. URL <https://doi.org/10.1007/BF02710419>.
- [71] W. Israel. Singular hypersurfaces and thin shells in general relativity. *Nuovo Cim. B*, 44S10:1, 1966. doi: 10.1007/BF02710419. [Erratum: *Nuovo Cim. B* 48, 463 (1967)].
- [72] Jan Hladík and Zdeněk Stuchlík. Photon and neutrino redshift in the field of braneworld compact stars. *Journal of Cosmology and Astroparticle Physics*, 2011(07):012–012, Jul

2011. ISSN 1475-7516. doi: 10.1088/1475-7516/2011/07/012. URL <http://dx.doi.org/10.1088/1475-7516/2011/07/012>.
- [73] T. Padmanabhan. *Theoretical Astrophysics*, volume 3. Cambridge University Press, 2002. doi: 10.1017/CBO9780511840166.
- [74] Wayne Hu. Covariant linear perturbation formalism, 2004.
- [75] E. M. Lifshitz. On the gravitational stability of the expanding universe. *Zhurnal Eksperimentalnoi i Teoreticheskoi Fiziki*, 16:587–602, January 1946.
- [76] N. Kaiser. Small-angle anisotropy of the microwave background radiation in the adiabatic theory. *Monthly Notices of the Royal Astronomical Society*, 202:1169–1180, March 1983. doi: 10.1093/mnras/202.4.1169.
- [77] Joseph Silk. When were Galaxies and Galaxy Clusters formed? *Nature*, 218:453,454, May 1968. doi: 10.1038/218453a0.
- [78] R. K. Sachs and A. M. Wolfe. Perturbations of a Cosmological Model and Angular Variations of the Microwave Background. *Apj*, 147:73, January 1967. doi: 10.1086/148982.
- [79] Martin White and Wayne Hu. The sachs-wolfe effect, 1996.
- [80] Lev Davidovich Landau. On the vibrations of the electronic plasma. *Yad. Fiz.*, 10:25, 1946. URL <https://cds.cern.ch/record/437300>.